SEPARATION OF POLAR AND NON-POLAR MOLECULES IN A NON-UNIFORM ELECTRIC FIELD

Thesis for the Degree of Ph. D.
MICHIGAN STATE UNIVERSITY
Charles D. Beals
1967

ABSTRACT

SEPARATION OF POLAR AND NON-POLAR MOLECULES IN A NON-UNIFORM ELECTRIC FIELD

by Charles D. Beals

A theoretical and experimental investigation of the dielectrophoresis of dilute aqueous solutions of polymethacrylic acid in a separation cell with cylindrical geometry was undertaken in this study in order to examine the feasibility of using the dielectrophoretic effect as a separation technique.

Analysis of the forces acting on a dipolar molecule in an A.C. or D.C. non-uniform electric field shows that the molecule will migrate in the direction of highest field strength. Solution of the transport equations describing the system yields equilibrium temperature, velocity, and concentration profiles as a function of radial position. The equilibrium separation factor or ratio of top to bottom cell concentration is found from the radial concentration profile. The theoretical separation factor is found to increase with increasing cell length, applied voltage, and molecular polarizability and to decrease with increasing values of the ratio of the outer to inner cylinder radii.

Charles D. Beals

Separations were obtained experimentally at various values of the solute concentration, cell length, and applied power. The use of radioactive tracer and resistance techniques enabled accurate concentration measurement. Both cells used in the experimental investigation were found to have an optimum operating power at which the observed separations were maximized. Operating at optimum power, a cell 24 inches long yielded a separation of 24 percent at a polymer concentration of 0.01 gm./ℓ. and a 12 inch cell, at the same concentration, gave a 3.5 percent separation. Increasing separations were found as the polymer concentration approached zero. This is attributed to increased molecular polarizabilities caused by polyion elongation in extremely dilute solutions.

The experimental results obtained using radioactively tagged polymer for concentration determination, verify the values obtained from resistance measurements for runs made at or below the optimum cell power. For these conditions, favorable agreement between the experimental and predicted results is also found. For runs made above the optimum cell power, the resistance results show greater separations than the counted results and seem to be in error.

SEPARATION OF POLAR AND NON-POLAR MOLECULES
IN A NON-UNIFORM ELECTRIC FIELD

By

Charles D. Beals

A THESIS

Submitted to
Michigan State University
in partial fulfillment of the requirements
for the degree of

DOCTOR OF PHILOSOPHY

Department of Chemical Engineering

1967

To Carrol

ACKNOWLEDGMENT

The author wishes to express his appreciation to Dr. Donald K. Anderson for his guidance during the course of this work.

The author is indebted to the Division of Engineering Research of the College of Engineering at Michigan State University for providing financial support.

Appreciation is extended to William B. Clippinger for his advice and assistance in the construction of the laboratory apparatus and also to Dr. J. Sutherland Frame for his consultation pertaining to theoretical derivations included in this research.

The understanding and patience of the author's wife, Carrol, is sincerely appreciated.

TABLE OF CONTENTS

Page

LIST OF FIGURES

Figure Page

Tabl

I

II

III

IV

V

VI

LIST OF TABLES

INTRODUCTION

The term "dielectrophoresis" was introduced by H. A. Pohl[50] in 1951 and is defined as the motion of matter caused by polarization effects in a non-uniform electric field. This subject has received very little attention in the past, whereas its counterpart in magnetic studies has provided one of the most powerful tools to structural inorganic chemistry. Some possible uses of the dielectrophoretic technique include; chemical separations, an alternate technique for determining dipole moments, and a method of fractionating polymers by molecular weight. Another use of this method may be found in separating chemically similar substances, such as cis- and trans-isomers, on which the common methods of separation are quite often ineffective.

The criteria for a separation to be effected by the dielectrophoretic technique is that the solute and solvent have different electric dipole moments. A dipolar molecule has a finite separation of equal amounts of plus and minus charge. If this charge separation is caused by the molecular structure of the molecule, as in water or p-nitroaniline, the molecule is said to have a permanent dipole moment. The magnitude of this moment is given by the product of the quantity of its charge times the distance between the charges.

A molecule is said to have an induced dipole moment if a charge separation is caused by the influence of an electric field. This induced moment is caused in some molecules because their charges are relatively loosely bound and can be forced to migrate due to the force exerted on them by the electric field. The magnitude of the dipole moment of a polarizable molecule is given by the product of a constant, called the polarizability, times the electric field strength operating at the site of the molecule.

When a dipolar molecule is placed in an electric field it will experience a torque, which will tend to orient it in a direction parallel to the field direction. If the field is spatially uniform, no translational movement will result. If the field is spatially non-uniform, one pole of the dipole will be in a stronger field than the other and the force on it will accordingly be greater. This results in a net translational movement in the direction of highest field strength. It will be shown that the direction of dipolar movement is independent of the polarity of the field, making the method applicable in either A.C. or D.C. fields.

Comparing dielectrophoresis to the more common phenomena "electrophoresis," it is seen that dielectrophresis:

1. Produces motion of the particle which is not affected by the direction of the applied field.
2. Requires highly divergent fields such as are produced by concentric cylinders or spheres.
3. Requires relatively high field strengths.

4. Is, in general, a relatively weak effect and will be easily observable only in systems which have a strong field and high electric moment.

On the other hand electrophoresis:

1. Produces motion of the particles in which the direction of motion is dependent on the direction of the field. Reversal of the field reverses the direction of travel.
2. Is observable with particles of any size.
3. Operates in either divergent or uniform fields.
4. Requires relatively low voltages.
5. Requires relatively small charges per unit volume of the particle.

Pohl[51] has used the dielectrophoretic technique to produce some interesting phenomena which include; selective precipitation, mixing, separation of course suspensions, and pumping of nonconducting liquids.

In this study, the dielectrophoresis of a polyelectrolyte solution in a concentric wire-cylinder electrode system is investigated. A theoretical analysis of the steady state temperature, velocity, and concentration profiles for this system is presented. Experimental measurements are obtained by resistance measurements and are verified by a radioactive tracer technique.

BACKGROUND WORK

Dielectrophoresis

The theoretical and experimental aspects of dielectrophoresis have been, in a limited sense, treated in the past. Mueller,[46] and Pohl,[50] and Loesche and Hultschig[38] independently studied the size and direction of the dielectrophoretic effect. Mueller in a theoretical analysis concluded that the effect would be small for particles of molecular size. Loesche and Hultschig also concluded this from their study of the theory and their experiments. Other investigators[57,27] have, however, using very high field strengths and extremely non-uniform geometries, obtained appreciable separations of small molecules with this method. Loesche and Hultschig[38] and Debye et al.[9] have shown that measurable concentration changes are observed in the dielectrophoresis of polymers.

The first experimental evidence of the movement of polar molecules in solution was given by Karagounis[27,28] in 1948. He placed a solution of nitrobenzene in benzene in the annular volume of a concentric tungsten wire and metallic cylinder. The apparatus was equipped with a continuous feed system and product was taken from a glass capillary which surrounded the wire. Upon applying an electric field to this system, he observed that after some time the concentration of nitrobenzene close to the wire was greater than that of the bulk solution. An applied voltage of 10,000 volts gave concentration changes of up to 12 percent. In a second apparatus the mixture was passed through a net, with horizontal wires forming the negative electrode and vertical ones the positive electrode. After passing through the net, the liquid was less concentrated in polar molecules than the liquid remaining in the apparatus, demonstrating that the net acted as a dipole filter. A third apparatus consisted of a porous metal tube concentric with a larger outer tube. Using these two tubes as electrodes and applying up to 16,000 volts D.C. across them, separations of up to 39.5 percent were measured with tetraethylammomium picrate in benzene (dipole moment = 18.0 Debye). This method was also used to obtain a 4.5 percent separation at 16,000 volts of a mixture of cis-and trans-azobenzene, where transazobenzene has a dipole moment of zero.

Debye _et al._,[9] in 1954, reported that the dielectrophoretic effect could be observed in 1 percent solutions of polystyrene, a highly polarizable molecule, with an applied voltage of 7,000 volts. The apparatus consisted of a cylinder coaxial with a fine central wire. It was proposed that since there was a concentration rearrangement within the cell, an accompanying change in capacitance of the system should also occur. The increase in capacity was determined as a measure of the concentration change in the cell. It was observed that after applying the voltage the establishment of the new capacity required about three minutes. A diffraction technique was alternately used to obtain more accurate concentration measurements. The possibility of using dielectrophresis for polymer fractionation was suggested by this work.

Loesche and Hultschig presented a theoretical and experimental work on dielectrophoresis in 1955. In the theoretical treatment, the dielectrophoretic force was equated to the sum of the osmotic and frictional forces acting on a dipolar molecule. The following basic differential equation was obtained.

$$MF \frac{\partial F}{\partial r} - kT \frac{1}{C} \frac{\partial C}{\partial r} = v\, S_t$$

where:

$M = \alpha + \frac{\mu^2 p}{3kT}$ = Total solute dipole moment

$S_t = 6\pi\mu r_m$ = Stoke's resisting force

and:

α = polarizability

μ_p = dipole moment of polar molecule

k = Boltzman's constant

T = temperature

F = electric field strength

r = direction of molecular movement

C = concentration

v = molecular velocity in the r direction

μ = viscosity

r_m = effective radius of dipolar molecule

and all quantities are expressed in a consistent set of units. This equation considers only the dipolar molecules in the solution, and when extended to polymer solutions, the Debye inner field approximation[8] is used to obtain the dipole moment. The time dependence of the concentration rearrangement in a cylindrical geometry was expressed by

$$\frac{\partial C}{\partial t} = - \frac{1}{A_r} \frac{\partial (CvA_r)}{\partial r}$$

where:

$A_r = 2\pi rL$

r = radial position from the center of the cylinder.

L - length of the cylinder.

The general solution to the differential equation was not obtained. A relationship was obtained for the variation of concentration with time at very small times and an approximate steady state radial concentration distribution was determined. The experimental work consisted of studying the dielectrophoresis of nitrobenzene in carbon tetrachloride and polyvinylacetate in nitrobenzene. The apparatus and measuring technique are similar to those used by Debye *et al.*[9] A separation of 0.04 percent was obtained at 750 volts for nitrobenzene in carbon tetrachloride, and separations of almost

1 percent were measured at 120 volts for the polyvinylacetate solutions. It was shown that for the polymer solutions, the maximum concentration change was proportional to the degree of polymerization. It is well to note here that although these separations are very small, this can be attributed to the low voltages used and the short length of the separation cell (4 cm.)

Pohl,[51] in 1858, obtained expressions for the dielectrophoretic particle velocity in cylindrical and spherical geometries. The work also includes the derivation of the expression for the dielectrophoretic force on a spherical particle for the above geometries. Experimentally, it was shown that enrichment factors* of up to 2.5 could be obtained when separating polyvinylchloride suspended in an equal volume mixture of benzene and carbon tetrachloride. The process was termed "dielectro-precipitation."

Perhaps the most notable work done on the dielectrophoresis of small molecules was reported by Swinkels and Sullivan[57] in 1961. Their theoretical analysis yielded the expression, previously stated by Karogounis, for the ratio of polar to non-polar molecules at any given position in a non-uniform field. This was accomplished by applying the Boltzman Distribution Law to the expression for the net force

---

*The enrichment factor was the ratio of the concentration of polyvinylchloride taken from close to the central cylinder of a coaxial cylinder apparatus to the concentration at the outer cylinder.

on a polar molecule in the field. This expression is applicable for the steady state concentration distribution in a system with no external forces acting other than the electric field. A more detailed description of this derivation is presented later. The experimental work consisted of a study of the dielectrophoresis of nitrobenzene in carbon tetrachloride. The apparatus was constructed to approximate a point electrode with a spherical outer electrode. This was equipped with a dropwise feed system and product was removed from a capillary surrounding the wire electrode. Concentrations were measured spectrophotometrically. For nitrobenzene in carbon tetrachloride, the solute concentration increased about 5 percent with an applied potential of 30,000 volts, and for p-nitroanaline with 50,000 volts applied, a separation of 25 percent was observed.

Analyzing the previous work on dielectrophoresis, it is seen that in order to obtain readily measurable separations with this technique either a very large electric field or a very large molecular dipole moment is required. Most molecules have permanent dipole moments of less than 5 or 6 Debye, thus a molecule with a very large polarizability is desired. This suggests the possibility of using a polyelectrolyte molecule which is capable of having an extremely large induced dipole moment in a moderate electric field.

Polyelectrolytes

A polyelectrolyte is a macromolecule carrying a large number of ionic charges with small counterions surrounding it, rendering the total system electrically neutral. The unique properties possessed by polyelectrolytes are attributed to the configuration of the polymeric chain and the distribution of counterions associated with it. Whenever an uncharged polymer chain is converted to one carrying a large number of ionized groups, the mutual repulsion of fixed charges may lead to a very large chain expansion. Since the molecular polarizability is proportional to the cube of the end to end length of the polyion chain,[10] this expansion will greatly increase the induced moment of a polyelectrolyte in an electric field.

For a weak polyacid, such as polymethacrylic acid, the degree of ionization can be controlled by the addition of a strong base to the aqueous polyacid solution. Wall[63,64] has shown that increasing the degree of neutralization correspondingly increases the degree of ionization of a weak polyacid. Several investigators[18,29,49] have observed large increases in the viscosity of polymethacrylic acid solutions as the degree of neutralization increases from 0 to 50 percent. The increased viscosity is attributed to polyion expansion caused by the mutual repulsion of the ionized groups. Viscosity results have also shown that decreasing the polymer concentration leads to increased chain expansions. This results from decreased shielding of the fixed charges since the counterions are distributed further from the polyion chain in increasingly dilute solutions.

The molecular polarizability is also dependent on the freedom of the counterions to move along the direction of the extended chain. Eigen and Schwartz[10] have shown that polyelectrolytes in an electric field exhibit enormous dipole moments which are attributed to this freedom of counterion movement. O'Konski[47] termed this effect surface conductivity. Dielectric constant studies by Mandel and Jenard[41] support the view that polyelectrolytes exhibit a longitudinal polarization due to the mobility of bound counterions.

Polymethacrylic acid has been the subject of many of the experimental investigations of polyelectrolyte behavior. The availability of information about this polymer as well as its large polarizability have been the primary considerations leading to its use in this study of dielectrophoresis.

THEORY

Previous Theoretical Considerations

Several attempts have been made to describe the concentration changes observed when a dipolar particle is subjected to an electric field. These have been qualitatively discussed in the previous section. The basic considerations and assumptions used by Swinkels and Sullivan[57] in their derivation of the steady state concentration distribution as a function of field strength will be given here.

Consider a dipolar molecule in an electric field. Assuming that the applied field is non-uniform in a direction, r, and decreases with increasing r, the net translational force acting on a dipole of moment M is:

$$f = M \frac{dF}{dr} \tag{1}$$

where F is the electric field intensity acting at the site of a molecule. M, the total moment, is the combination of contributions due to the polarizability of the molecule, α, and its permanent dipole moment. The induced moment is given by

$$m_i = \alpha F. \tag{2}$$

The contribution of permanently polar molecules is given by an average moment, $\mu L(x)$, where μ is the absolute value of the dipole moment, $L(X)$ is the Langevin function and x is $\mu F/kT$, with k and T being the Boltzman constant and temperature respectively. For a detailed description of the concept of an average moment, the reader is referred to Debye.[7] Thus, the total moment M is

$$M = \alpha F + \mu L(x).$$

Considering a solution of polar and non-polar molecules and introducing subscripts p and n for them respectively, the difference in force on the polar and non-polar molecules is

$$\Delta f = f_p - f_n = [\mu L(x) + F(\alpha_p - \alpha_n)] \frac{dF}{dr} \qquad (4)$$

Applying the Boltzman distribution law to the system under consideration, the ratio of polar to non-polar molecules is given by

$$\left[\frac{N_p}{N_n}\right]_{F = F_r} = \left[\frac{N_p}{N_n}\right]_{F = 0} \exp\,(-E_r/kT) \qquad (5)$$

where E_r is the energy difference between polar and non-polar molecules at a point where the electric field intensity is F_r. If this energy difference is zero at $r = \infty$, then

$$E_r = -\int_0^{Fr} [\mu L(x) + (\alpha_p - \alpha_n)F]\, dF. \qquad (6)$$

Introducing the approximate form of the Langevin function for small values of x, $\mu F/3kT$, and integrating,

$$E_r = -\frac{1}{2}\left[\frac{\mu^2}{3kT} + \alpha_p - \alpha_n\right] F_r^2. \qquad (7)$$

Equation (5) then takes the form

$$\left[\frac{N_p}{N_n}\right]_{F = F_r} = \left[\frac{N_p}{N_n}\right]_{F_r = 0} \exp\left\{\left(\frac{\mu^2}{3kT} + \alpha_p - \alpha_n\right) F_r^2/2kT\right\}. \qquad (8)$$

The assumptions included in the previous derivation are:

1. The field is continuous but non-uniform in the r direction.
2. Interactions between neighboring molecules are neglected.
3. Only the mean polarizability of a molecule is considered in determining its induced moment.
4. The variation of field intensity over a molecular distance is neglected in the calculation of the induced moment.

It is immediately evident from Equation (8) that separations of polar mixtures may be obtained in either an A.C. or D.C. field, since the concentration ratio is dependent on the square of the field strength.* An analogous expression has been obtained by Frank[15] from a thermodynamic analysis of polar mixtures.

Statement of the Problem

A more fundamental approach to the problem of obtaining equilibrium concentration distributions for a

---

*This requires that when the $\mu^2/3kT$ terms in Equation (8) is important, the molecules can re-orient within the time represented by one cycle of an A.C. field, and when the α_p term is important, the mobile charge associated with a molecule can shift within one cycle of an A.C. field.

particular geometry is to solve the transport equations for the system. This is accomplished by first solving for the temperature and velocity profiles for the given system. They are then used in the solution of the equation of continuity of species.

The system under consideration is a very dilute polyelectrolyte-water solution in the annular space between two concentric cylinders connected to reservoirs at both ends. Assume that the cylinder is long enough, compared to its radius, such that end effects may be neglected. The inner cylinder, in this case, is a fine wire. Further, assume that in the limit of extreme dilution, the concentration dependences of density, viscosity, coefficient of volume expansion, and diffusivity are negligible. The competing effects of sedimentation and thermal diffusion are also neglected in this treatment.

On applying a potential across the wire and outer cylinder of the above system, three effects begin to occur simultaneously. First, the dipolar molecules are oriented and attracted to the wire. Second, back diffusion starts to occur due to the concentration change caused by dielectrophoresis. Third, the applied voltage produces a current in the solution causing Joule heating. This establishes a temperature gradient through the solution, with the inner electrode at a higher temperature than the outer one, and natural convection takes place. The separations obtained are caused by this combination of effects. It may be stated that no loss in generality is incurred by saying dipolar "molecules" rather than "particles" as the following treatment is applicable in either case, as long as the system conform to the stated assumptions.

Temperature Distribution

For the system under consideration, define the radius of the inner cylinder, or wire, as R_i and the outer radious R_o. The ratio of outer to inner radius is then a constant, κ. From Bird, Stewart, and Lightfoot,[4] the following simplified energy equation is obtained

$$0 = k_1 \frac{1}{r} \frac{\partial}{\partial r} \left(r \frac{\partial T}{\partial r}\right) + S_e \tag{9}$$

where:

k_1 = thermal conductivity of solution

r = radial dimension

T - temperature

S_e = power produced/unit volume due to electrical dissipation.

The simplification of the basic energy equation includes neglecting:

a. viscous heating

b. all variables with angular (θ) dependences

c. all velocities except those in the length (z) direction

d. variation of temperature with time

e. the temperature variation in the z direction.

The power generated by Joule heating is obtained from examining the radial variation of resistance in a cylindrical geometry:

$$dR = \frac{\rho_1 dr}{2\pi r L} \tag{10}$$

where:

dR = a differential increment of resistance

ρ_1 = the resistivity of the medium

dr = a differential increment of distance in the r direction

L = the length of the cylinder.

From basic electrical relationships it can be shown that

$$P_{(r)} = \frac{\Delta VI}{\ell n\ \kappa}\ \ell n\ \frac{r}{R_i} \tag{11}$$

where:

$P_{(r)}$ = total power generated by Joule heating as a function of r

ΔV = applied voltage across the cell

I = current across the cell.

Similarly the electrical source term, S_e, is

$$S_e = \frac{\Delta VI}{2\pi L\ \ell n\ \kappa} \left(\frac{1}{r^2}\right). \tag{12}$$

Introducing the dimensionless variable

$$y = \frac{r}{R_i}, \tag{13}$$

the expression for S_e becomes

$$S_e = \frac{\Delta VI}{2\pi L R_i^2\ \ell n\ \kappa} \left(\frac{1}{y^2}\right) \tag{14}$$

Figure 1 shows the variation of $\frac{1}{y^2}$ as a function of y. This is directly proportional to the power produced per unit volume as a function of radial position. Examination of Figure 1 shows that S_e decreases very rapidly over a very short radial increment. This indicates that for geometries of practical interest (i.e. $\kappa > 20$), a reasonable assumption is that all the heat is produced at or very near to the wire. This simplifies the mathematics by reducing Equation (9) to

$$0 = k_1 \frac{1}{r} \frac{\partial}{\partial r} (r \frac{\partial T}{\partial r}), \tag{15}$$

with the boundary conditions that

at $r = R_i$, $T = T_i$

$r = R_o$, $T = T_o$.

Making use of Equation (13) and letting

$$\Theta = \frac{T - T_i}{T_o - T_i}, \tag{16}$$

Equation (15) becomes, after some rearrangement,

$$\frac{d^2\Theta}{dy^2} + \frac{1}{y} \frac{d\Theta}{dy} = 0. \tag{17}$$

The boundary conditions on Equation (17) are also made dimensionless and are:

at $r = R_i$, $y = 1$; $T = T_i$, $\Theta = 0$

$r = R_o$, $y = \kappa$; $T = T_o$, $\Theta = 1$.

It is seen that by the substitution

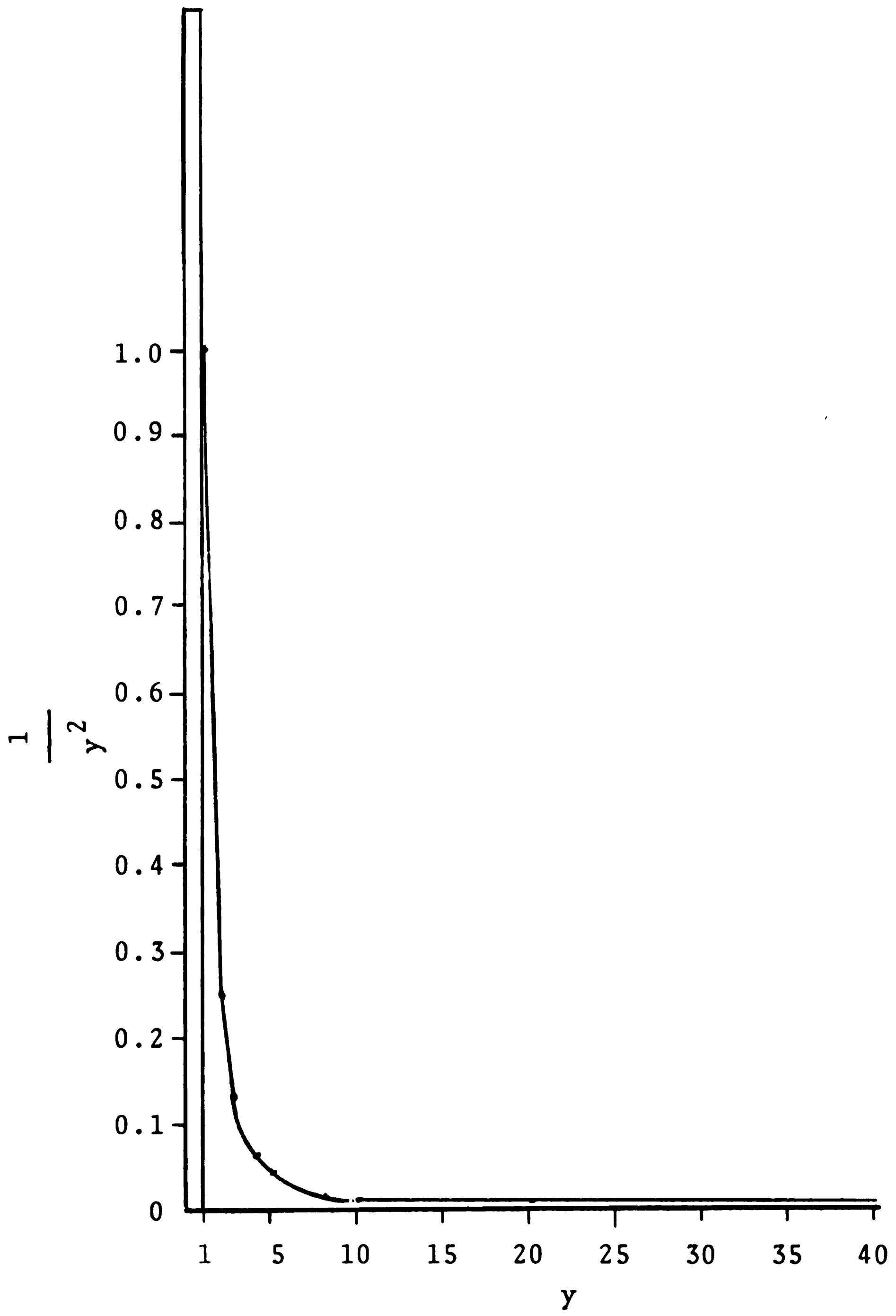

Figure 1. Variation of power per unit volume with y.

$$\frac{d\Theta}{dy} = Q, \tag{18}$$

Equation (17) may be reduced to a readily soluble first order differential equation in Q,

$$\frac{dQ}{dy} + \frac{1}{y} Q = 0, \tag{19}$$

the solution of which is

$$Q = \frac{c_1}{y} = \frac{d\Theta}{dy}, \tag{20}$$

where c_1 is a constant of integration. Equation (20) solved in terms of Θ becomes

$$\Theta = c_1 \, \ell n \, y + c_2 \tag{21}$$

where c_2 is the second constant of integration. The constants c_1 and c_2 are then eliminated by applying the dimensionless boundary conditions to Equation (21), and the radial temperature distribution in terms of the characteristic parameters of the cell is

$$T = T_i + (T_o - T_i) \frac{\ell n \, y}{\ell n \, \kappa} . \tag{22}$$

Velocity Distribution

Having obtained a mathematical relationship for the temperature as a function of radial position, the problem of the velocity profile for the cell may be considered.

From Bird, Stewart, and Lightfoot,[3] the generalized equation of motion, simplified to satisfy the system under consideration, is

$$0 = \frac{\partial p}{\partial z} + \mu \frac{1}{r} \frac{\partial}{\partial r} \left(r \frac{\partial V_z}{\partial r} \right) + \rho g_z, \tag{23}$$

where

p = pressure

z = length variable

μ = viscosity

V_z = fluid velocity in the z direction

ρ = density

g_z = acceleration of gravity in the z direction

In obtaining Equation (23), the simplification of the equation of motion included neglecting the variation of the z component of the velocity with time, terms resulting from bulk flow, terms with an angular dependence, and the second order viscous term. Expanding the density, ρ, in a Taylor series in T about a reference temperature $\bar{T}$:

$$\rho = \rho|_{\bar{T}} + \frac{\partial \rho}{\partial T}\Big|_{\bar{T}} (T - \bar{T}) + \ldots\ldots.., \tag{24}$$

and expressing the volume coefficient of expansion as

$$\beta = -\frac{1}{\rho} \left(\frac{\partial \rho}{\partial T} \right)_p , \tag{25}$$

Equation (24) may be rewritten as

$$\rho = \bar{\rho} - \bar{\rho}\bar{\beta}(T - \bar{T}) + \ldots\ldots.., \tag{26}$$

where $\bar{\rho}$ is the density evaluated at $\bar{T}$ and similarly $\bar{\beta}$ is the volume coefficient of expansion evaluated at $\bar{T}$. Noting that

$$g_z = -g \tag{27}$$

and that the pressure gradient in the fluid is due only to the weight of the fluid

$$\frac{\partial p}{\partial z} = -\bar{\rho} g, \tag{28}$$

Equation (23) may be rewritten

$$\frac{d^2 V_z}{dr^2} + \frac{1}{r}\frac{dV_z}{dr} = -\frac{\bar{\rho}\bar{\beta} g}{\mu}(T - \bar{T}). \tag{29}$$

Inserting the dimensionless radial variable, y, and the temperature from Equation (22), Equation (29) takes the form

$$\frac{d^2 V_z}{dy^2} + \frac{1}{y}\frac{dV_z}{dy} \quad \frac{\bar{\beta}\bar{\rho} g R_i^2 (T_o - T_i)}{\mu \, \ell n \, \kappa} (\ell n \, y) = -\frac{\bar{\beta}\bar{\rho} g R_i^2}{\mu}(T_i - \bar{T}). \tag{30}$$

Letting

$$A = -\frac{\bar{\rho}\bar{\beta} g R_i^2 (T_o - T_i)}{\mu \, \ell n \, \kappa}, \tag{31}$$

and

$$B = -\frac{\bar{\rho}\bar{\beta} g R_i^2 (T_i - \bar{T})}{\mu}, \tag{32}$$

Equation (30) becomes

$$\frac{d^2 V_z}{dy^2} + \frac{1}{y}\frac{dV_z}{dy} = A \, \ell n \, y + B, \tag{33}$$

subject to the boundary conditions:

$$\begin{aligned} \text{at } y &= 1, \; V_z = 0 \\ y &= \kappa, \; V_z = 0 \end{aligned} \tag{34}$$

Again it is seen that with the proper substitution,

$$\frac{dV_z}{dy} = Z, \tag{35}$$

Equation (33) may be reduced to the readily integrable first order differential equation

$$\frac{dZ}{dy} + \frac{1}{y} Z = A \ln y + B. \tag{36}$$

Rearrangement of Equation (36) to an exact form and subsequent integration yields

$$yZ = \frac{Ay^2}{2} \ln y - \frac{Ay^2}{4} + \frac{By^2}{2} + c_3, \tag{37}$$

where c_3 is a constant of integration. Reinserting Equation (35), in terms of the velocity gradient, into Equation (37) and integrating again gives

$$V_z = \frac{Ay^2}{4} \ln y - \frac{Ay^2}{4} + \frac{By^2}{4} + c_3 \ln y + c_4 \tag{38}$$

where c_4 is the second constant of integration. Applying the boundary conditions to Equation (38), the constants of integration are

$$c_3 = \frac{(A - B)}{4 \ln \kappa} (\kappa^2 - 1) - \frac{A\kappa^2}{4}, \tag{39}$$

and

$$c_4 = \frac{(A - B)}{4}, \tag{40}$$

and Equation (38) becomes

$$V_z = \frac{Ay^2}{4} \ln y - \frac{(A-B)}{4} y^2 + \frac{(A-B)}{4 \ln \kappa} (\kappa^2-1) \ln y - \frac{A\kappa^2 \ln y}{4} + \frac{(A-B)}{4}. \tag{41}$$

The velocity profile is now defined except for obtaining a relationship which determines the average temperature,

$\overline{T}$, about which the Taylor series expansion was made. The expression which defines $\overline{T}$ is obtained from requiring that the net volume flow in the z direction be zero, which expressed mathematically is

$$\int_{R_i}^{R_o} 2\pi V_z \; r \; dr = 0,$$

or equivalently

$$\int_{1}^{\kappa} V' \; y \; dy = 0, \tag{42}$$

where V' is a dimensionless velocity defined by

$$V' = \frac{4 \; V_z}{A - B}. \tag{43}$$

Equation (41) expressed in terms of the dimensionless velocity is

$$V' = \frac{A}{(A - B)} \ln y(y^2 - \kappa^2) - (y^2 - 1) + \frac{(\kappa^2 - 1)}{\ln \kappa} \ln y. \tag{44}$$

Inserting Equation (44) into Equation (42) and rearranging, the expression which defines $\overline{T}$ is

$$0 = \int_1^{\kappa} y \; dy - \int_1^{\kappa} y^3 dy + \frac{A}{A - B} \int_1^{\kappa} y^3 \ln y \; dy$$

$$+ \left[\frac{\kappa^2 - 1}{\ln \kappa} - \left(\frac{A}{A - B}\right) \kappa^2\right] \int_1^{\kappa} y \ln y \; dy. \tag{45}$$

Inspection shows that the result obtained from solving Equation (45) will be a relationship for B in terms of the parameters A and κ. This relates the reference temperature $\bar{T}$ to the ΔT across the cell and the characteristic constant of the cell, κ. The reader is referred to Appendix I for the details of this manipulation, the result of which is

$$B = A \left\{ 1 - \left[\frac{-\kappa^4 \ln \kappa + (3/4)\kappa^4 - \kappa^2 + 1/4}{1 - \kappa^4 + \frac{1}{\ln \kappa}(\kappa^2 - 1)^2} \right] \right\}, \tag{46}$$

which in terms of $\bar{T}$ is

$$\bar{T} = T_i + \frac{T_i - T_o}{\ln \kappa} \left\{ 1 - \left[\frac{-\kappa^4 \ln \kappa + (3/4)\kappa^4 - \kappa^2 + 1/4}{1 - \kappa^4 + \frac{1}{\ln \kappa}(\kappa^2 - 1)^2} \right] \right\}. \tag{47}$$

Equation (41) may now be written, using Equation (46) to eliminate the unknown B, as

$$\begin{aligned} 4V_z = {} & A(1 - y^2) \frac{-\kappa^4 \ln \kappa + (3/4)\kappa^4 - \kappa^2 + 1/4}{1 - \kappa^4 + \frac{1}{\ln \kappa}(\kappa^2 - 1)^2} + A(y^2 - \kappa^2) \ln y \\ & + A \frac{-\kappa^4 \ln \kappa + (3/4)\kappa^4 - \kappa^2 + 1/4}{1 - \kappa^4 + \frac{1}{\ln \kappa}(\kappa^2 - 1)^2} \left(\frac{\kappa^2 - 1}{\ln \kappa} \right) \ln y, \end{aligned} \tag{48}$$

or in terms of a new dimensionless velocity,

$$V^* = \frac{4\ V_z}{A}, \tag{49}$$

as

$$V^* = \left[\frac{-\kappa^4\ \ell n\ \kappa + (3/4)\kappa^4 - \kappa^2 + 1/4}{1 - \kappa^4 + \frac{1}{\ell n\ \kappa}(\kappa^2 - 1)^2}\right](1 - y^2) + (y^2 - \kappa^2)\ \ell n\ y$$
$$+ \left[\frac{-\kappa^4\ \ell n\ \kappa + (3/4)\kappa^4 - \kappa^2 + 1/4}{1 - \kappa^4 + \frac{1}{\ell n\ \kappa}(\kappa^2 - 1)^2}\right]\left(\frac{\kappa^2 - 1}{\ell n\ \kappa}\right)\ell n\ y. \qquad (50)$$

Thus, Equation (50) is the complete velocity expression in terms of the radial variable y and the cell's characteristic value κ. The velocity equation was programmed in Fortran computer language and profiles were obtained with the aid of a Control Data 3600 computer. The program used is shown in Appendix II. Figures 2-7 show calculated velocity profiles for various values of κ from 5 to 100. Figure 8 demonstrates the relative magnitude of several calculated velocity profiles in relation to the cell parameter κ.

Concentration Distribution

Having expressed the temperature and velocity distributions in mathematical form, the radial concentration as well as the equilibrium reservoir concentrations may now be obtained. From Bird, Stewart, and Lightfoot,[5] the generalized equation of continuity of species in cylindrical coordinates is

$$\frac{\partial C_A}{\partial t} + \left(\frac{1}{r}\ \frac{\partial}{\partial r}(N_{Ar}) + \frac{1}{r}\ \frac{\partial N_{A\Theta}}{\partial \Theta} + \frac{\partial N_{Az}}{\partial z}\right) = R_A \qquad (51)$$

where

C_A = concentration of species A, the polyelectrolyte, in a binary mixture, hereafter referred to as C

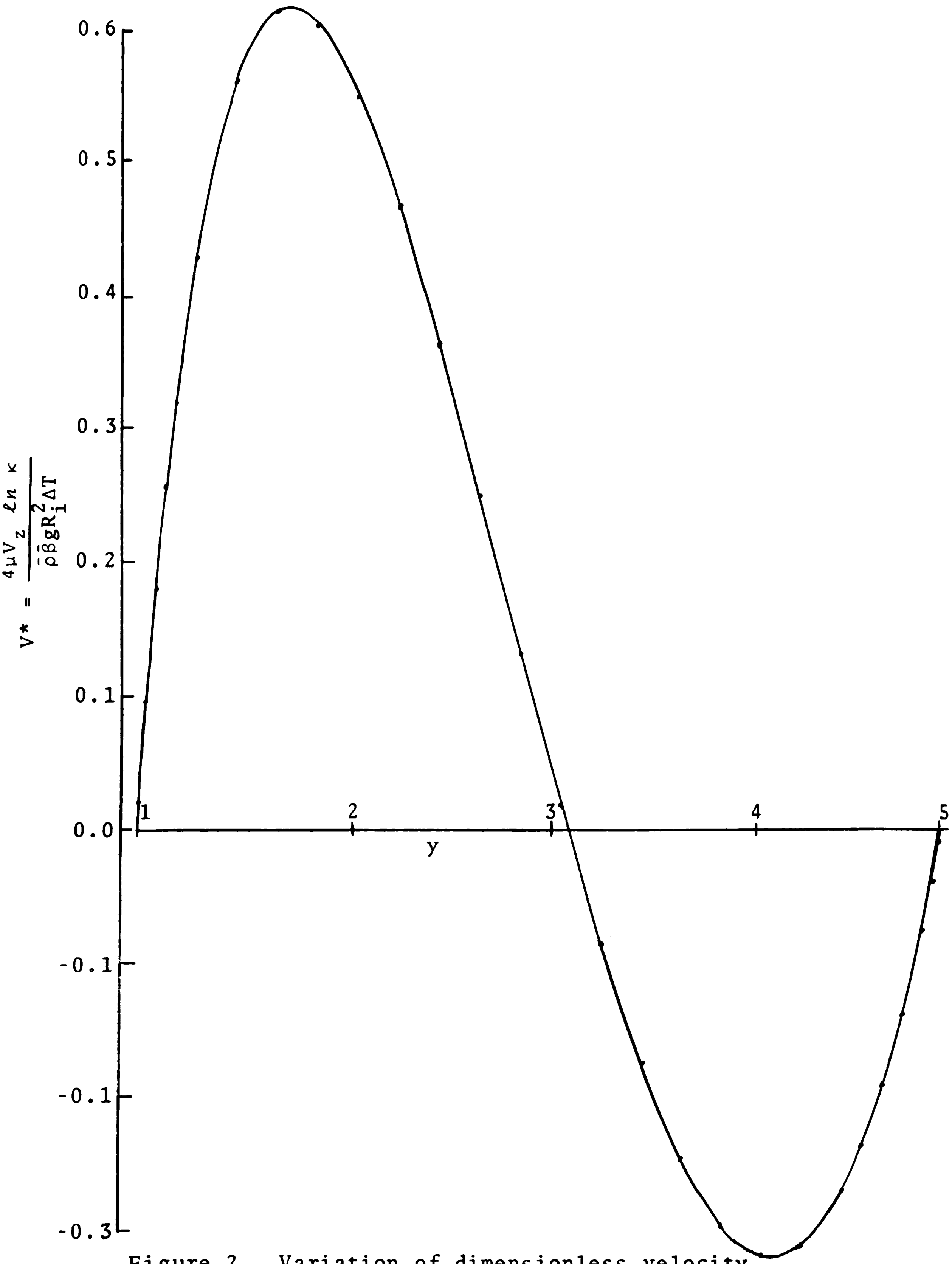

Figure 2. Variation of dimensionless velocity, V^*, with y for $\kappa = 5$.

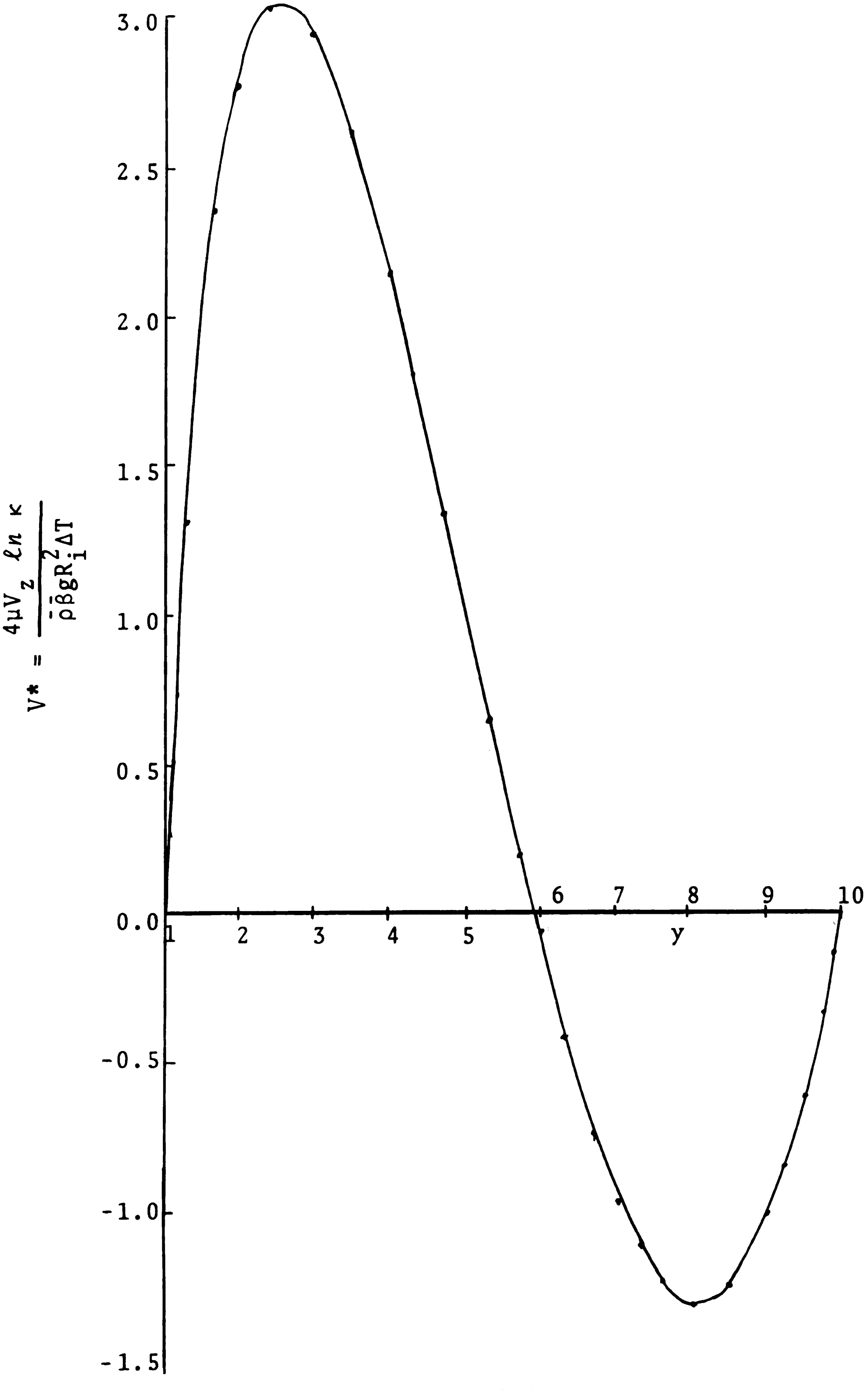

Figure 3. Variation of dimensionless velocity, V*, with y for κ = 10.

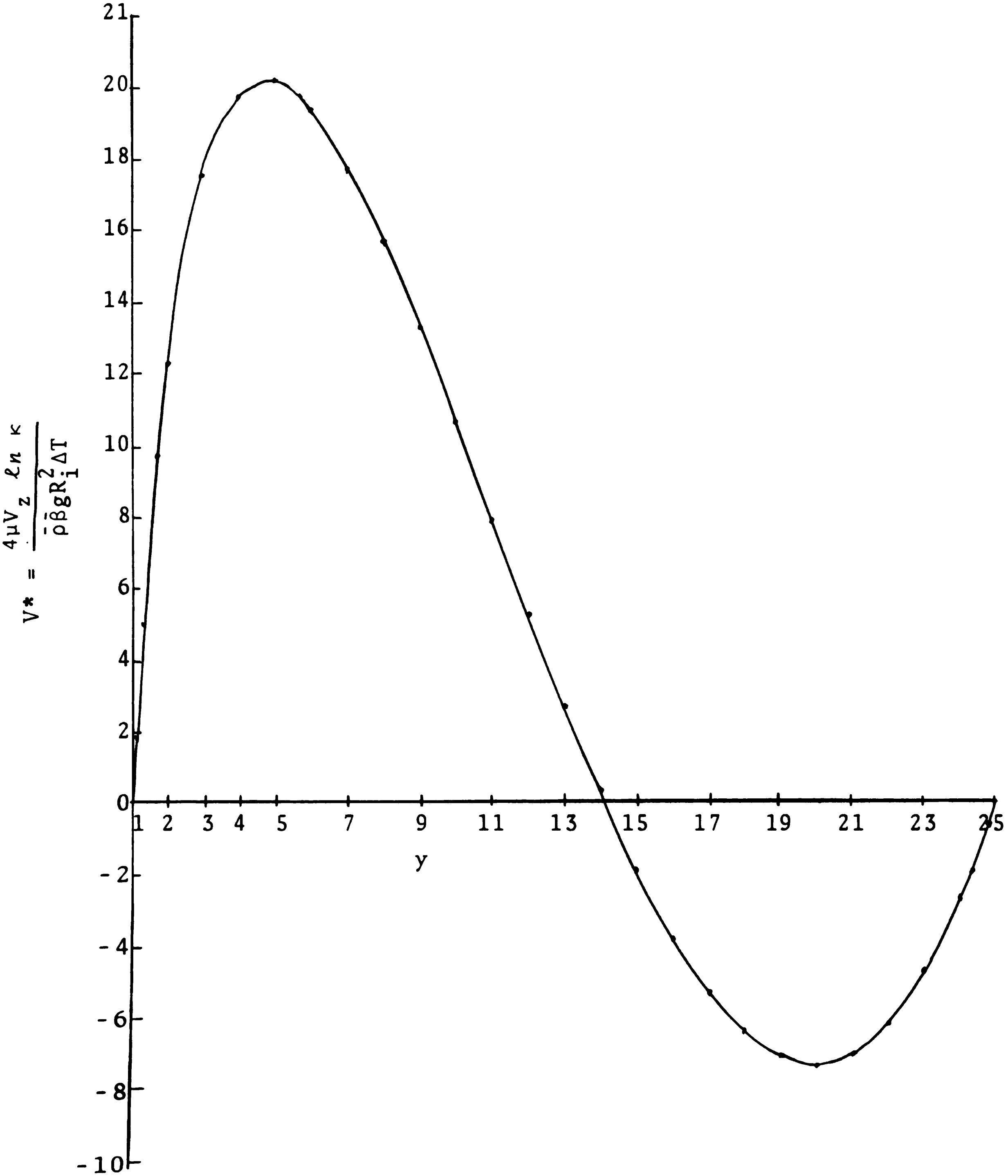

Figure 4. Variation of dimensionless velocity, V*, with y for κ = 25.

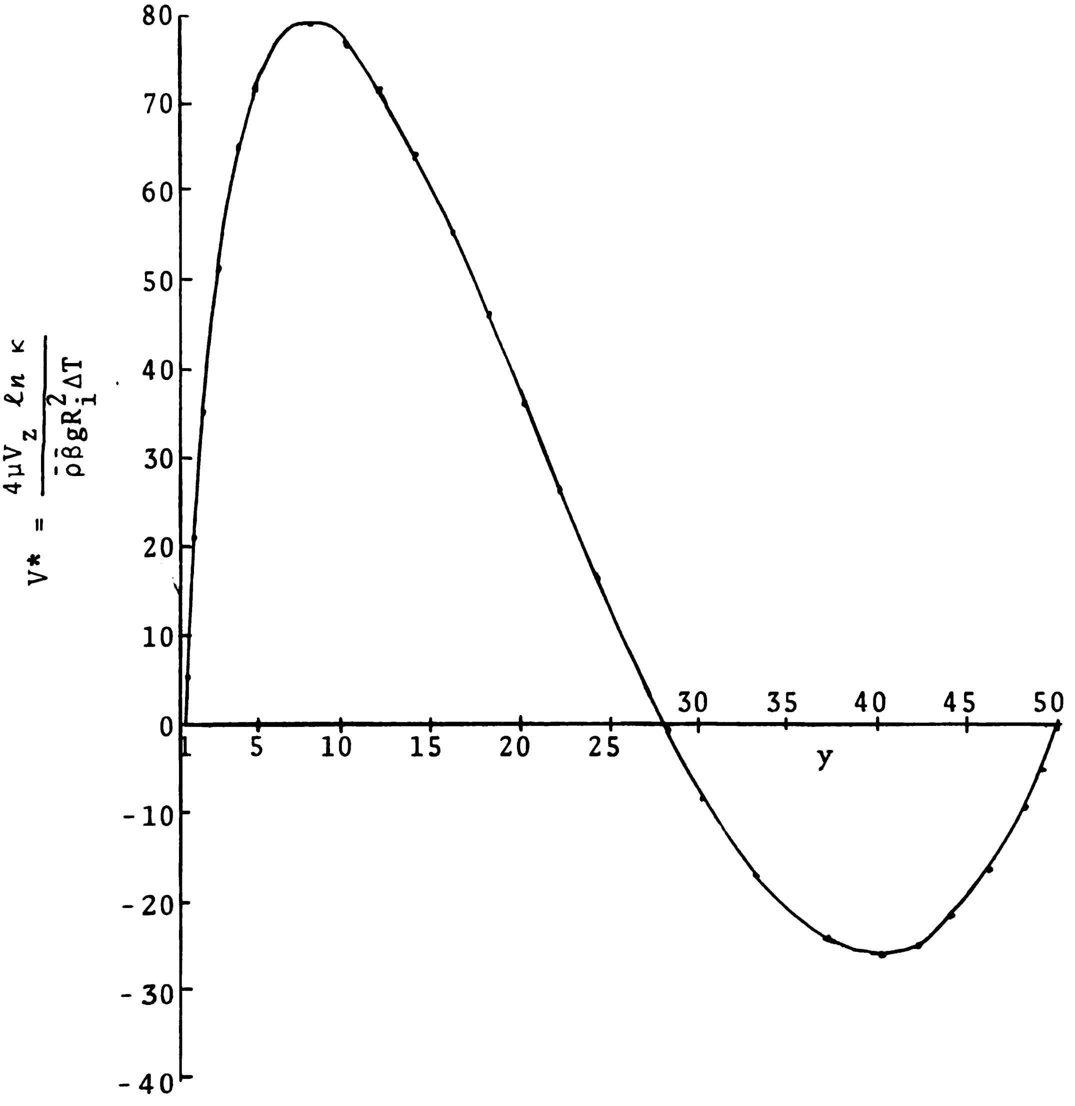

Figure 5. Variation of dimensionless velocity, V*, with y for κ = 50.

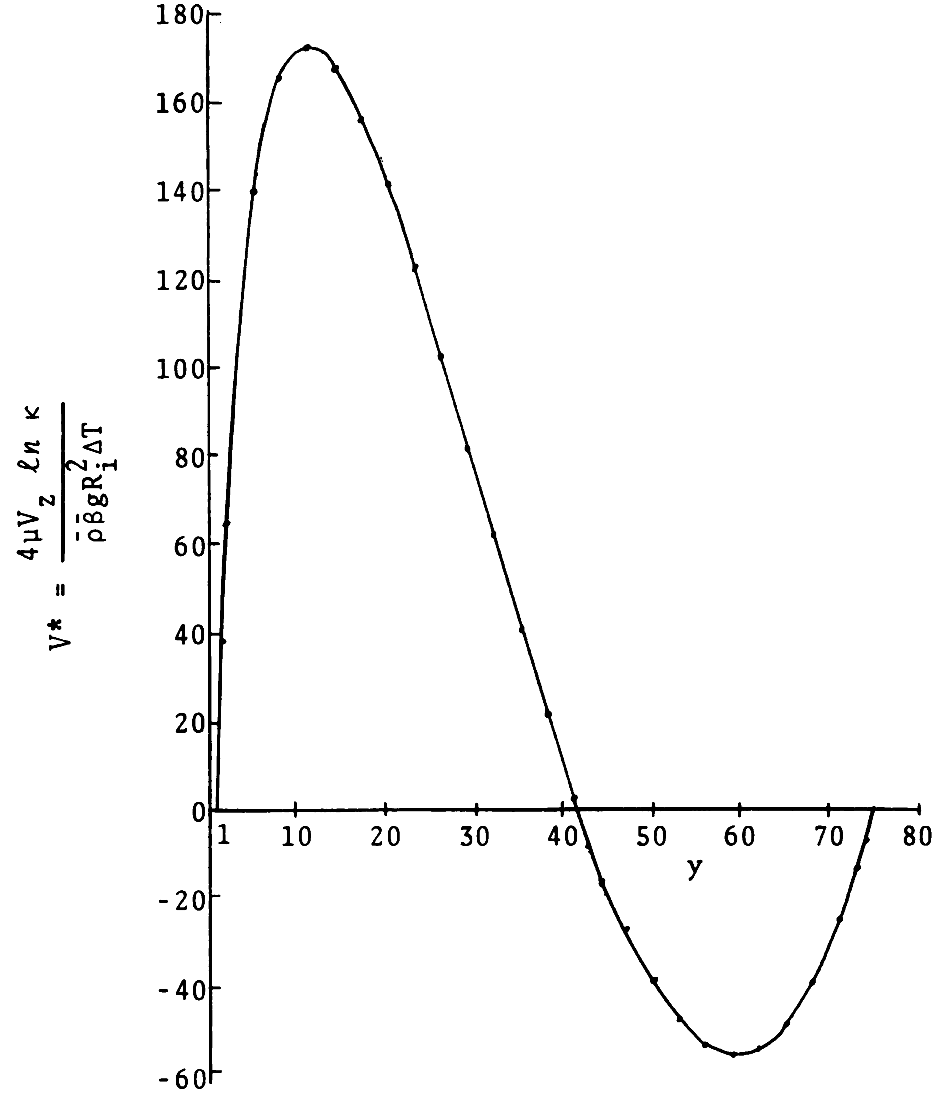

Figure 6. Variation of dimensionless velocity V^*, with y for $\kappa = 75$.

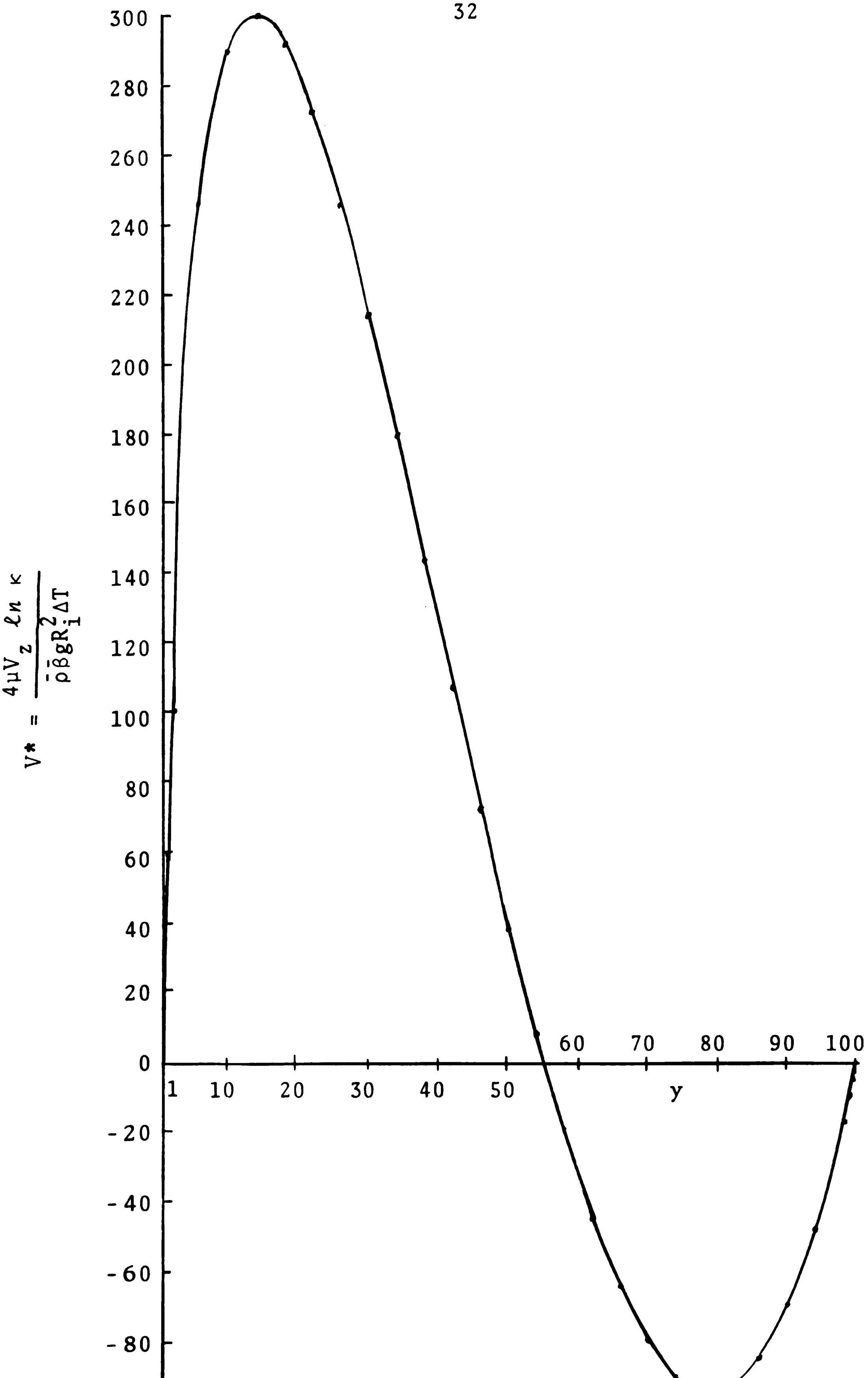

Figure 7. Variation of dimensionless velocity, V*, with y for $\kappa = 100$.

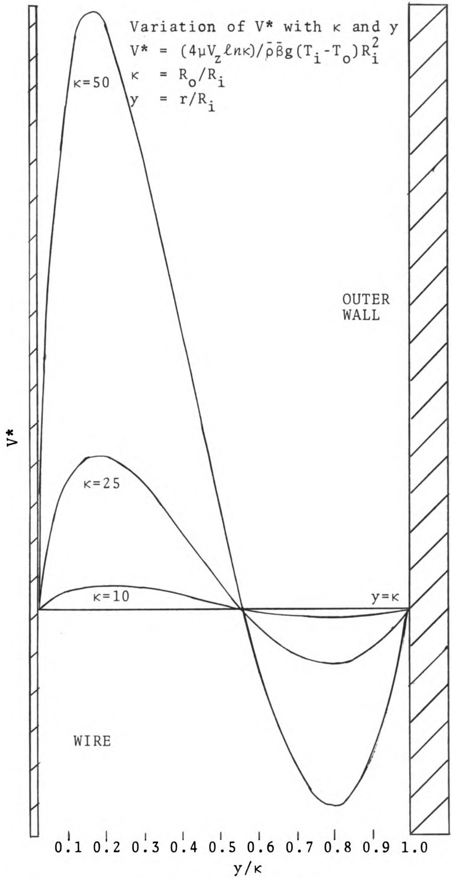

Figure 8. Comparison of several velocity profiles.

N_{Ar} = flux of A in the r direction

$N_{A}\theta$ = flux of A in the Θ direction

N_{Az} = flux of A in the z direction

R_A = rate of production of A per unit volume by chemical reaction.

Equation (51), with the assumptions of steady state, no chemical reaction, and no Θ dependencies, may be simplified to

$$\frac{1}{r}\frac{\partial}{\partial r}(r\ N_{Ar}) = -\frac{\partial N_{Az}}{\partial z} \tag{52}$$

Since N_{Ar} is the net flux of the polyelectrolyte in the r direction, it is seen that this term will be the combination of contributions due to dielectrophoresis and diffusion. The expression for N_{Ar} is obtained from considering the chemical potential of the polyelectrolyte in an electric field,

$$\mu_c = \mu_0 + (\nu + 1)RT\ \ell n\ \frac{m}{1000} - \frac{N}{2}\left(\frac{\mu_p}{3kT} + \alpha_p\right)F_r^2 \tag{53}$$

where

μ_c = total chemical potential of a dipole in an electric field[32,57]

μ_0 = constant

R = the gas constant

m = the solute molality

N = Avogadro's number

ν = number of ionized groups per polyion

and electrostatic interactions between ions have been neglected for infinitely dilute solutions. The term $\mu_0 + (\nu + 1)\ RT\ \ell n \frac{m}{1000}$ represents the portion of the chemical potential due to the ideal behavior of a dilute solute which is dissociated into (ν + 1) particles per molecule.[32] Assuming the polyelectrolyte to have a very small dipole moment compared to the magnitude of its induced moment, and further assuming that the number of ionized groups per polyion is much greater than one, Equation (53) may be reduced to

$$\mu_c = \mu_0 + \nu RT\ \ell n \frac{m}{1000} - \frac{N\alpha_p}{2} F_r^2. \tag{54}$$

The driving force for molecular movement in the r direction is obtained by taking the derivation of μ_c with respect to r,

$$-\frac{d\mu_c}{dr} = -\nu RT \frac{d\ \ell n\ m}{dr} + \frac{N\alpha_p}{2}(2F_r)\frac{dF_r}{dr}. \tag{55}$$

Noting that at infinite dilution the molality may be approximated by the concentration C, Equation (55) may be written

$$-\frac{d\mu_c}{dr} = -\nu RT \frac{d\ \ell n\ C}{dC} \cdot \frac{dC}{dr} + N\alpha_p F_r \frac{dF_r}{dC} \cdot \frac{dC}{dr}. \tag{56}$$

The driving force may then be equated to the resisting force as

$$6\pi\mu N r_m v_r = \left[-\nu RT \frac{d\ \ell n\ C}{dC} + N\alpha_p F_r \frac{dF_r}{dC}\right]\frac{dC}{dr} \tag{57}$$

where

μ = solution viscosity.

Rearranging Equation (57) the velocity in the r direction is

$$v_r = \frac{\nu RT}{6\pi\mu N r_m}\left[-\frac{d\ \ell n\ C}{dC} + \frac{N\alpha_p F_r}{\nu RT}\frac{dF_r}{dC}\right]\frac{dC}{dr}. \tag{58}$$

The flux of polyelectrolyte in the r direction is given by

$$N_{Ar} = C\ v_r \tag{59}$$

which, combined with Equation (58), yields

$$N_{Ar} = \frac{\nu RT}{6\pi\mu N r_m}\left[1 + \frac{N\alpha_p F_r}{\nu RT}\ \frac{dF_r}{d\ \ell n\ C}\right]\frac{dC}{dr}. \tag{60}$$

With

$$\frac{dC}{d\ \ell n\ C} = C, \tag{61}$$

after some simplification, the flux in terms of an approximate form of the diffusion coefficient, D_{AB}, may be written

$$N_{Ar} = -\ D_{AB}\frac{dC}{dr} + \frac{D_{AB}\alpha_p F_r C}{\nu kT}\ \frac{dF_r}{dr}, \tag{62}$$

where

$$D_{AB} = \nu RT/6\pi N\mu r_m$$

For the system of coaxial cylinders, the field strength as a function of radial position is

$$F_r = \frac{\Delta V}{r\ \ell n\ \frac{R_o}{R_i}} \tag{63}$$

and

$$\frac{dF_r}{dr} = -\ \frac{\Delta V}{\ell n\ \frac{R_o}{R_i}} \cdot \frac{1}{r^2}. \tag{64}$$

Substituting Equations (63) and (64) into Equation (62), the expression for the net flux in the r direction takes the form

$$N_{AR} = - D_{AB} \frac{dC}{dr} - \frac{D_{AB}(\Delta V)^2 \alpha_p}{\nu KT \, \ell n^2 (R_o/R_i)} \cdot \frac{C}{r^3}. \qquad (65)$$

Equation (65) is then simplified to

$$N_{AR} = - D_{AB} \left(\frac{dC}{dr} + \beta \frac{C}{r^3} \right) \qquad (66)$$

by letting

$$\beta = \frac{(\Delta V)^2 \alpha_p}{\nu KT \, \ell n^2 \, R_o/R_i}. \qquad (67)$$

The left-hand side of Equation (52) then becomes

$$\frac{1}{r} \frac{\partial}{\partial r}(r \, N_{Ar}) = -D_{AB} \left[\frac{\partial^2 C}{\partial r^2} + \frac{1}{r} \frac{\partial C}{\partial r} - \frac{2\beta C}{r^4} + \frac{\beta}{r^3} \frac{\partial C}{\partial r} \right]. \qquad (68)$$

The flux of polyelectrolyte in the z direction, N_{Az}, is due to mass flow in the z direction and is

$$N_{Az} = CV_z. \qquad (69)$$

Since the velocity in the z direction is a function of radial position only, the right-hand side of Equation (52) may be written

$$- \frac{\partial N_{Az}}{\partial z} = - V_z \frac{\partial C}{\partial z}. \qquad (70)$$

Equating Equation (68) and Equation (70) yields

$$V_z \frac{\partial C}{\partial z} = D_{AB} \left[\frac{\partial^2 C}{\partial r^2} + \left(\frac{1}{r} + \frac{\beta}{r^3} \right) \frac{\partial C}{\partial r} - \frac{2\beta}{r^4} C \right], \qquad (71)$$

which is the differential equation describing the concentration as a function of radial position and length in the cell. Equation (71) is separable but application of this technique did not render it soluble. The first simplification employed in solving Equation (71) is the assumption that

$$\frac{\partial C}{\partial z} \equiv K. \qquad (72)$$

This substitution reduces it to a second order differential equation in r only. Letting

$$y = r/R_i \qquad (73)$$

and making use of Equation (72), the dimensionless form of Equation (71) is

$$KV_z = \frac{D_{AB}}{R_i^2}\left[\frac{d^2C}{dy^2} + \left(\frac{1}{y} + \frac{\beta}{R_i^2 y^3}\right)\frac{dC}{dy} - \frac{2\beta C}{R_i^2 y^4}\right]. \qquad (74)$$

An irregular singular point at r = 0 in Equation (71) has now been shifted to y = 1. The singularity may be removed, facilitating a series solution, by changing the variable y with the substitution

$$s = \frac{1}{y^2}. \qquad (75)$$

In terms of the new variable s

$$\frac{dC}{dy} = -\ 2s^{3/2}\ \frac{dC}{ds} \qquad (76)$$

and

$$\frac{d^2C}{dy^2} = 4s^3 \frac{d^2C}{ds^2} + 6s^2 + \frac{dC}{ds}. \qquad (77)$$

Substituting Equations (75), (76), and (77) into Equation (74), reduces it, after simplification, to

$$\frac{d^2C}{ds^2} + \left(\frac{1}{s} - \frac{\beta}{2R_i^2}\right)\frac{dC}{ds} - \frac{\beta C}{2R_i^2 s} = \frac{R_i^2 K}{D_{AB}} V_z. \qquad (78)$$

The velocity, V_z, is that defined by Equation (50), expressed in its dimensional form. Equation (50) may be inserted into Equation (78) in terms of the dimensionless profile if the coefficient of V_z in Equation (78) is multiplied (1/4)A, where A is defined by Equation (31). The terms in Equation (50) can be rearranged to

$$V_z^* = c_{11}\, y^2 \ln y + c_{22} \ln y + c_{33}\, y^2 + c_{44} \qquad (79)$$

where

$$c_{11} = \frac{1}{\ln \kappa}$$

$$c_{22} = \left[\frac{T'(\kappa^2 - 1)}{\ln \kappa} - \left(\frac{\kappa^2}{\ln \kappa} + \frac{1 - \kappa^2}{\ln^2 \kappa}\right)\right]$$

$$c_{33} = \left(-T' - \frac{1}{\ln \kappa}\right)$$

$$c_{44} = -c_3 = \left(T' + \frac{1}{\ln \kappa}\right)$$

and

$$T' = \frac{-\kappa^4 + \frac{1}{\ell n\ \kappa}(1.75\kappa^4 - \kappa^2 - 3/4) - \frac{1}{\ell n^2\ \kappa}(\kappa^2 - 1)^2}{1 - \kappa^4 + \frac{1}{\ell n\ \kappa}(\kappa^2 - 1)^2}.$$

Letting

$$\beta' = \frac{\beta}{2R_i^2}, \tag{80}$$

multiplying c_{11}, c_{22}, c_{33}, and c_{44} by the factor $\frac{R_i^2 KA}{4D_{AB}}$, denoting them as c_1', c_2', c_3', c_4', respectively, and transforming Equation (79) into terms in s, Equation (78) may be written as

$$\frac{d^2C}{ds^2} + \left(\frac{1}{s} - \beta'\right)\frac{dC}{ds} - \frac{\beta' C}{s} = -\frac{c_1'}{2s}\ell n\ s - \frac{c_2'}{2}\ell n\ s + \frac{c_3'}{s} + c_4'. \tag{81}$$

It is interesting to note that the term, β', in Equation (81) is just the exponential portion of Equation (8) applied to a polyelectrolyte and evaluated at the inner cylinder. This similarity leads one to suspect that the general solution to Equation (81) may be some combination of exponential functions. The boundary conditions on the concentration distribution, in terms of r, are

$$N_{AR} = -D_{AB}\left(\frac{dC}{dr} + \beta\frac{C}{r^3}\right) = 0;\ \text{at } r = R_i \text{ and } r = R_o. \tag{82}$$

In terms of y they become

$$\frac{dC}{ds} = \frac{\beta C}{R_i^2 y^3};\ \text{at } y = 1 \text{ and } y = \kappa, \tag{83}$$

and in terms of s they are further transformed to

$$\frac{dC}{ds} = \frac{\beta}{2R_i^2} C = \beta' C; \quad \text{at } s = 1 \text{ and } s = \kappa^{-2} \tag{84}$$

The general procedure for solving Equation (81) is to first set the right-hand side of the equation equal to zero and obtain a complimentary solution by the series method of Frobenius. The particular solution may then be obtained by the method of undetermined coefficients. The solution by this method is given in Appendix III. A simpler technique, suggested by Frame,[14] involves inserting an appropriate substitution into Equation (81). This reduces the problem to the solution of two first order differential equations. As both procedures yield the same result, the latter is presented here. A new variable, ϕ, is introduced, where

$$\phi = \frac{dC}{ds} - \beta' C, \tag{85}$$

and

$$\frac{d\phi}{ds} = \frac{d^2C}{ds^2} - \beta' \frac{dC}{ds}. \tag{86}$$

Substituting Equations (85) and (86) into Equation (81), it is reduced to

$$\frac{d\phi}{ds} + \frac{1}{s}\phi = -\frac{c_1'}{2s}\ln s - \frac{c_2'}{s}\ln s + \frac{c_3'}{s} + c_4', \tag{87}$$

with the boundary condition

$$\phi = 0; \text{ at } s = 1. \tag{88}$$

The problem is now reduced to that of a first order differential equation with a variable coefficient and is readily soluble by the methods of elementary differential equations. The complimentary solution, ϕ_c, to Equation (87) is obtained by setting the right-hand side of the equation equal to zero, and solving the left side. Thus,

$$\frac{d\phi_c}{ds} + \frac{1}{s}\phi_c = 0, \tag{89}$$

or

$$\frac{d\phi_c}{\phi c} = -\frac{ds}{s}, \tag{90}$$

which yields on integration

$$\ell n\ \phi_c = -\ell n\ s + c_5 \tag{91}$$

where

c_5 = constant of integration.

Simplification of Equation (91) gives

$$\phi_c = \frac{c_5}{s}. \tag{92}$$

The calculations of Appendix III lead to the assumption of a particular solution for Equation (87) of the form

$$\phi_p = A\ s\ \ell n\ s + B\ \ell n\ s + Cs + D \tag{93}$$

where

A,B,C,D, = arbitrary constants to be evaluated by the method of undermined coefficients.

The values of the coefficients are found by putting the assumed solution, Equation (93), into the differential equation, Equation (87), and equating coefficients of like terms in s. The manipulation is straightforward, the results being

$$A = -\frac{c'_2}{4}$$

$$B = -\frac{c'_1}{2}$$

$$C = \frac{c'_4}{2} + \frac{c'_2}{8}$$

and $$D = c'_3 + \frac{c'_1}{2} .$$

Thus the particular solution is

$$\phi_p = \frac{c'_2}{4} s \,\ell n\, s - \frac{c'_1}{2} \ell n\, s + \left(\frac{c'_4}{2} + \frac{c'_2}{8}\right) s + \left(c'_3 + \frac{c'_1}{2}\right) , \quad (94)$$

and the total solution, ϕ, by linear combination of solutions, is

$$\phi = \phi_c + \phi_p = \frac{c_5}{s} - \left[\frac{c'_2}{4} s \,\ell n\, s + \frac{c'_1}{2} \ell n\, s - \frac{c'_4}{2} + \frac{c'_2}{8} \quad s - \quad c'_3 + \frac{c'_1}{2}\right]. \quad (95)$$

The constant of integration, c_5, is determined by applying the boundary condition, Equation (88),

$$c_5 = -\left(\frac{c'_4}{2} + \frac{c'_2}{8}\right) - \left(c'_3 + \frac{c'_1}{2}\right) . \quad (96)$$

The expressions for c_5 and ϕ as a function of concentration, Equation (85), are then reintroduced into

Equation (95) giving

$$\frac{dC}{ds} - \beta'C = -\frac{1}{s}\left(\frac{c_4'}{2} + \frac{c_2'}{8} + c_3' + \frac{c_1'}{2}\right) - \left[\frac{c_2'}{4}\, s\, \ell n\, s + \frac{c_1'}{2}\, \ell n\, s - \left(\frac{c_4'}{2} + \frac{c_2'}{8}\right) s - \left(c_3' + \frac{c_1'}{2}\right)\right]. \qquad (97)$$

Equation (97) is seen to have an integrating factor,

$$e^{-\beta' s}. \qquad (98)$$

Letting the right side of Equation (97) again be called ϕ, and multiplying both sides by the integrating factor, Equation (97) reduces to

$$\frac{d}{ds}\left(e^{-\beta' s} C\right) = e^{-\beta' s}\, \phi, \qquad (99)$$

which yields

$$C = e^{\beta' s}\left[\int e^{-\beta' s} \phi\, ds + c_6\right] \qquad (100)$$

where

c_6 = a constant of integration.

The function

$$\int e^{-\beta' s} \phi\, ds, \qquad (101)$$

in terms of s is

$$- \left\{\left(\frac{c_4'}{2} + \frac{c_2'}{8} + c_3' + \frac{c_1'}{2}\right)\int \frac{e^{-\beta' s}}{s}\, ds\right\} - \left\{\frac{c_2'}{4}\int e^{-\beta' s}\, s\, \ell n\, s\, ds\right\}$$
$$- \left\{\frac{c_1'}{2}\int e^{-\beta' s}\, \ell n\, s\, ds\right\} + \left\{\left(\frac{c_4'}{2} + \frac{c_2'}{8}\right)\int e^{-\beta' s}\, s\, ds\right\}$$
$$+ \left\{\left(c_3' + \frac{c_1'}{2}\right)\int e^{-\beta' s}\, ds\right\}. \qquad (102)$$

The bracketed terms in Equation (102) are labeled Γ_1, Γ_2, Γ_3, Γ_4, and Γ_5 respectively and are evaluated separately. The results of these integrations are:

$$\Gamma_1 = - \left(\frac{c_4'}{2} + \frac{c_2'}{8} + c_3' + \frac{c_1'}{2} \right) \left[\ln s + \sum_1^{\infty} \frac{(-1)^n \, (\beta')^n \, s^n}{n \cdot n!} \right] \quad (103)$$

where

n = summation index

$$\Gamma_2 = \frac{c_2'}{4(\beta')^2} \left\{ \ln s \left[e^{-\beta' s} \, (\beta' s + 1) \right] + e^{-\beta' s} - \left[\ln s + \sum_1^{\infty} \frac{(-1)^n \, (\beta')^n \, s^n}{n \cdot n!} \right] \right\}$$

$$\Gamma_3 = \frac{c_1'}{2\beta'} \left\{ e^{-\beta' s} \ln s - \left[\ln s + \sum_1^{\infty} \frac{(-1)^n \, (\beta')^n \, s^n}{n \cdot n!} \right] \right\}$$

$$\Gamma_4 = - \left(\frac{c_4'}{2} + \frac{c_2'}{8} \right) \frac{e^{-\beta' s}}{(\beta')^2} \, (\beta' s + 1)$$

and

$$\Gamma_5 = - \frac{1}{\beta'} \left(c_3' + \frac{c_1'}{2} \right) e^{-\beta' s}$$

The relations; Γ_1, Γ_2, Γ_3, Γ_4, and Γ_5, are inserted into Equation (100). The right-hand side of Equation (100), after multiplication by $e^{\beta' s}$ and combination of terms with like powers of s, is

$$C=c_6e^{\beta's}-\left(\frac{c_4'}{2}+\frac{c_2'}{8}+c_3'+\frac{c_1'}{2}+\frac{c_2'}{4(\beta')^2}+\frac{c_1'}{2\beta'}\right)e^{\beta's}\left[\ell n\ s+\sum_1^\infty\frac{(-1)^n(\beta')^n s^n}{n\cdot n!}\right]$$

$$+\frac{c_2'}{4\beta'}\ s\ \ell n\ s+\left(\frac{c_2'}{4(\beta')^2}+\frac{c_1'}{2\beta'}\right)\ell n\ s-\left(\frac{c_4'}{2\beta'}+\frac{c_2'}{8\beta'}\right)s-\left(\frac{c_3'}{\beta'}+\frac{c_1'}{2\beta'}+\frac{c_4'}{2(\beta')^2}-\frac{c_2'}{8(\beta')^2}\right). \tag{104}$$

In order to evaluate c_6, the boundary condition at the wall must be examined. The flux at each wall is zero, thus the net driving force at each surface must also be zero. It will be shown that if the driving force at the outside wall is zero, the radial concentration gradient evaluated at the outside wall is also very close to zero. Modification of Equation (56) relates the concentration gradient to the known variables for a given experimental situation. The defining relationship, evaluated at $r = R_o$, is

$$\left.\frac{N\alpha_p(\Delta V)^2}{\nu r^3\ \ell n^2\ R_o/R_i}\right|_{r\,=\,R_o} = \left.\frac{RT}{C}\frac{dC}{dr}\right|_{r\,=\,R_o}, \tag{105}$$

where, for a typical experimental run,

$\Delta V = 100$ volts $= 0.333$ e.s.u.

$\alpha_p = 0.6 \times 10^{-13}$ cm.^{3}

$\ell n^2\ R_o/R_i = 12.8$

$r^3|R_o = 0.0118$ cm.^{3}

$C = 0.01$ gm./ℓ.

$T = 300^{o}K.$

$\nu = 2,350$

The concentration gradient at the wall obtained from using the above values for the variables is about 10^{-4} gm./ℓ./cm. Comparing the gradient at the wire to that at the wall shows that for the above geometry the value at the wire is about 46,000 times that at the wall and essentially is independent of all the variables except R_i and R_o. This justifies assuming that

$$\left.\frac{dC}{dr}\right|_{r = R_o} \simeq 0, \qquad (106)$$

which transformed into the s coordinate is

$$\left.\frac{dC}{ds}\right|_{s = \kappa^{-2}} \simeq 0. \qquad (107)$$

The constants in Equation (104) are redefined by

$$C = c_6 e^{\beta' s} - A_1' e^{\beta' s}\left[\ln s + \sum_{1}^{\infty} \frac{(-1)^n \; (\beta')^n \; s^n}{n \cdot n!}\right] + A_2' s \ln s$$

$$+ A_3' \ln s - A_4' s - A_5' \qquad (108)$$

where

$$A_1' = \frac{c_4'}{2} + \frac{c_2'}{8} + c_3' + \frac{c_1'}{2} + \frac{c_2'}{4(\beta')^2} + \frac{c_1'}{2\beta'}$$

$$A_2' = \frac{c_2'}{4\beta'}$$

$$A_3' = \frac{c_2'}{4(\beta')^2} + \frac{c_1'}{2\beta'}$$

$$A_4 = \frac{c_4'}{2\beta'} + \frac{c_2'}{8\beta'}$$

and

$$A_5' = \frac{c_3'}{\beta'} + \frac{c_1'}{2\beta'} + \frac{c_4'}{2(\beta')^2} - \frac{c_2'}{8(\beta')^2} .$$

Applying the boundary condition, Equation (107), to Equation (108) yields

$$c_6 = \frac{A_1'\kappa^2 e^{\frac{2\beta'}{\kappa^2}} + A_1'\beta' e^{\frac{\beta'}{\kappa^2}}\left[-2\,\ell n\,\kappa + \sum_1^\infty \frac{(-1)^n\,(\beta')^n}{n \cdot n!\,\kappa^{2n}}\right]}{\beta' e^{\frac{\beta'}{\kappa^2}}} +$$

$$\frac{-A_2'\,(1 - 2\,\ell n\,\kappa) - \kappa^2 A_3' + A_4'}{\beta' e^{\frac{\beta'}{\kappa^2}}}. \qquad (109)$$

Inspection of Equations (108) and (109) shows that very term includes one of the prime constants; A_1', A_2', A_3', $'_4$, or A_5', and that every term in these constants contains ither c_1', c_2', c_3', or c_4'. The primes on these constants signify that each term in Equations (108) and (109) is multiplied the factor $\frac{R_i^2\ KA}{4D_{AB}}$. Dividing both sides of Equation (108) this group defines a dimensionless concentration,

$$C^* = \frac{4CD_{AB}}{R_i^2\ KA} \qquad (110)$$

d returns c_1', c_2', c_3', and c_4' to the constants c_{11}, c_{22},

c_{33}, and c_{44} respectively, defined by Equation (79). Equation (108) in terms of C* takes the form

$$C^* = c_6 e^{\beta' s} - A_1 e^{\beta' s}\left[\ell n\ s + \sum_1^\infty \frac{(-1)^n\ (\beta')^n\ s^n}{n \cdot n!}\right] + A_2\ s\ \ell n\ s + A_3\ \ell n\ s - A_4 s - A_5 \qquad (111)$$

where

$$c_6 = \frac{A_1 \kappa^2 e^{\frac{2\beta'}{\kappa^2}} + A_1 \beta' e^{\frac{\beta'}{\kappa^2}}\left[-2\ \ell n\ \kappa + \sum_1^\infty \frac{(-1)^n\ (\beta')^n}{n \cdot n! \kappa^{2n}}\right]}{\beta' e^{\frac{\beta'}{\kappa^2}}} + \frac{-A_2\ (1 - \ell n\ \kappa) - \kappa^2 A_3 + A_4}{\beta' e^{\frac{\beta'}{\kappa^2}}}$$

nd

$$A_1 = \frac{c_{44}}{2} + \frac{c_{22}}{8} + c_{33} + \frac{c_{11}}{2} + \frac{c_{22}}{4(\beta')^2} + \frac{c_{11}}{2\beta'}$$

$$A_2 = \frac{c_{22}}{4\beta'}$$

$$A_3 = \frac{c_{22}}{2(\beta')^2} + \frac{c_{11}}{2\beta'}$$

$$A_4 = \frac{c_{44}}{2\beta'} + \frac{c_{22}}{8\beta'}$$

$$A_5 = \frac{c_{33}}{\beta'} + \frac{c_{11}}{2\beta'} + \frac{c_{44}}{2(\beta')^2} - \frac{c_{22}}{8(\beta')^2}$$

A Fortran computer program for Equation (111) was developed and run on a Control Data 3600 computer. The program, shown in Appendix IV, yielded values of C* as a function of y for various values of the parameters β' and κ. The shape of the dimensionless concentration profile, shown in Figure 9, shows an extremely large concentration gradient for very small radii. This is to be expected as the electrical portion of the driving force is inversely proportional to r^3. The variation of the radial concentration ratio, C^*_i/C^*_o, with β' at several values of κ is shown in Figure 10.

The equilibrium top and bottom reservoir concentrations are found by relating C* to the length variable z, and evaluating z at L, the length of the separation cell. From he relation

$$K = \frac{dC}{dz} \tag{72}$$

ith the condition that

$$\text{at } z = 0,\ C = C_B,$$

e constant K is defined as

$$K = \frac{C - C_B}{z}. \tag{112}$$

bstituting Equation (112) into Equation (110) and rearrang-
g yields

$$\frac{C}{C_B} = \frac{C^*}{C^* - 0' \ell n\ \kappa\ (z)}, \tag{113}$$

re

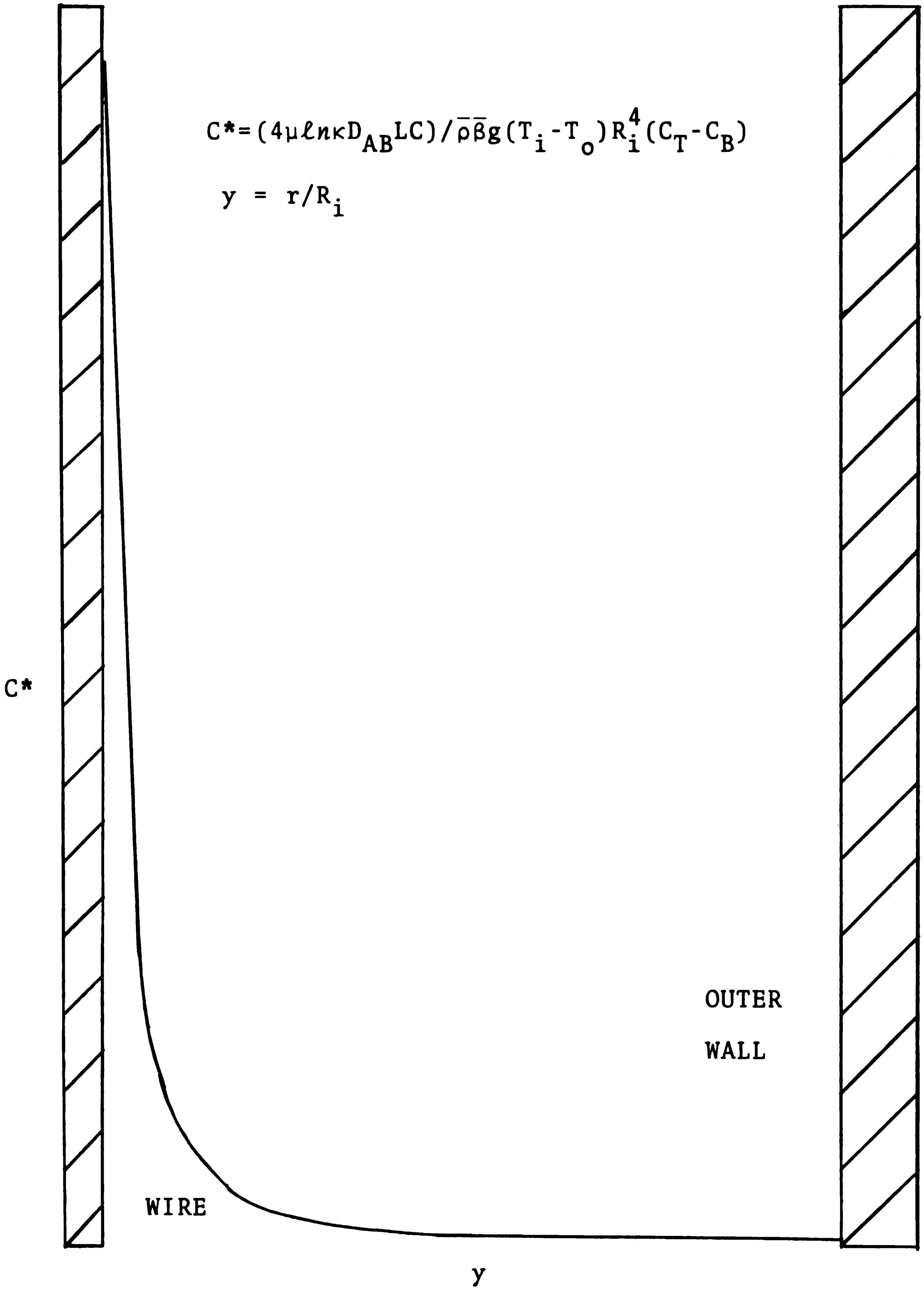

Figure 9. Variation of the dimensionless concentration, C*, with y.

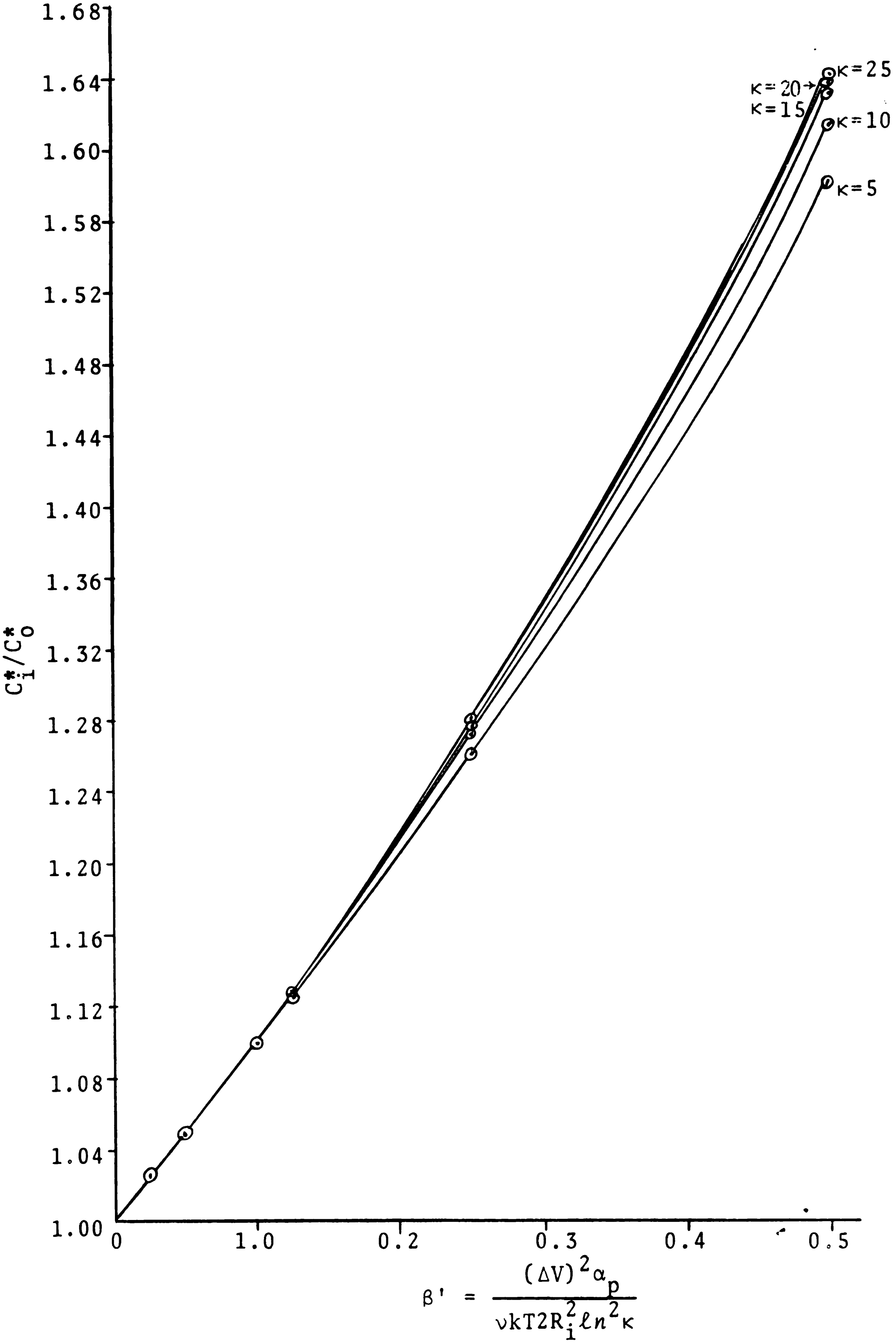

Figure 10. Variation of the radial concentration ratio, C_i^*/C_o^* with β' for various values of κ.

$$0' = \frac{4D_{AB}\mu}{R_i^4 \Delta T \bar{\rho} \bar{\beta} g}. \tag{114}$$

Equation (113) is seen to be the relationship between the concentration, C, at some point in the cell relative to the concentration in the bottom reservoir as a function of vertical position in the cell. The separation factor, C_T/C_B, is obtained from evaluating Equation (113) at z = L, as

$$\frac{C_T}{C_B} = \frac{C^*}{C^* - 0' \; \ell n \; \kappa \; (L)}. \tag{115}$$

Separation factors were obtained as functions of κ, β', and L from the computer program shown in Appendix IV-A. The variation of separation factor with length at a constant κ for several values of β' is shown in Figure 11. The effect of length on separation factor for several values of κ at a constant value of β' is shown in Figure 12. Figure 13 shows the effect of κ on separation factor for several values of β'. For a discussion of these curves the reader is referred to page 76.

The expressions for the dimensionless velocity and concentration profiles may be expressed in terms of dimensionless groups. For the velocity expression,

$$V^* = \frac{4\mu \; \ell n \; \kappa \; V_z}{\bar{\rho} \bar{\beta} g R_i^2 \Delta T} = 16 \frac{Re}{Gr} \; \ell n \; \kappa \tag{116}$$

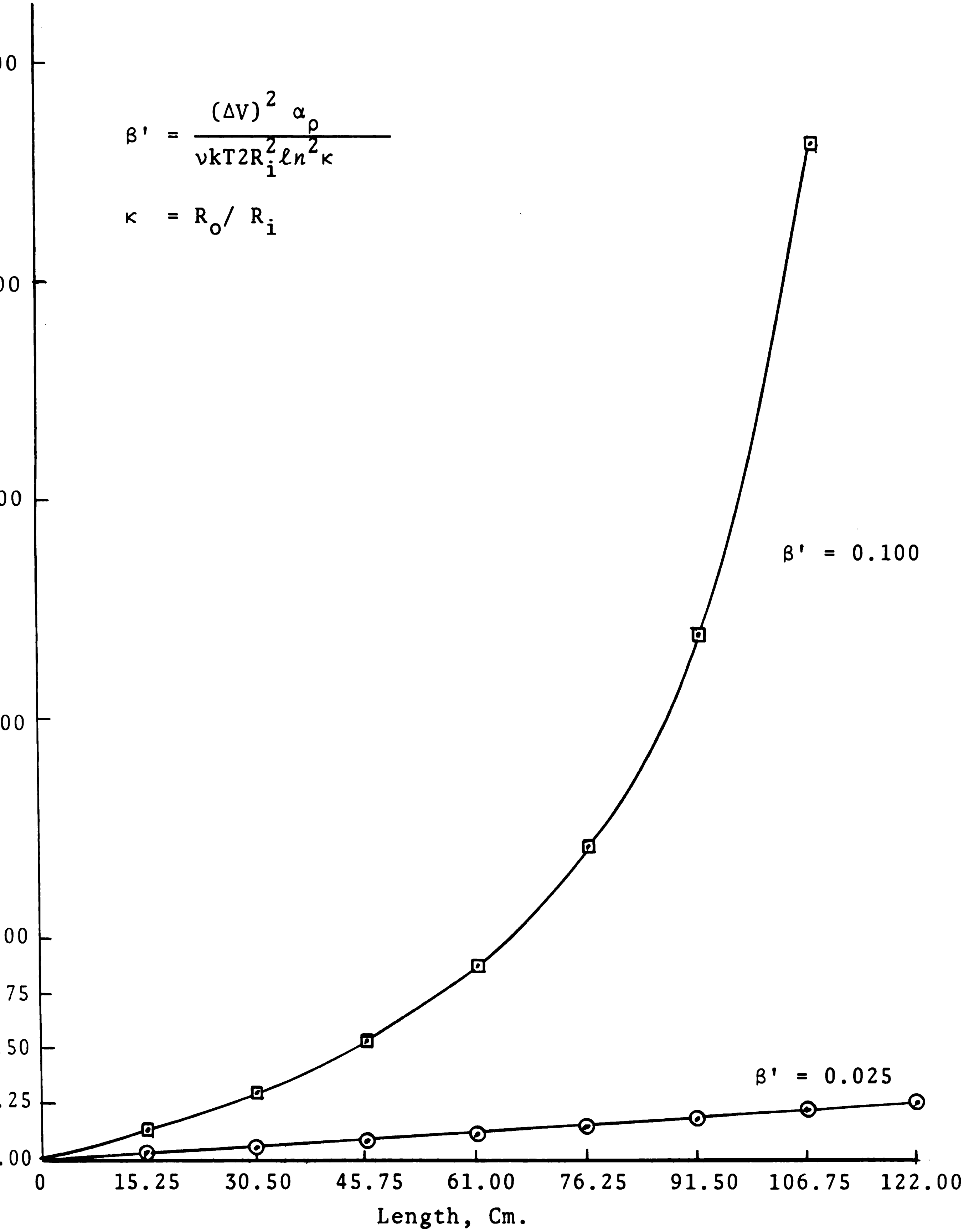

igure 11. Variation of the separation factor with L at κ = 35 for several values of β'.

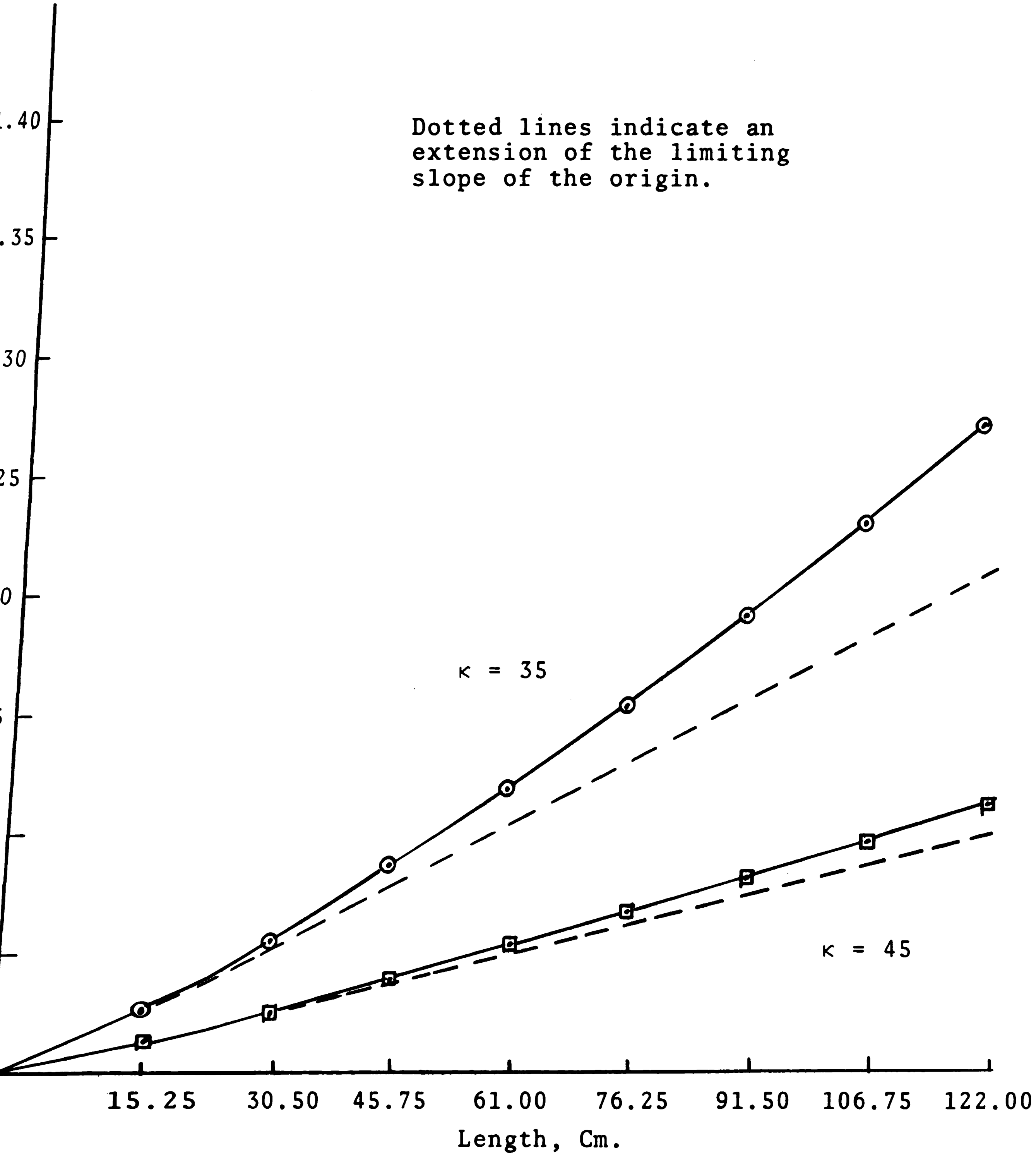

12. Variation of separation factor with L at β' = 0.025 for several values of κ.

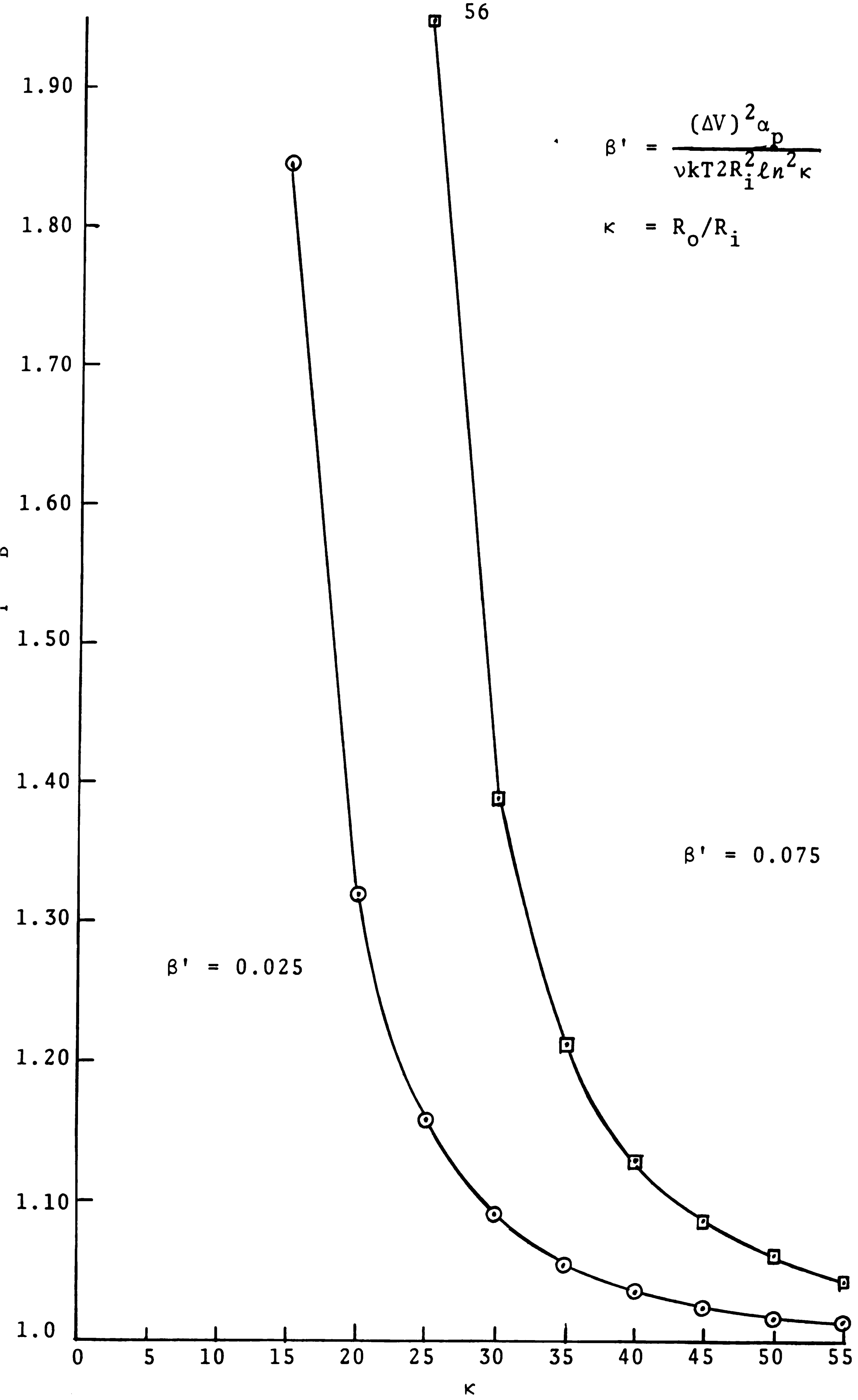

Figure 13. Variation of the separation factor with κ at L = 30.5 cm. for several values of β'.

where

Re = Reynolds number

Gr = Grashof number.

The concentration expression is

$$C^* = \frac{4L\ D_{AB}\mu\ \ell n\ \kappa\ C}{R_i^2\ (C_T - C_B)\ \bar{\rho}\bar{\beta}g\Delta T} = 64\ \frac{L/D}{(Gr)(Sc)}\ \frac{C\ \ell n\ \kappa}{C_T - C_B}. \qquad (117)$$

where

L/D - the length to diameter ratio

Sc = Schmidt number.

EXPERIMENTAL METHOD

Apparatus

Experimental measurement of the dielectrophoretic separations was accomplished with a coaxial tube and wire separation cell. A schematic diagram of the separation cell is shown in Figure 14. Two cells of this same general design were used in the experimental program.

The first cell was constructed of Type 304 Stainless Steel. The tube, or working portion of the cell, was made from 0.25 inch O.D. tubing with 0.035 inch walls and was 12 inches long. It was equipped with an electrical connection, spot-welded equidistant from the ends of the tube. Teflon sleeves, which screwed onto the tube, insulated the working portion of the cell from the reservoirs. The central wire was 0.005 inch diameter platinum wire. The wire was fastened with a plug at the bottom of the cell and was attached to a spring loaded clamp, equipped with an electrical lead, at the top of the cell. The reservoirs were made of 0.875 inch O.D. stainless tubing with 0.156 inch walls and were 2 inches long. They also were equipped with electrical connections. Caps, made from 1.5 inch diameter extruded teflon rod covered both bottom and top reservoirs. Extreme care was taken to ensure that the holes drilled in the caps

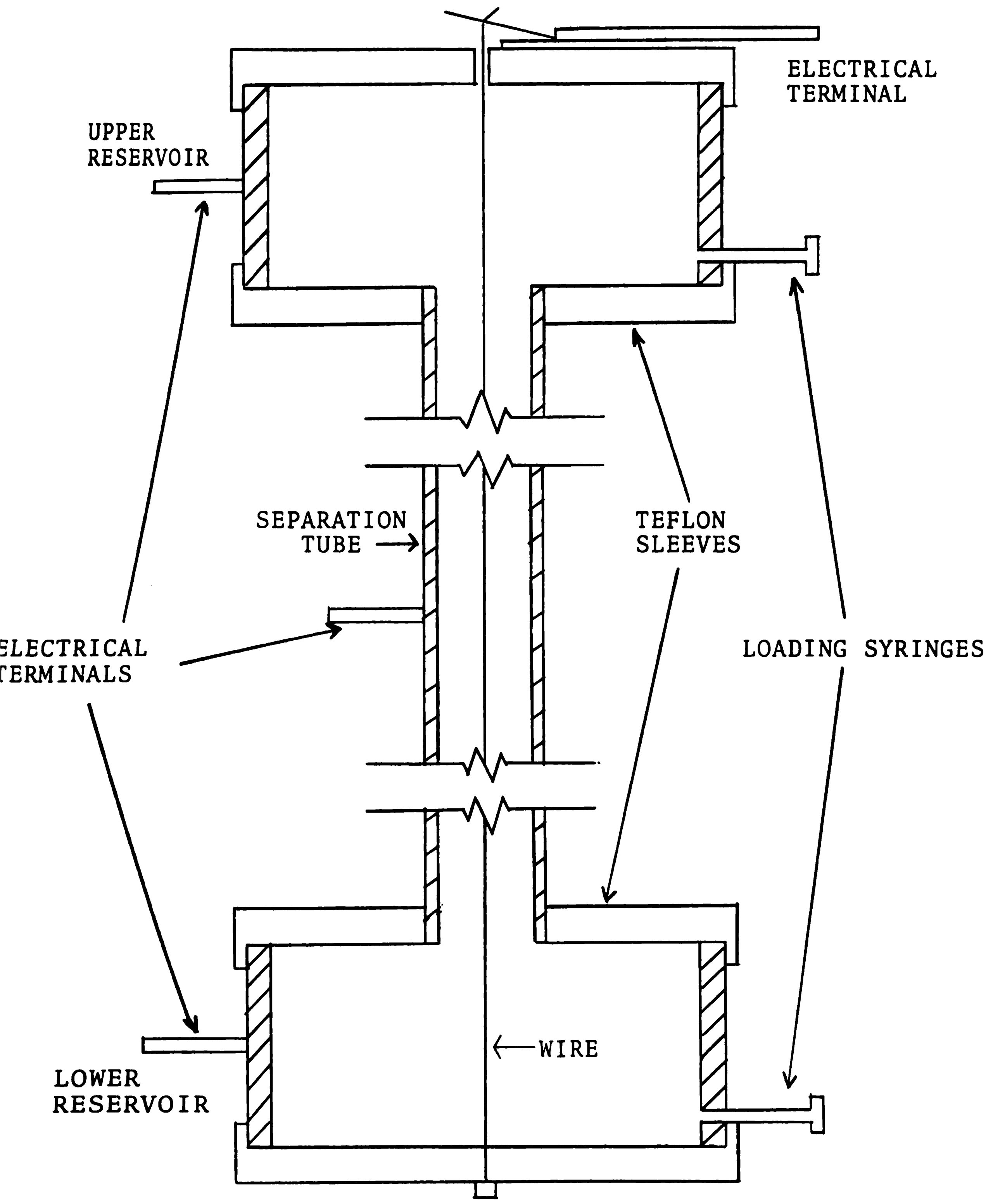

ure 14. Schematic diagram of dielectrophoresis cell.

enabled accurate positioning of the wire in the center of the working tube. The cap at the top of cell I was threaded such that there was a space of 0.5 inches from the top of the reservoir to the bottom of the cap. This ensured that when the cell was filled, the liquid level was always above the metal reservoir, enabling both the upper and lower reservoirs to be used as conductivity cells. Both reservoirs were fitted with capped hypodermic needles, located at the bottom of the reservoir, for loading and sampling.

Data taken using cell I indicated that the polymer degraded in the cell. This was eliminated by the use of a second cell made of tantalum. Cell II was of the same general design as cell I with the following modifications. The separation tube was 0.25 inch O.D. seamless tantalum tubing with 0.020 inch walls and was 24 inches long. The small wall thickness prohibited the use of screw connections to the teflon sleeves. Slip fittings were used to make these onnections. This required that the teflon be machined to it tightly over the tantalum tubing. Minute irregularities n the surface of the tantalum caused the connections to leak hen the apparatus was full. This was eliminated by sealing he connections with high vacuum stopcock grease. The reser- irs, also tantalum, were made of 0.75 inch O.D. tubing with e same wire, filling syringes, electrical connections, and re clamps as were used in cell I.

Both cells could be modified with a forced feed system and capillary device. This enabled the collection of solution which was close to the wire. A glass capillary tube was inserted into a thin teflon disc. This was placed between the top reservoir and the separation tube. In this position, the wire was coaxial with the capillary tube. The forced feed system consisted of a piece of tygon tubing connected to the bottom hypodermic needle. The tubing was L shaped so that the open end of the tubing was above the top of the capillary tube. Feed could then be introduced into the cell by controlled addition of polymer solution at the open end of the tygon tubing. This forced the solution close to the wire through the capillary tube and into the (previously empty) top reservoir.

Electrical System

A schematic diagram of the electrical apparatus used o produce the electric field is shown in Figure 15. The lectrical equipment consisted of two parts; (a) the circuit equired to produce a potential difference across the wire d tube of the separation cell, and (b) the circuit necessary measure the solution resistance in the cell reservoirs durg an experimental run.

The applied voltage to the experimental cell was duced by amplification of the output signal of a Hewlettkard, model 200 C.D., wide range oscillator. A slide-wire

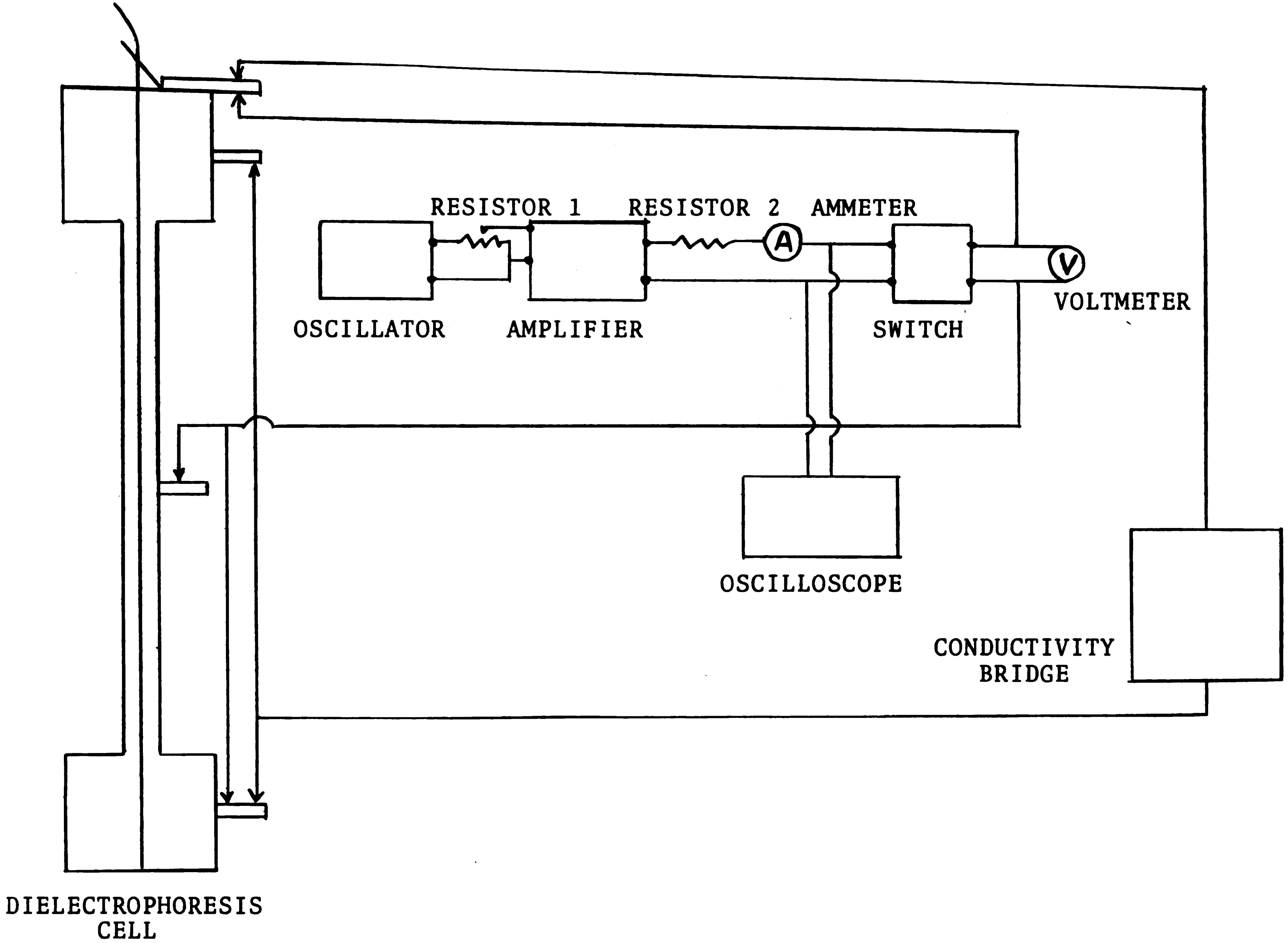

Figure 15. Schematic diagram of electrical system in relation to the dielectrophoresis cell.

resistor was placed in parallel between the output of the oscillator and the input terminals of a General Radio Company, model 1233-A, amplifier. This permitted very fine control of the input voltage to the amplifier. The amplifier output was connected to an "on-off" switch which controlled the input signal to the cell. A variable resistor in series with the amplifier output enabled accurate voltage control and current was measured with a Weston, model 425, milliammeter. Thus, with the switch "on", the amplifier output was applied to the separation cell, whereas the circuit could be broken, enabling resistance measurement of the solution in the reservoirs, without having to turn off the oscillator and amplifier.

The input voltage to the cell was measured with a Simpson, model 260, variable scale voltmeter at the output of the amplifier on the cell side of the switch. This gave an accurate measure of the voltage across the separation cell as the only sources of error were due to the resistances of the leads and electrical connections. Although the voltage loss due to dissipation in the leads and connections is extremely low compared to the voltage drop across the cell, care was taken to keep all connections corrosion free and the leads to the cell as short as possible. The input signal to the cell was monitored with a Dumont, model 304-H. cathode-ray oscilliscope in order to correct any fluctuations in the oscillator or amplifier outputs. Either a sine or square wave input to the cell could be obtained by varying the oscillator gain control.

The solution resistances in the top and bottom cell reservoirs were measured during an experimental run with an Industrial Instruments Inc. RC-18 conductivity bridge. During a conductivity measurement, the input voltage to the cell was turned "off" and each reservoir was used as a conductivity cell with the platinum wire serving as one electrode and the reservoir the other. This enabled the measurement of concentration changes without sampling the reservoirs.

For experimental runs in which natural convection controlled the solution flow, the input voltage to the experimental cell was also applied across the wire and lower reservoir. This was necessary to ensure that the solution in the bottom reservoir was warmer than the downflow from the separation tube, otherwise the downflow would not have entered the lower reservoir.

Synthesis of Polymethacrylic Acid

Polymethacrylic acid was prepared from a free radical polymerization of the monomer, methacrylic acid, obtained from Eastman Organic Chemical Company. The monomer was vacuum distilled to remove the inhibitor and 100 gm. of the product were charged to a 2 ℓ. flask. Added to this were 300 ml. of Reagent Grade methanol, 300 ml. of distilled water, and varying amounts of benzoyl peroxide. The benzoyl peroxide is the initiator for the polymerization, and its concentration controls the average molecular weight of the polymer product. For product molecular weights of about one million, about 0.2 gm. of initiator is required. The reaction mixture was stirred by bubbling nitrogen through the system and was maintained at 70° C. by immersing the reaction vessel in a constant temperature bath. The reaction proceeded for about four hours when the appearance of a cloudy, viscous solution indicated completion.[60]

The swollen polymer product was dissolved in 1 ℓ. of methanol and was precipitated with 3 ℓ. of diethyl ether. This purification procedure was repeated several times to ensure the complete removal of monomer and catalyst. The polymer has the formula

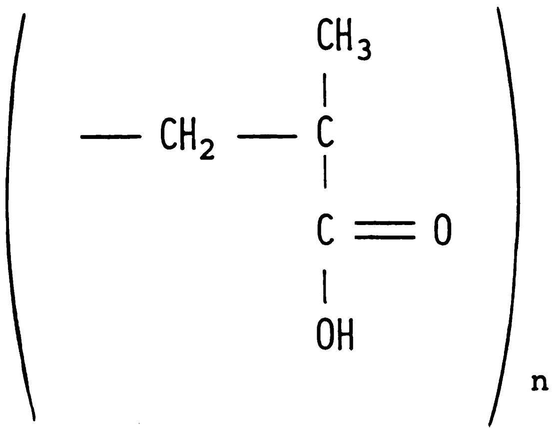

$$\left(\begin{array}{lll} & & CH_3 \\ & & | \\ -CH_2 & - & C \\ & & | \\ & & C=O \\ & & | \\ & & OH \end{array} \right)_n$$

where

n = the degree of polymerization.

The purified polymer was fractioned by the method of Flory.[12] The product was dissolved and then precipitated by drop-wise addition of diethyl ether to collect products of different molecular weights. The polymer fractions were dried under vacuum for 48 hours and then ground to a powder giving a yield of about 35 percent usable polymer.

Polymer molecular weights were determined viscometrically by the method of Katchalsky and Eisenberg.[29] Polymer of molecular weight 9.6 x 10^4 to 1.18 x 10^6 was obtained by this method of preparation.

Solution Preparation

Polymethacrylic acid is soluble in water. However, dissolution becomes increasingly difficult as the polymer molecular weight is increased. The experimental polymer solutions were prepared by adding a weighed amount of polymer powder to a 1 ℓ. volumetric flask. The contents were diluted with 500 ml. of triply de-ionized water with a conductivity of approximately 10^{-6} (ohm-cm.)$^{-1}$. To this was added the amount of sodium hydroxide necessary to obtain the desired degree of neutralization. The mixture was gently agitated ith a magnetic stirrer until all the polymer was dissolved. n the case of very high molecular weight polymer, this required several days. The concentration of the stock solution was 1.0 gm./ℓ. Prior to an experimental run, a solution of the desired concentration was prepared by dilution of the stock solution.

Radioactively tagged polymer solutions were prepared by addition of a known amount of $Na^{22}OH$ to the experimental solutions during their preparation from the stock material. In all cases the concentration of $Na^{22}OH$ was too low to significantly change the degree of neutralization of the polyion, yet was high enough to give reliable counting statistics.

The first tagged polymer solutions were prepared with radioactive sodium obtained from the Nuclear Chicago Corporation. In its initial form, the tracer was $NA^{33}Cl$ in 1 M. HCL with an activity of 10μc./ml. of solution. The tracer was carrier free (i.e., all of the sodium was radioactive). The $Na^{22}Cl$ was converted to $Na^{22}OH$ in H_2O by ion exchange of the original material and was diluted to the desired concentration.

A second batch of radioactive sodium was obtained from Volk Radio Chemical Company. The Na^{22} came as 200 μc. of $Na^{22}Cl$ in 1.0 ml. aqueous solution with a specific activity of 69 mc./mmole of total sodium in solution. Calculation showed that about 0.05 percent of the sodium is radioactive and the rest is carrier. The same preparation procedure as described above was used for this material.

Procedure for Experimental Run of Dielectrophoresis Cell

1) An aqueous polymethacrylic acid solution of the desired concentration and neutralization was prepared by dilution of the stock solution. For runs in which the concentration was to be determined by the solution activity, the volume of $Na^{22}OH$ solution added was included in the dilution volume.

2) The separation cell was rinsed several times with conductivity water and then twice with the polymer solution.

3) The cell was placed in a horizontal position with the syringe needles up. Polymer solution was injected into the bottom needle with a hypodermic syringe until solution flowed from the upper needle. Entrapped air was eliminated by forcing solution into the bottom needle while holding the cell at a 45^o angle from the horizontal. The procedure was then reversed using the top needle. This was continued until no air bubbles were seen in the overflow.

4) The loaded cell was weighed to check for evaporation losses later.

5) The cell was clamped to a ring stand. Care was taken to ensure vertical alignment of the separation tube.

6) The resistances in the top and bottom reservoirs as well as the separation tube were measured. This was primarily to ensure that the central wire was properly aligned so there was no short circuit.

7) The apparatus was placed in an incubator maintained at 10^{o} C., and the electrical leads were connected.

8) The resistance of the solution in the top and bottom reservoirs was measured until it was constant, indicating that the cell and its contents had come to temperature equilibrium.

9) The oscillator, amplifier, and oscilloscope were turned on and the desired frequency was set on the oscillator. With the conductivity bridge leads disconnected at the instrument, the switch was turned "on", applying an A.C. potential to the separation cell. The desired voltage or power was obtained by adjustment of the second variable resistor.

10) The resistance of the solution in the top and bottom reservoirs was measured as a function of time. This was accomplished by turning the switch "off" and rapidly measuring the resistances. The voltage was then reapplied to the cell, making sure that the conductivity bridge leads were disconnected. The resistances were measured with the bridge operating at 1000 cps.

11) After a run was completed, the cell was reweighed to ensure no loss of solution due to evaporation. When tagged polymer solutions were used, 10 ml. samples were withdrawn from the top and then the bottom cell reservoirs.

These were stored in plastic vials for further concentration measurement. The cell was then dismantled, thoroughly cleaned with a dilute HCl solution, rinsed several times with de-ionized water, reassembled, and filled with de-ionized water. The cell was then ready for the next run.

Determination of the Separation Factor

A measure of the separations obtained in the dielectrophoresis runs is given by the separation factor. This is defined as the ratio of top to bottom reservoir concentration. As is seen from the linearity of Figure 16, the reciprocal of the solution resistance may be used as a measure of its concentration. The separation factor is then, in terms of resistance,

$$\frac{C_T}{C_B} = \frac{R_B}{R_T} \; . \qquad (118)$$

Equation (118) implies that the reservoirs have the same cell constants. To eliminate any cell constant effects, the resistances in Equation (118) are divided by their initial values yielding

$$\frac{C_T/C_{iT}}{C_B/C_{iB}} = \frac{R_B/R_{iB}}{R_T/R_{iT}} \qquad (119\text{-a})$$

Noting that the initial concentration is the same in both reservoirs and subtracting "one" from both side of Equation (119), the concentration change may be written as

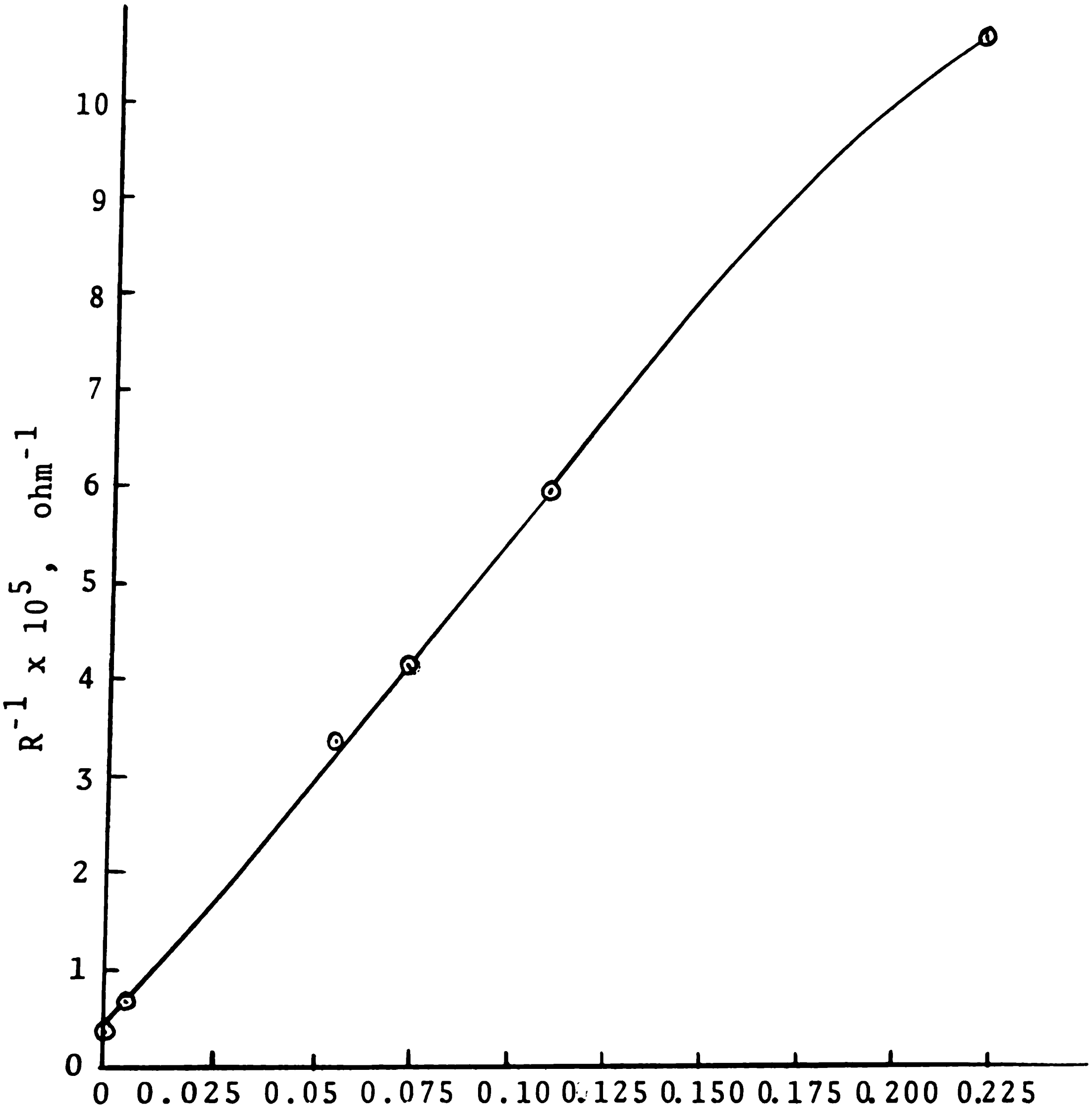

Figure 16. Variation of reciprocal resistance with concentration for polymethacrylic acid, molecular weight = 453,000, temperature = 25°C.

$$\frac{C_T - C_B}{C_B} = \frac{R_B/R_{iB} - R_T/R_{iT}}{R_T/R_{iT}} \tag{120}$$

The concentration change represented by Equation (120) is termed the fractional separation, and is the separation factor minus one. The percent separation is calculated from the experimental resistance data by substituting the appropriate measured resistance values into the right-hand side of Equation (120) and multiplying by 100. The determined values may then be plotted as a function of time.

For the runs made with tagged polymer, the Na^{22} activity in the top and bottom samples is a measure of the polymer concentration. The solution activity is determined as follows. Five ml. of each sample taken at the completion of a run, as well as five ml. of feed are measured into plastic scintillation bottles with a five ml. burrette. To each of these are added 20 ml. of scintillation liquid.* The number of radioactive counts per unit time is measured for each sample in a Packard Tri-Carb Liquid Scintillation Spectrophotemeter. The solution activity is directly proportional to the polymer concentration. Thus the separation factor is

$$\frac{C_T}{C_B} = \frac{\text{counts from top sample/unit time}}{\text{counts from bottom sample/unit time,}} \tag{119-b}$$

---

*The scintillation liquid was a mixture of 1.4 gm. P.P.O., 10.0 mg. P.O.P.O.P., 125 ml. anisole, 750 ml. p-dioxane, and 125 ml. 1,2 o-dimethoxyethane.

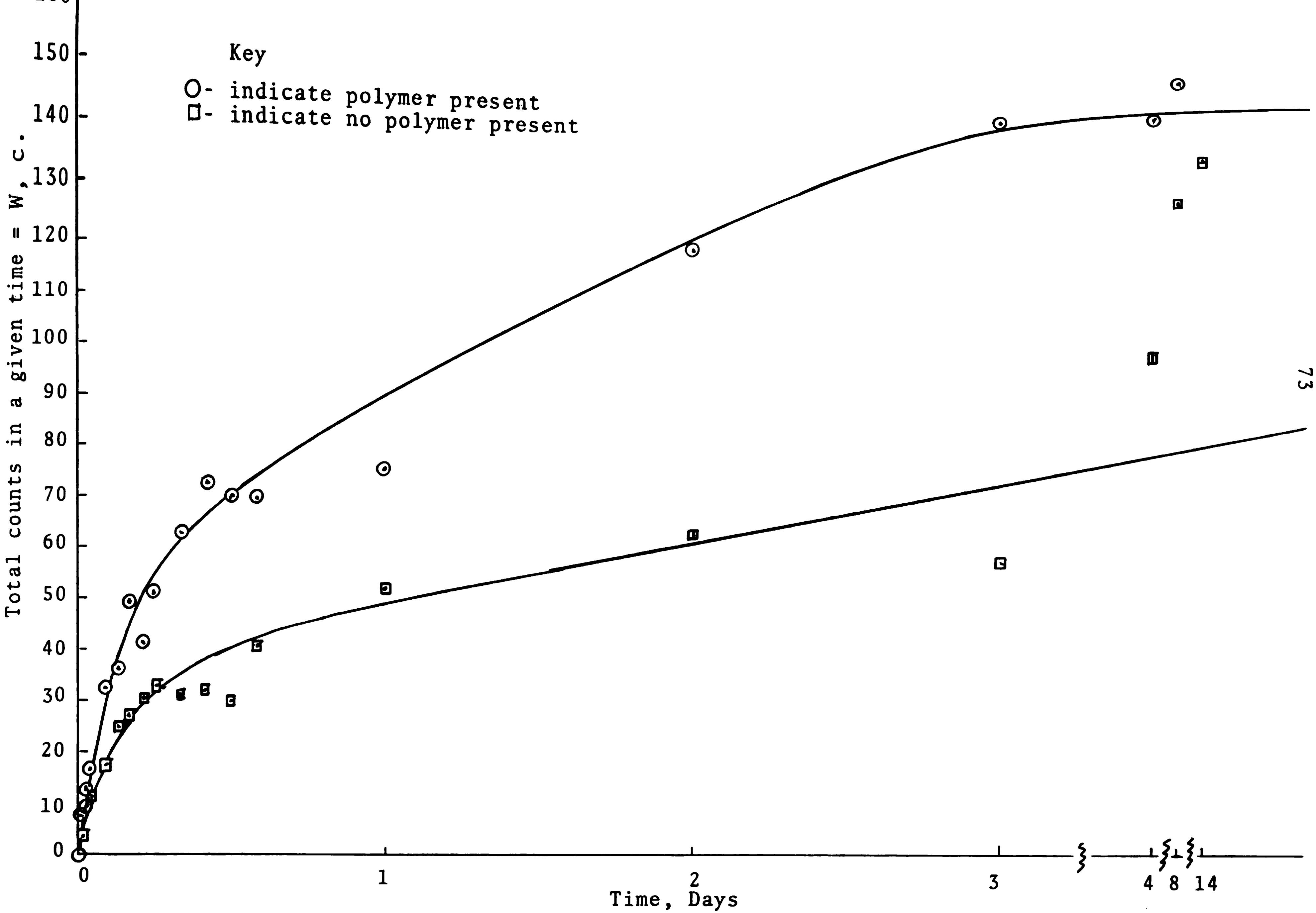

Figure 17. Variation of radioactivity in glass sample bottles with time.

and may be calculated by direct substitution of the values obtained from the scintillation counter.

The Isotopic Exchange Effect

Some of the first samples measured with the radioactive tracer technique were stored in glass sample bottles at the completion of the run. The feed sample had also been placed in a glass container, usually prior to the start of the run. Subsequent determination of the top, bottom, and feed activities invariably showed the feed to have the lowest value. This erroneously indicated that the feed was less concentrated than either the top or bottom products.

Investigation of this abnormality showed that the erroneous measurements were due to isotopic exchange of the Na^{22} with the Na in the glass sample bottles. Tests were run simultaneously in which one set of glass sample bottles was filled with $Na^{22}OH$ in H_2O and another identical set was filled with tagged polymer solution. The amount of radioactive sodium used was the same in both cases. The samples were allowed to stand for varying lengths of time after which each bottle was emptied and thoroughly rinsed with de-ionized water, methanol, and acetone. The sample bottles were then filled with scintillating liquid and counted. Figure 17 shows the variation of the bottle activity with time for both tests. Examination of Figure 17 shows not only that isotopic exchange occurs but also that the amount of exchange is greater for $Na^{22}OH$ in water than for the equivalent tagged polymer solution. Background counts were subtracted out of this data, and the counting time in each case was 150 minutes. The ratio of the corresponding values from the tests show that with no polymer present about 50 percent more isotopic exchange occurs than does for the tagged polymer. This indicates that some fraction of radioactive sodium is effectively bound to the polyion decreasing the amount of Na^{22} which is free in solution for isotopic exchange. A more elaborate investigation of this phenomena could possibly yield information about the nature and amount of counterion binding in very dilute solutions.

The erroneous measurements due to isotopic exchange were eliminated in later experiments by using plastic sample bottles.

RESULTS AND DISCUSSION

Theoretical

The equation describing the dimensionless concentration distribution for dielectrophoresis in a cylindrical geometry, Equation (111), is given on page 49. The variation of C* with radial position is shown in Figure 9. The extreme gradient, noted at very low values of y, is attributed to the inverse proportionality of the dielectrophoretic driving force to the cube of the inner cylinder radius. This suggests that the inner cylinder radius will seriously affect the magnitude of the radial concentration ratio and should be as small as possible.

Figure 10 shows the variation of the radial concentration ratio with the factor β' for several values of the cell constant, κ. The curves show a slightly greater than linear dependence of the concentration ratio on β'. It is seen that for values of β' less than 0.1 the concentration ratio is independent of κ. At larger values of β', the concentration ratio increases with increasing κ. The concentration ratios merge to a common curve for values of κ larger than 25. A comparison of the values obtained from Equation (111) to the values obtained from Swinkles and Sullivan's expression for the concentration ratio, Equation (8), is informative. Equation (8), applied to the system under consideration, is modified to

$$\frac{C_i^*}{C_o^*} = \exp \frac{\alpha_p(\Delta V)^2}{2\nu kT} \left(\frac{1}{\ell n^2 \frac{R_o}{R_i}}\right)\left(\frac{1}{R_i^2} - \frac{1}{R_o^2}\right) \qquad (121)$$

where

$$R_i^2 <<< R_o^2$$

Noting that

$$\beta' = \frac{\alpha_p(\Delta V)^2}{2\nu kT\ \ell n^2 \frac{R_o}{R_i}} \left(\frac{1}{R_i^2}\right), \qquad (80)$$

and neglecting the R_o term, Equation (121) takes the form

$$\frac{C_i^*}{C_o^*} = e^{\beta'} \qquad (122)$$

This approximation is accurate to 0.4 percent for $\kappa = 25$ and becomes better with increasing κ. Equation (122) predicts radial concentration ratios of 1.650 for $\beta' = 0.5$, 1.2840 for $\beta' = 0.25$, 1.1052 for $\beta' = 0.1$, and 1.0254 for $\beta' = 0.025$. The corresponding values calculated from Equation (111) for $\kappa = 35$ (which lies on the limiting curve in Figure 10) are 1.6441, 1.2822, 1.1045, and 1.0252. Comparison of the values shows that the results from Equation (111) are slightly lower for every value of β' than those obtained from Equation (122). Since Equation (111) includes the velocity in the vertical direction, the comparison indicates that essentially equilibrium radial concentration profiles are obtained even when natural convection causes flow in the system. It should also be noted that the chemical potential energy is not accounted for in the derivation of Equation (122). This leads to very little error, however, since it is a negligibly small fraction of the electrical potential energy.

Theoretical separation factors for dielectrophoresis in a cell with radial geometry were calculated from Equation (115). The constant, O', in Equation (115) was calculated so as to approximate the experimental conditions. The calculations are shown in Appendix VIII. The diffusivity was taken from Kern's[32] data and μ, $\bar{\rho}$, and $\bar{\beta}$ were approximated by using the values for water at the average solution temperature. The ΔT was determined from heat transfer considerations. The theoretical data are shown in Appendix V.

The effect of length on the predicted separation factor at $\kappa = 35$ for several values of β' is shown in Figure 11. Comparison of the curves shows that much greater separations are obtained as the factor β' is increased at any given cell length. This demonstrates the importance of the molecular polarizability since the value of κ is the same for both curves. The curve for $\beta' = 0.100$ shows greatly increasing separations at large values of L. The same effect would be observed for the $\beta' = 0.025$ curve if much larger values of L were considered. This curve shows that for the values of β' and κ of most interest, the separation factor more than doubles, when the separation tube length is doubled.

The variation of separation factor with length at $\beta' = 0.025$ for several values of κ is shown in Figure 12. The curve for $\kappa = 35$ shows the decrease from linearity of the separation factor as a function of length. The dashed lines indicate the limiting slope at the origin. Comparison of the curves for different values of κ shows that for a given β' and length, the separation factor decreases with increasing κ.

The effect of κ on the separation factor at a given length is shown for several values of β' in Figure 13. The curves show that as κ decreases the separation factors become very large. The values may be exaggerated at low values of κ due to the neglect of the electrical dissipation term in Equation (9). Although this assumption is good for values of κ larger than about 15, for values lower than this the electrical dissipation term, S_e, should be included in Equation (9). Including it decreases ΔT which leads to larger values of C^* and correspondingly lower separation factors. The trend of increasing separation factors with decreasing values of κ would still be expected as may be seen from examining the curves for values of κ from 40 to 55.

In general, the theoretical analysis shows that increasing β', decreasing κ, and increasing the length of the separation tube all lead to increased values of the theoretical separation factor.

Experimental Results

Experimental separations of aqueous polymethacrylic acid solutions were measured at various polymer molecular weights, solute concentrations, applied powers, and voltages as are tabulated in Tables I and II. The experimental data for the dielectrophoresis runs are tabulated in Appendix VI and plotted in Appendix VII.

The variation of solute resistance in the top and bottom cell reservoirs as a function of time is illustrated in Figure 18. Examination of the curves shows that the resistance in the top reservoir decreases very rapidly initially and then continues to decrease at a somewhat slower rate until a steady value is obtained. The resistance in the bottom reservoir also decreases rapidly at first but goes through a minimum after about six hours and then gradually increases to a steady value. The rapid initial decrease in the bottom reservoir resistance is attributed to a solution temperature increase due to Joule heating in the reservoir. The initial resistance drop in the top reservoir is due to the temperature increase caused by the natural convection of the solution close to the wire. After an equilibrium temperature is

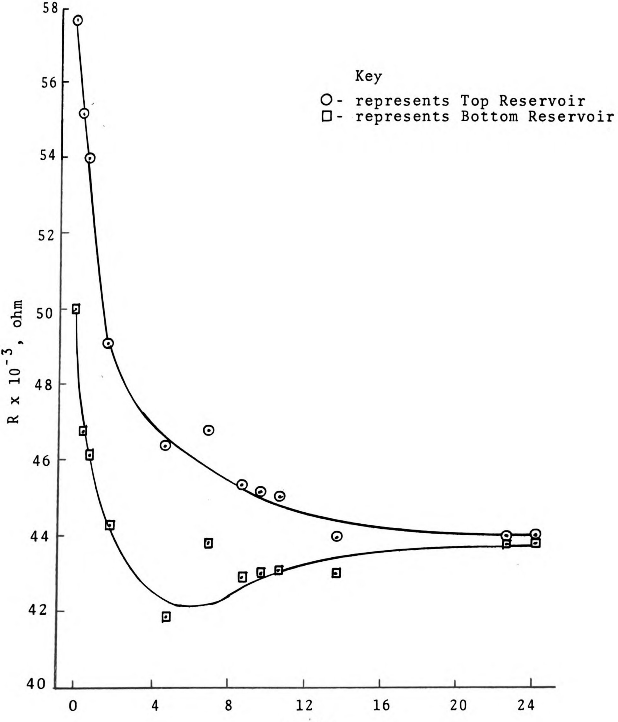

Figure 18. Variation of resistance with time for Run 32, C = 0.000225 gm./ℓ., α' = 20%, cell I, and $P_{avg.}$ = 2.8 watts.

established, about six hours for this case, dielectrophoresis and natural convection cause the polymer concentration to increase in the top reservoir (decreasing its resistance), and to decrease in the bottom reservoir (increasing its resistance). After about 18-24 hours the equilibrium separation is obtained. The variation of the separation factor as a function of time is shown in Figure 19. The negative values observed at low times are attributed to a greater initial temperature increase in the bottom than in the top reservoir. This is expected as the bottom is directly heated from the Joule effect, whereas the only heat input to the top is from natural convection. The negative values should not be interpreted as "negative separations."

The effect of power on the separations obtained in cell I, operating with forced feed, is shown in Figure 20. The data are taken from Table II. The shape of the curve indicates that there is an optimum value of power which gives the largest separation for a given system. A decrease in the separation factor would be expected at higher values of power due to increased thermal or convective turbulence. A maximum separation factor of 1.0265 is seen at a power of about 2.7 watts. Since the measurements were made with very slow feed addition, this represents the equilibrium radial concentration difference that may be obtained in a single pass through the cell. As seen from the polarizability calculations in Appendix VIII, this corresponds to an experimental value of $\beta' = 0.0262$ for cell I operating at 100 volts.

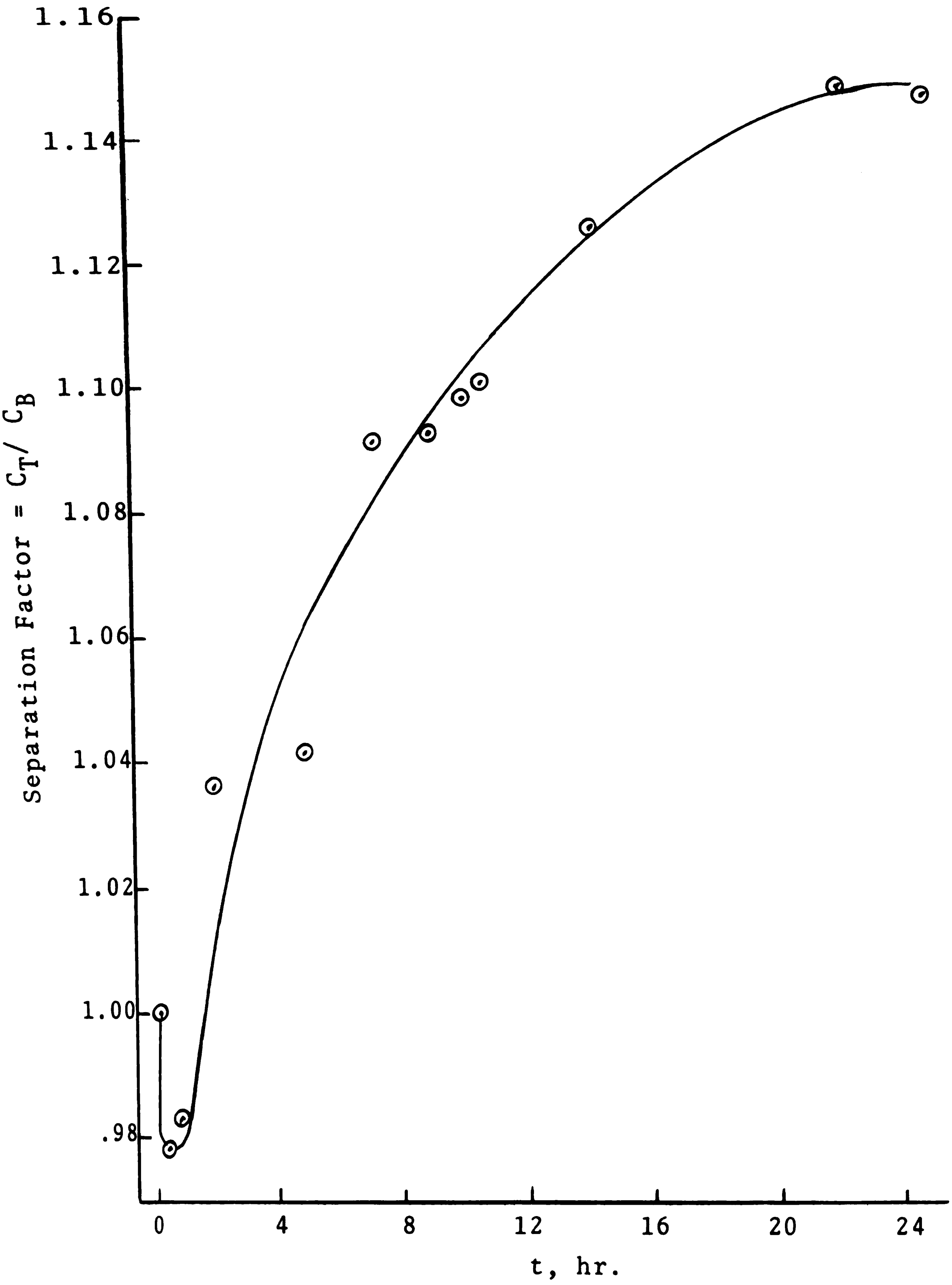

Figure 19. Variation of separation factor with time for Run 32.

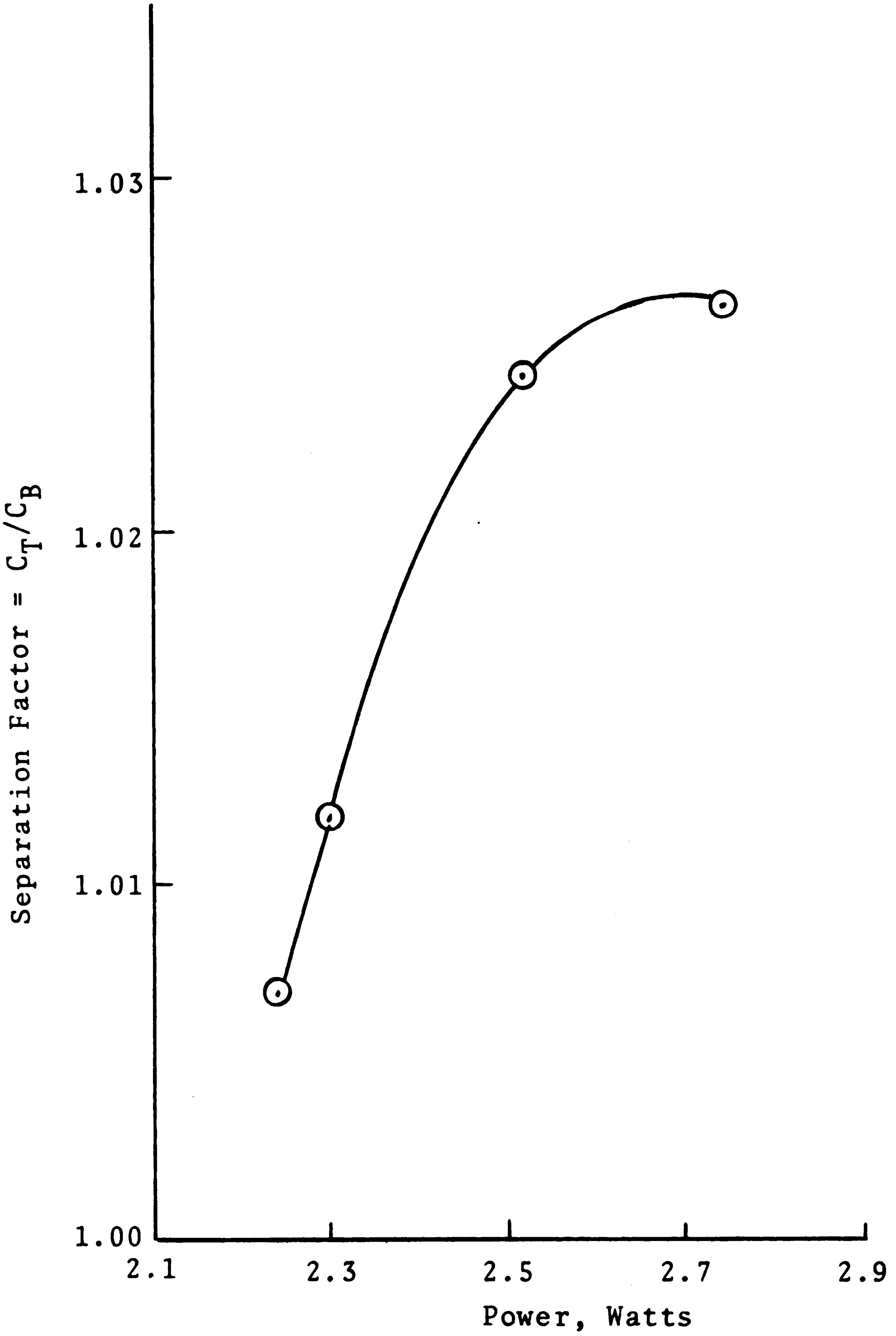

Figure 20. Effect of power on separation factor for tagged data at $C = 0.01$gm./ℓ. in cell I with forced feed.

The effect of power on the separation factor for the resistance data taken on cell I, operating with countercurrent staging, at a concentration of 0.000225 gm./ℓ. is shown in Figure 21. A maximum separation of 47 percent is seen to occur at a power of 2.6 watts. Although there is scatter in the data, this is in the same range as the value of 2.7 watts suggested by the forced feed measurements.

Figure 22 shows the variation of the separation factor with power for tagged data taken in cell II, operating with countercurrent staging, with a polymer concentration of 0.01 gm./ℓ. The curve shows a maximum separation of 24 percent at a power of 4.55 watts. Analysis of Figures 21 and 22 suggests that an optimum operating power exists which is about 2.6 watts for cell I and about 4.5 watts for cell II.

The tabulated results in Table I show the separations determined from resistance and radioactivity data as well as the experimental conditions. As the radioactivity technique for concentration measurement was not used for Runs 11-51, a comparison of the results from Runs 61-82 should be made to verify the reliability of the earlier results. Comparison shows that when considering runs in which the applied power is below or up to the optimum cell power, the agreement is quite good. When considering runs made at powers above the optimum for the cell, the resistance data shows considerably larger separations than the tagged data. This is due to

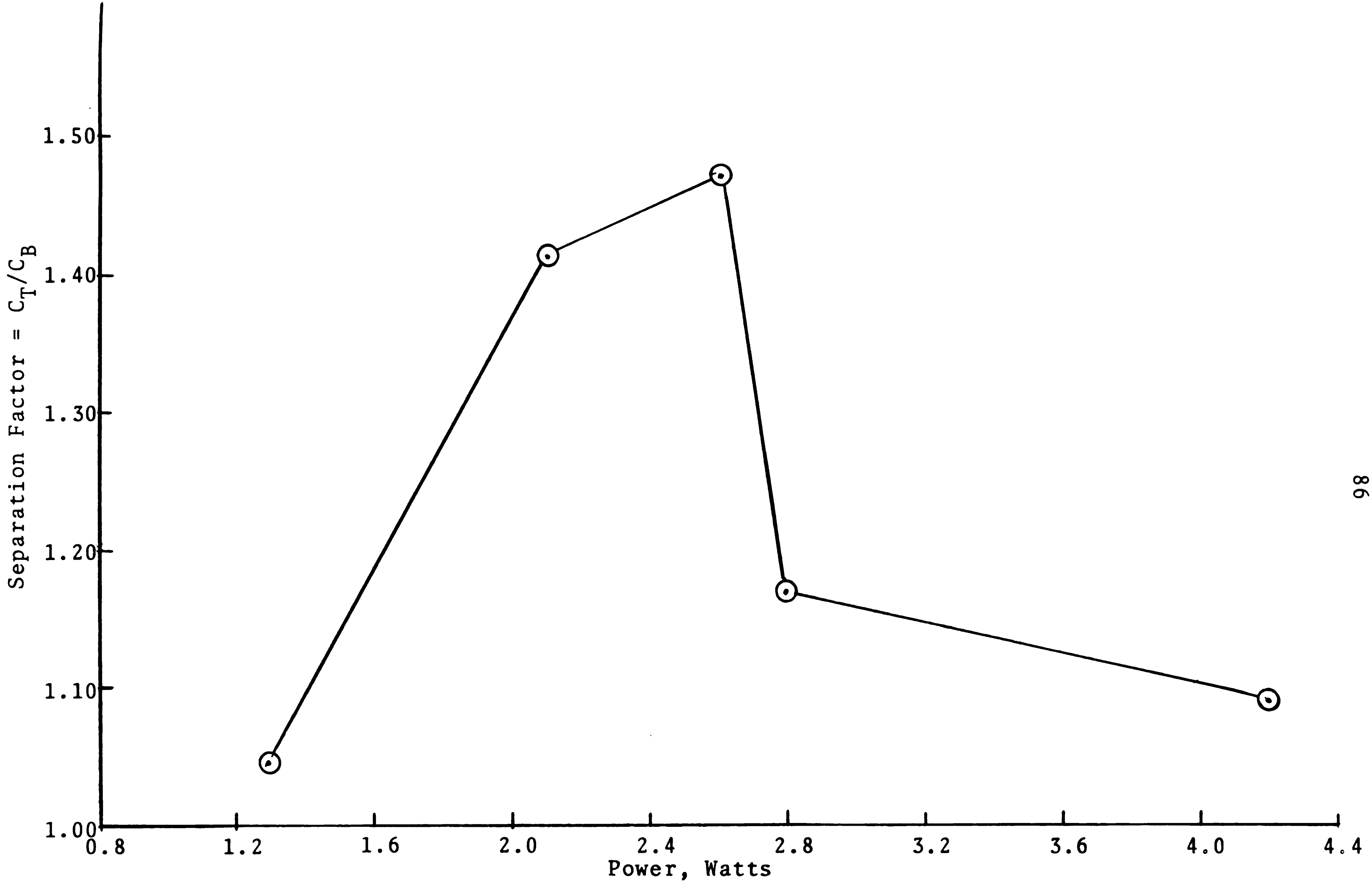

Figure 21. Effect of power on separation factor for resistance data at C = 0.000225 gm./ℓ. in cell I.

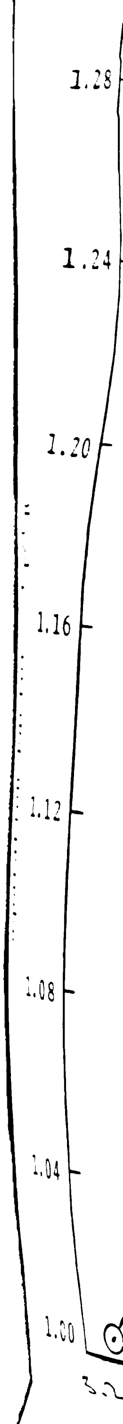

Fig

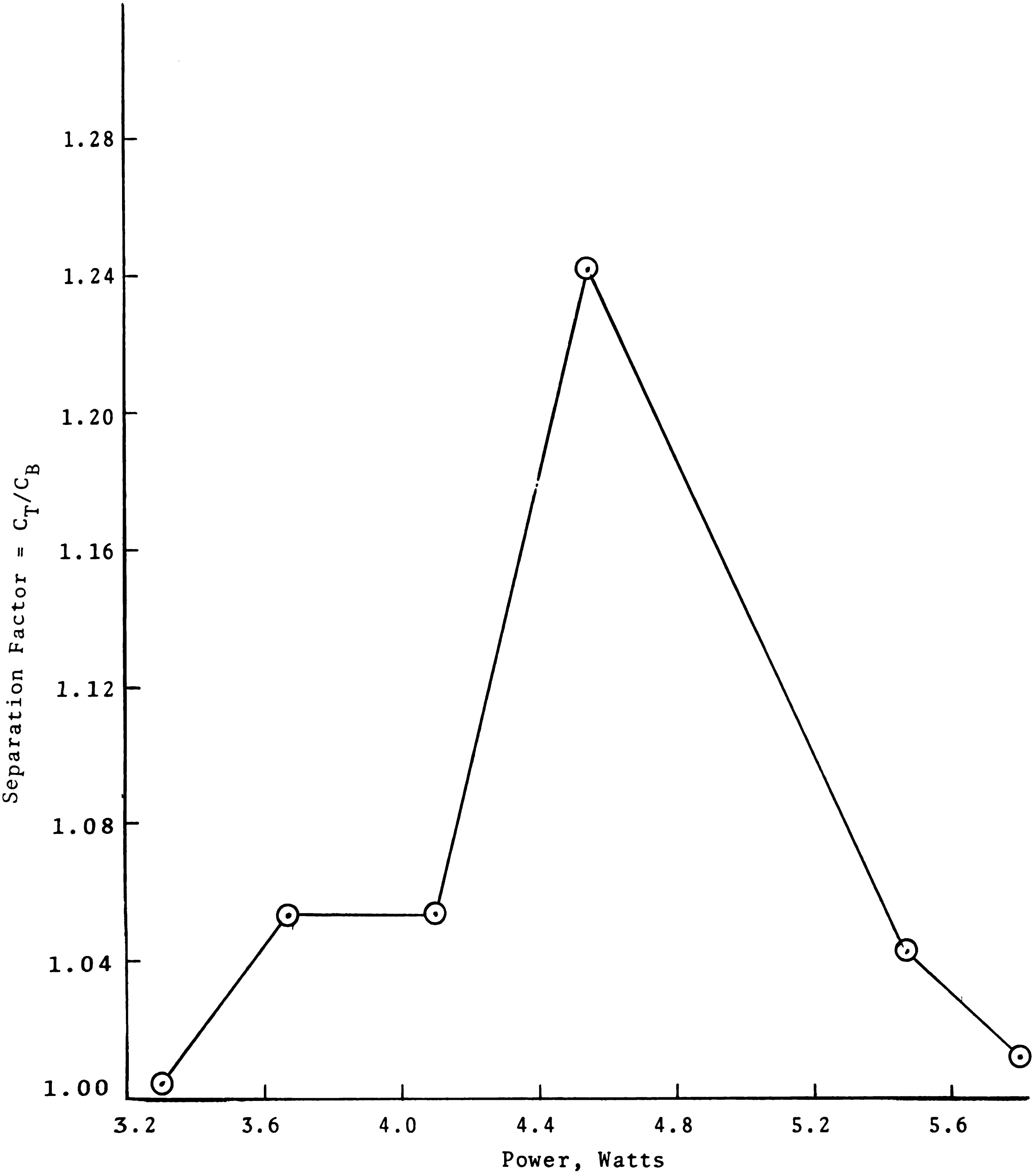

Figure 22. Effect of power on separation factor for tagged data at C = 0.01 gm./ℓ. in cell II.

uncertainty in the resistance measurements caused by increased solution temperatures. It is felt that the tagged values of the percent separation are more accurate than the resistance values due to their lack of dependence on temperature, geometry, and impurities. Some of the results shown in Table I show negative values of the percent separation, indicating that the bottom reservoir became enriched in polymer. These runs were all made with the tracer obtained from Volk Radiochemical Company and are included only to broaden the comparison between the two concentration measurement methods. Comparing the resistance to tagged results for the runs having negative values shows that, in every case except one, whenever the tracer indicated a negative separation the resistance data did also. The separation observed in the exception was so small that within the limits of experimental error it could have been either positive or negative.

It is felt that the negative separations observed in the runs made with Volk tracer were caused by a di-valent impurity in the tracer. The contaminant was probably magnesium, as Na^{22} is made from MgO; however, this is not definitely determined since a sample analysis was not obtained from the supplier. The presence of di-valent ions in a dilute polymethacrylic acid solution would cause a coiling of the polymeric chain due to the formation of complexes involving non-adjacent carboxyls. Wojtczak[65] indicates that for 20 percent neutralized polymer the molecule would be more compact than in its unneutralized state. This would greatly reduce the polarizability (dependent on the cube of the molecular length), and in turn, the dielectrophoretic effect. Alternately, the reverse effects of sedimentation and thermal diffusion would be enhanced by this process and could be responsible for the reversed separations.

The variation of separation factor with concentration for runs of approximately equal power in cell I is shown in Figure 23. The data are taken from Table I. The curve shows a large increase in the separation factor as the concentration approaches zero. This is explained by the increase in chain extension of the polymer molecules as the concentration decreases. The increased chain end to end distance is reflected as a cubed increase in the polarizability, which leads to a large increase in the separation factor. Although a solute concentration dependence is not directly apparent from the theoretical expression for the separation factor (Equation (115)), decreasing the concentration increases the parameter β' in C^* and decreases $\bar{\rho}$ in O'. Both effects lead to an increase in the theoretical separation factor.

Polarizability and theoretically predicted separation factor calculations are given in Appendix VIII. The values of the theoretically predicted polarizability of polymethacrylic acid were calculated from the expression

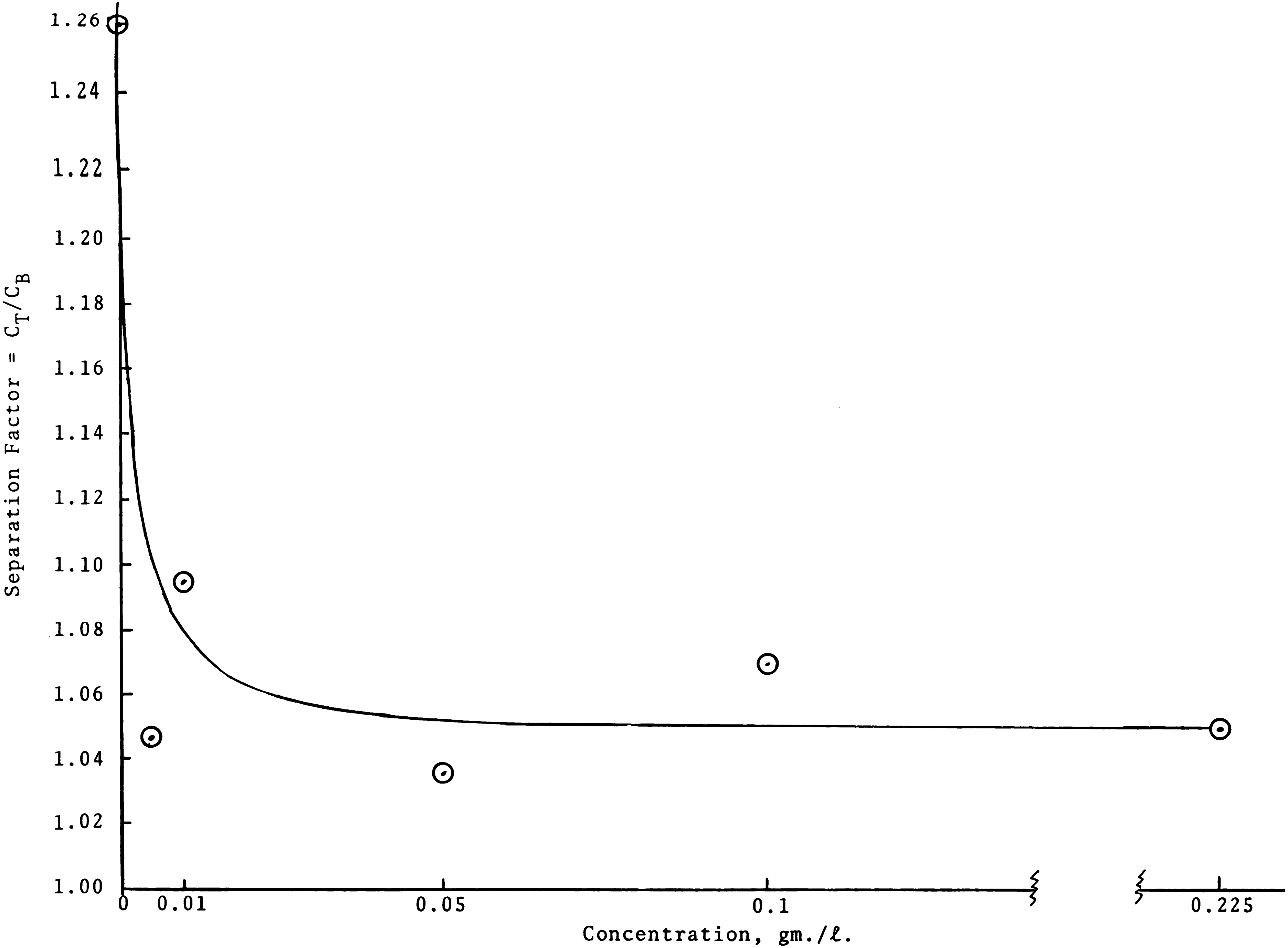

Figure 23. Effect of concentration on separation factor for runs of approximately equal power in cell I.

given by Eigen and Schwartz.[10] The average end to end chain distance at 20 percent neutralization was determined from bond length considerations, yielding $\alpha_p = 4.38 \times 10^{-13}$cm.^{3}, and from an expression given by Krause,[36] yielding $\alpha_p = 1.26 \times 10^{-14}$cm.^{3}. The theoretical values differ by a factor of 35 which is not unusual considering that any difference in the chain length is cubed in the polarizability expression. Experimental values of the polarizability were determined from the forced feed runs made with cells I and II. The values were calculated from a modification of Equation (8). The data show a value of $\beta' = 0.0262$ for cell I ($\kappa = 36$) which, at 100 volts and 300°K, corresponds to a polarizability of 0.59×10^{-13}cm.^{3}. The value of β' for cell II is 0.0837 which correspondents to a polarizability of 2.06×10^{-13}cm.^{3}. The experimental polarizabilities are equivalent to a dipole moment of about 2×10^5 to 7×10^5 Debye in a field of 1000 volts/cm.

Theoretically predicated separation factors for cells I and II, operating with staging, were calculated from Equations (111) and (115) using the experimentally determined values of β'. The theoretical separation factor for cell I, operating at 100 volts, optimum power, and with 0.01 gm./ℓ. polymer, is 1.049. This represents 1.85 theoretical stages for the cell. The experimentally obtained separation factor for cell I under similar conditions is 1.035, representing 1.32 theoretical stages. This is determined from averaging the separations obtained in Runs 40-44 shown in Table I. For cell II, under the same conditions, the predicted separation factor is 1.255 corresponding to 2.9 equilibrium stages. The experimental separation factor determined from radioactivity measurement, with the cell at optimum power, is 1.243. This represents 2.78 experimentally determined stages. The results illustrate the extreme dependence of the separation factor on the length of the cell, since the only major difference between the experimental cells is that cell II is twice as long as cell I. The agreement of the experimental and theoretical values seems to justify the assumption made in Equation (72) that the concentration gradient in the z direction is constant.

Table I. Summary of experimental dielectrophoresis results.

Run Number	Concentration gm./ℓ.	Molecular Weight	Neutralization %	Power Watts	V Volts	Cell	Frequency c.p.s.	Percent Separation	
								Resistance Data	Tagged Data
11	0.1	96,000	15	0.7	21	I	60	7.0	
15	0.01	860,000	50	1.5	50	I	5,000	14.6	
16	0.01	860,000	50	1.7	48	I	5,000	7.5	
17	0.005	860,000	50	1.8	80	I	5,000	5.2	
23A	0.07	860,000	15	1.09	75	I	10,000	0.9	
23B	0.07	860,000	15	1.65	102	I	10,000	12.0	
25	0.225	453,000	20	6.2	35	I	6,000	4.8	
28	0.000225	453,000	20	2.1	100	I	6,000	41.3	
30	0.000225	453,000	20	4.2	100	I	6,000	9.0	
31	0.000225	453,000	20	1.3	100	I	6,000	4.8	
32	0.000225	453,000	20	2.8	100	I	6,000	17.0	
34	0.000225	453,000	20	2.6	100	I	6,000	47.0	
38	0.005	1,180,000	20	1.75	121	I	5,000	3.9	
39	0.005	1,180,000	20	1.85	115	I	5,000	1.9	
40	0.01	1,180,000	20	1.8	95	I	5,000	6.6	
41	0.01	1,180,000	20	1.5	104	I	5,000	1.5	
43	0.01	1,180,000	20	1.48	100	I	6,000	3.4	
44	0.01	1,180,000	20	1.36	98	I	6,000	2.6	
45	0.05	1,180,000	20	1.87	52	I	6,000	3.7	
47	0.05	1,180,000	20	2.05	53	I	6,000	3.2	

Table I, Continued.

Run Number	Concentration gm./ℓ.	Molecular Weight	Neutralization %	Power Watts	V Volts	Cell	Frequency c.p.s.	Percent Separation Resistance Data	Percent Separation Tagged Data
48	0.05	1,180,000	20	1.9	45	I	6,000	5.4	
51	0.05	1,180,000	20	2.15	50	I	6,000	4.8	
61	0.01	1,180,000	20	3.67	82	II	6,000	0.9	5.35
63	0.01	1,180,000	20	5.47	105	II	6,000	24.0	4.32
64	0.01	1,180,000	20	5.8	93	II	6,000	66.0	1.13
65	0.01	1,180,000	20	4.55	60	II	6,000	17.0	24.30
66	0.01	1,180,000	20	4.1	93	II	6,000	6.0	5.26
67*	0.01	1,180,000	20	5.02	117	II	6,000	7.5	1.23
68*	0.01	1,180,000	20	4.53	115	II	6,000	-4.4	-4.40
69*	0.01	1,180,000	20	4.53	118	II	6,000	1.9	1.33
70*	0.01	1,180,000	35	4.48	92.5	II	6,000	2.5	4.04
71*	0.01	1,180,000	35	4.95	96	II	6,000	-2.9	-1.44
72*	0.01	1,180,000	35	5.05	94	II	6,000	-7.1	-0.86
73*	0.01	1,180,000	35	4.5	89	II	6,000	1.2	-0.69
75*	0.01	1,180,000	20	4.45	122	II	6,000	-1.1	1.02
76*	0.01	1,180,000	20	4.5	110	II	6,000	-4.6	-3.9
78*	0.01	1,180,000	20	4.5	108	II	6,000	0.9	0.93
82	0.01	1,180,000	20	4.45	140	II	6,000	9.3	9.66

*Indicates runs made with Volk Chemical Company tracer.

Table II. Summary of forced feed results.

Run Number	Concentration gm./ℓ.	Molecular Weight	Neutralization %	Frequency c.p.s.	Cell	Power Watts	V Volts	Feed Time Hours	Percent Separation Tagged Data
54	0.01	1,180,000	20	6,000	I	2.3	120	1.42	1.20
56	0.01	1,180,000	20	6,000	I	2.24	118	1.33	0.71
57	0.01	1,180,000	20	6,000	I	2.52	120	1.58	2.45
59	0.01	1,180,000	20	6,000	I	2.75	120	0.83	2.65
60	0.01	1,180,000	20	6,000	II	4.2	88	1.42	8.75

CONCLUSIONS

The theoretical investigation of dielectrophoresis of polyelectrolytes in a system with cylindrical geometry shows that the predicted separation factors increase with increasing β', which is directly proportional to the molecular polarizability and applied voltage and inversely proportional to the inner cylinder radius. The predicted separations were also found to increase with increasing tube length, L, and decrease with increasing values of the ratio of the outer to inner cylinder radii, κ. The results show that the radial concentration ratio for a system with flow is only slightly less than the static equilibrium value. This enables the radial concentration ratio obtained from Equation (111) to be approximated by the form obtained from considering only dielectrophoresis; the exponential of β'. The radius of the inner cylinder is seen to critically affect the radial concentration ratio and should be as small as possible.

The experimental investigation demonstrated that dielectrophoresis may be used to separate polymethacrylic acid from water. An optimum applied power, at which the observed separations were maximized, was found for both of the experimental cells investigated. For cell I (12 inches long), the optimum operating power was 2.6 watts, and for cell II (24 inches long) it was found to be 4.5 watts. The optimum power is interpreted as being the ideal balance between the natural convection forces (which increases the separation) and the thermal mixing forces (which decrease the separation). The same dependence was noted in equilibrium radial concentration ratio measurements.

The separation factor increases greatly with decreasing solute concentrations for extremely dilute solutions. This is attributed to increased molecular polarizabilities resulting from polyion chain extension in increasingly dilute solutions.

The experimental results obtained using radioactive sodium for concentration determination verify the values obtained from resistance measurements for runs made at or below the optimum cell power. For runs made above the optimum power, it is felt that the radioactivity results are the most reliable.

The experimental separation factors, obtained at optimum cell powers, compare favorably to the predicted values calculated from experimental values of β'. This substantiates the theoretically predicted affect of length on the separation factor and indicates that the assumption of a constant concentration gradient in the z direction was reasonable.

FUTURE WORK

It is suggested that future work continue along the following lines:

Experimental

1. Runs should be made with longer cells since the cell length greatly affects the equilibrium separation.

2. Consideration should be given to the continuous operation of a long cell. The present design could be modified with the addition of feed and product streams and if the cell was long enough, appreciable staging would result. A study of this nature might greatly enhance the practicality of dielectrophoresis.

3. Experimental runs should be made with radioactive polymethacrylic acid which is tagged on the polymer chain. This would eliminate any uncertainty in the measurements due to impurities in the radioactive sodium.

4. For the present system, a device should be constructed such that the wire could be pulled through the apparatus. This would impart an upward velocity, equal to the wire velocity, to the material immediately adjacent to the wire which is at the highest radial polymer concentration. The modification could readily be incorporated in the theoretical velocity and concentration expressions.

Theoretical

1. The power generation term could be included in the solution of the temperature profile. This would affect only the particular solution of the energy equation and would extend its applicability to low values of κ.

2. The equation of continuity of species could be solved without assuming that the concentration gradient in the z direction is constant since the equation is separable. A numerical method would probably be required.

APPENDIX I

The Solution to Equation (45) in Terms of $\bar{T}$

APPENDIX I

The Solution to Equation (45) in Terms of T.

$$0 = \int_1^{\kappa} y \; dy - \int_1^{\kappa} y^3 \; dy + \frac{A}{A - B} \int_1^{\kappa} y^3 \; \ln y \; dy$$

$$+ \left[\frac{\kappa^2 - 1}{\ln \kappa} - \left(\frac{A}{A - B} \right) \kappa^2 \right] \int_1^{\kappa} y \; \ln y \; dy \qquad (45)$$

The procedure necessary to obtain an expression for T from Equation (45) is to integrate each term in Equation (45) and then solve for the group $\frac{A}{A - B}$, which can be rearranged to give B as a function of A and κ. Denoting the individual integrals in Equation (45) as 1, 2, 3, and 4, Equation (45) takes the form

$$0 = \int 1 + \int 2 + \int 3 + \int 4 \qquad (I\text{-}1)$$

where:

$$\int 1 = \int_1^{\kappa} y \; dy = \frac{y^2}{2} \Big|_1^{\kappa} = \frac{1}{2} (\kappa^2 - 1) \qquad (I\text{-}2)$$

$$\int 2 = - \int_1^{\kappa} y^3 \; dy = - \frac{y^4}{4} \Big|_1^{\kappa} = - \frac{1}{4} (\kappa^4 - 1) \qquad (I\text{-}3)$$

$$\int 3 = \frac{A}{A-B}\int_{1}^{\kappa} y^3 \ \ell n\ y\ dy = \frac{A}{A-B}\left(\frac{y^4}{4}\ \ell n\ y - \frac{y^4}{16}\right)\Bigg|_{1}^{\kappa}$$

$$= \frac{A}{A-B}\left(\frac{\kappa^4}{4}\ \ell n\ \kappa - \frac{\kappa^4}{16} + \frac{1}{16}\right) \tag{I-4}$$

and

$$\int 4 = \left[\frac{\kappa^2 - 1}{\ell n\ \kappa} - \left(\frac{A}{A-B}\right)\kappa^2\right]\int_{1}^{\kappa} y\ \ell n\ y\ dy$$

$$= \left[\frac{\kappa^2 - 1}{\ell n\ \kappa} - \left(\frac{A}{A-B}\right)\kappa^2\right]\left(\frac{y^2}{2}\ \ell n\ y - \frac{y^2}{4}\right)\Bigg|_{1}^{\kappa}$$

$$= \left[\frac{\kappa^2 - 1}{\ell n\ \kappa} - \left(\frac{A}{A-B}\right)\kappa^2\right]\left(\frac{\kappa^2}{2}\ \ell n\ \kappa - \frac{\kappa^2}{4} + \frac{1}{4}\right). \tag{I-5}$$

Adding the individual integrals and factoring all terms multiplied by $\frac{A}{A-B}$, Equation (45) becomes

$$\frac{A}{A-B} = \frac{\frac{1}{2}(1 - \kappa^2) + \frac{1}{4}(\kappa^4 - 1) - \left(\frac{\kappa^2 - 1}{\ell n\ \kappa}\right)\left(\frac{\kappa^2}{2}\ \ell n\ \kappa - \frac{\kappa^2}{2} + \frac{1}{4}\right)}{\left(-\frac{\kappa^4}{4}\ \ell n\ \kappa + \frac{3}{16}\kappa^4 - \frac{\kappa^2}{4} + \frac{1}{16}\right)}, \tag{I-6}$$

which on inversion and further simplification is

$$\frac{A-B}{A} = \frac{-\kappa^4\ \ell n\ \kappa + \frac{3}{4}\kappa^4 - \kappa^2 + \frac{1}{4}}{1 - \kappa^4 + \frac{1}{\ell n\ \kappa}(\kappa^2 - 1)^2}. \tag{I-7}$$

Rearrangement of Equation (I-7) gives the following relationship for B as a function of A and κ,

$$B = A \left\{ 1 - \left[\frac{-\kappa^4 \ln \kappa + \frac{3}{4}\kappa^4 - \kappa^2 + \frac{1}{4}}{1 - \kappa^4 + \frac{1}{\ln \kappa}(\kappa^2 - 1)^2} \right] \right\}. \qquad (46)$$

APPENDIX II

Fortran Program for Velocity Profiles

Fortran Program for Velocity Profiles

```
 7 FORMAT(E5.1)
 8 FORMAT(E10.4)
 9 FORMAT(1HV,14,14)
   DIMENSION Y(40),R(2)
   READ7,(Y(I),I=I,29),(R(J),J=1,2)
   J=1
10 I=0
 2 I=I+1
 3 TESVAL=R(J)-Y(I)
 4 IF(TESVAL)6,6,5
 5 CONST     =((1./(LOGF(R(J))*LOGF(R(J))))*(2.*R(J)*R(J)-1.-R(J)**4)
  3+(1./LOGF(R(J)))*(1.75*R(J)**4-3/4-R(J)*R(J))-R(J)**4)/(1.-R(J)**4
  4+1./LOGF(R(J))-2.*R(J)*R(J)/LOGF(R(J))+R(J)**4/LOGF(R(J)))
   STAR     =Y(I)*Y(I)*(LOGF(Y(I))-1)/LOGF(R(J))-(R(J)*R(J)/LOGF(R(J)
  1)+(1-R(J)*R(J))/(LOGF(R(J))*LOGF(R(J))))*LOGF(Y(I))+1./LOGF(R(J))
11 ADDIT     =CONST     *(LOGF(Y(I))/LOGF(R(J))+Y(I)*Y(I)-1.-R(J)*R(J
  1)*LOGF(Y(I))/LOGF(R(J)))
12 VSTAR=STAR-ADDIT
   PUNCH9,I,J
   PUNCH8,VSTAR,CONST
   GO TO 2
 6 STOP
   END
   END
```

APPENDIX III

The General Procedure for Solving Equation (81)

APPENDIX III

The General Procedure for Solving Equation (81)

$$\frac{d^2C}{ds^2} + \left(\frac{1}{s} - \beta'\right)\frac{dC}{ds} - \frac{\beta' C}{s} = - \frac{c_1'}{2s}\,\ell n\ s - \frac{c_2'}{2}\,\ell n\ s + \frac{c_3'}{s} + c_4' \tag{81}$$

The general method for solving Equation (81) is to obtain a complimentary solution by applying a series technique, such as the method of Frobenius, and then use the method of undermined coefficients or variations of parameters to obtain a particular solution. The sum of the complimentary and particular solutions is the total solution of the equation, and the constants of integration may be eliminated by application of the boundary conditions of the problem.

Applying the method of Frobenius to Equation (81), let the right hand side of the equation equal zero, and assume a solution of the form,

$$C = \sum_{0}^{\infty} A_n\ s^{n + \ell} \tag{III-1}$$

where

n = summation index

ℓ = dummy variable

A_n = constant determined by n.

Differentiating Equation (III-1), substituting into Equation (81), and rearranging yields

$$A_o \left[\ell(\ell - 1) + \ell \right] s^{\ell-2} + \sum_{1}^{\infty} A_n (n + \ell)^2 \, s^{n+\ell-2}$$

$$- \sum_{0}^{\infty} A_n \, \beta' \, (n + \ell + 1) \, s^{n+\ell-1} = 0 \qquad \text{(III-2)}$$

where

$A_0 = A_n$ evaluated at n = 0.

The indicial equation, evaluating the possible values of ℓ, is obtained from the first term in Equation (III-2) as

$$\ell^2 = 0, \qquad \text{(III-3)}$$

yielding

$\ell = 0, 0.$

The second and third terms in Equation (III-2) may be combined by letting n = n + 1 in the second term. This relates the constant A_{n+1} to A_n as

$$A_{n+1} = \frac{A_n \, \beta'}{n + \ell + 1}, \qquad \text{(III-4)}$$

and if $\ell = 0$,

$$A_{n+1} = \frac{A_n \, \beta'}{n + 1} \qquad \text{(III-5)}$$

or

$$A_n = \frac{A_{n-1}\ \beta'}{n} . \tag{III-6}$$

Relating the constant A_n to A_0 yields

$$A_n = \frac{(\beta')^n\ A_0}{n!} . \tag{III-7}$$

Substituting Equation (III-7) into Equation (III-1) and noting that $\ell = 0$, the first part of the complimentary solution to Equation (81) is

$$C_I = A_0 \sum_0^\infty \frac{(\beta')^n\ s^n}{n!} = A_0\ e^{\beta' s} . \tag{III-8}$$

Another solution is seen to be required as the indicial equation yielded two values of ℓ. Since the values of ℓ are equal, the procedure for obtaining the second portion of the solution, C_{II}, is to take the derivative of C_I with respect to ℓ and evaluate it at $\ell = 0$. An alternate procedure is to use the method of variation of parameters which generates both C_I and C_{II}. Using the latter method, let

$$C_{II} = U_{(s)}\ C_I = U_{(s)}\ A_0\ e^{\beta' s} \tag{III-9}$$

where

$U_{(s)}$ = a function of s to be determined.

The differential equation describing $U_{(s)}$ is found by substituting Equation (III-9) into Equation (81), as

$$\frac{d^2U_{(s)}}{ds^2} + \left(\frac{1}{s} + \beta'\right)\frac{dU_{(s)}}{ds} = 0. \qquad \text{(III-10)}$$

The solution of Equation (III-10) is

$$U_{(s)} = a_1\left[\ell n\ s + \sum_1^{\infty}\frac{(-1)^n\ (\beta')^n\ s^n}{n \cdot n!}\right] + b_1 \qquad \text{(III-11)}$$

where

a_1, b_1 = constants of integration.

The second portion of the complimentary solution is then

$$C_{II} = U(s)C_I = A_0 e^{\beta' s}\left[a_1\left(\ell n\ s + \sum_1^{\infty}\frac{(-1)^n\ (\beta')^n\ s^n}{n \cdot n!}\right) + b_1\right], \qquad \text{(III-12)}$$

and the total solution is

$$C = C_I + C_{II} = c_6 e^{\beta' s} - A_1 e^{\beta' s}\left[\ell n\ s + \sum_1^{\infty}\frac{(-1)^n\ (\beta')^n\ s^n}{n \cdot n!}\right] \qquad \text{(III-13)}$$

where

$c_6 = A_0 + b_1A_0$

$A_1 = -A_0\ a_1$,

and c_6 and A_1 are the same as in Equation (111).

Examination of Equation (III-12) shows that the method of variation of parameters generates both parts of the complimentary solution from the first solution, C_I. The particular solution to Equation (81) is obtained by the method of undetermined coefficients. Assume that

$$C_p = A\ s\ \ell n\ s + B\ \ell n\ s + Cs + D \qquad \text{(III-14)}$$

is a solution of Equation (81), where Cp = particular solution of Equation (81) and A, B, C, and D are arbitrary constants to be evaluated. Substituting Equation (III-14) into Equation (81) and equating like powers of s yields

$$A = \frac{c_2'}{4\beta'} \qquad \text{(III-15)}$$

$$B = \frac{c_1'}{2\beta'} + \frac{c_2'}{4(\beta')^2}$$

$$C = -\left(\frac{c_4'}{2\beta'} + \frac{c_2'}{8\beta'}\right)$$

and

$$D = -\left(\frac{c_3'}{\beta'} - \frac{c_2'}{8(\beta')^2} + \frac{c_1'}{2\beta'} + \frac{c_4'}{2(\beta')^2}\right).$$

The total solution of Equation (81) is the sum of the complimentary and particular solutions. Thus

$$C = c_6 e^{\beta' s} - A_1 e^{\beta' s}\left[\ell n\ s + \sum_1^{\infty} \frac{(-1)^n\ (\beta')^n\ s^n}{n \cdot n!}\right] + A\ s\ \ell n\ s$$

$$+ B\ \ell n\ s + Cs + D \qquad \text{(III-16)}$$

Comparison of Equation (III-16) with Equation (108) shows that both methods of solution yield the same dependence of the concentration profile on the variable s. Evaluation of the constants c_6 and A_1 in Equation (III-16) is accomplished by applying the boundary conditions, Equation (84). The solution obtained is identical to Equation (111).

APPENDIX IV

Fortran Program for Radial Concentration Ratio Calcultations

Fortran Program for Radial Concentration Ratio Calculations

```
FTN5,3B

      PROGRAM CALC
      DO 2 K = 1, 10
      R = 5*K
      PRINT 102
      PRINT 103, R
      Do 3 J = 1, 20
      AJ = J
      P = 5. /( 10.* AJ)
      PRINT 104
      PRINT 103 , P
      X = LOGF(R)
      T = ((1.0/(X*X))*((2.0*R*R)-1.0-(R**4.0))+(1.0/X)*((1.75*(R**4))
     1 -(R*R)-.75)-(R**4.0))/(1.0-(R**4.0)+(1.0/X)*(1.0-(2.0*R*R)
     2 +(R**4.0)))
      C1 = (1.0/X)
      C2 =  (1.0/X)*T*(R*R-1.0)-(R*R)/X-(1/0-R*R)/(X*X)
      C3 = -T-1.0/X
      C4 = -C3
      A1 = C4/2.0 + C2/8.0 + C3 + C1/2.0 + C2/(4.0*P*P)+ C1/(2.0*P)
      A2 = C2/(4.0*P)
      A3 = C2/(4.0*P*P) + C1/(2.0*P)
      A4= C4/(2.0*P) + C2/(8.0*P)
      A5 = C3/P + C1/(2.0*P) + C4/(2.0*P*P) - C2/(8.0*P*P)
```

Fortran Program for Radial Concentration Ratio Calculations (Continued)

```
      B = (A1*R*R*EXPF(2.0*P/(R*R)) + A1*P*EXPF(P/(R*R))*(-2.0*X -P/R
     1 + P*P/(4.0*R**4.0) -P**3.0/(18.0*R**6.0)) - A2* (1.0-2.0*X)
     2 -R*R*A3 + A4)/(P*EXPF(P/(R*R)))
      SUM = -P/R + P*P/(4.0*R**4.0) - P*P*P/(18.0*R**6.0)
      RATIO = -(P*P*P/(18.0*R**6.0))/SUM
      N = R
      DO 1  I = 1, N
      Y = I
      S = 1.0/(Y*Y)
      W = LOGF(S)
      V = C1*Y*Y*LOGF(Y) + C2*LOGF(Y) + C3*Y*Y + C4
      C = B*EXPF(P*S) - A1  *EXPF(P*S)*(W - P*S + P*P*S*S/4.0 -
     1 P*P*P*S*S*S/18.0) + A2*S*W + A3*W -  A4*S -  A5
    1 PRINT 100, Y, C, V, S
      PRINT 101, T, C1, C2, C3, C4, SUM, RATIO
      PRINT 101, A1, A2, A3, A4, A5, B, X
    3 CONTINUE
    2 CONTINUE
  100 FORMAT (*0*,4(7X,E16.9 ))
  101 FORMAT (*0*, 7(3X,E10.3))
  102 FORMAT (*0 THE RADIUS RATIO FOR THE FOLLOWING IS * )
  103 FORMAT ( *0* , 7X , F7.4)
  104 FORMAT ( *0 THE VALUE OF BETA PRIVE IS *)
      END
RUN,3,3600
```

APPENDIX IV-A

Fortran Program for Separation Factor Calculations

Fortran Program for Separation Factor Calculations

```
FTN5,3B

      PROGRAM CALC
      DO 2 K = 1, 7
      R = 5*K+20
      PRINT 102
      PRINT 103, R
      DO 3 J = 1, 20
      AJ = J
      P = .025 * AJ
      PRINT 104
      PRINT 103 , P
      X = LOGF(R)
      T =  ((1.0/(X*X))*((2.0*R*R)-1.0-(R**4.0))+(1.0/X)*((1.75*(R**4))
     1 -(R*R)-.75)-(R**4.0))/(1.0-(R**4.0)+(1.0/X)*(1.0-(2.0*R*R)
     2 +(R**4.0)))
      C1 =  (1.0/X)
      C2 =   (1.0/X)*T*(R*R-1.0)-(R*R)/X-(1.0-R*R)/(X*X)
      C3 = -T-1.0/X
      C4 = -C3
      A1 = C4/2.0 + C2/8.0 + C3 + C1/2.0 + C2/(4.0*P*P)+ C1/(2.0*P)
      A2 = C2/(4.0*P)
      A3 = C2/(4.0*P*P) + C1/(2.0*P)
      A4= C4/(2.0*P) + C2/(8.0*P)
      A5 = C3/P + C1/(2.0*P) + C4/(2.0*P*P) - C2/(8.0*P*P)
```

Fortran Program for Separation Factor Calculation (Continued)

```
      B = (A1*R*R*EXPF(2.0*P/(R*R)) + A1*P*EXPF(P/(R*R))*(-2.0*X -P/R
     1 + P*P/(4.0*R**4.0) -P**3,0/(18.0*R**6.0)) - A2* (1.0-2.0*X)
     2 -R*R*A3 + A4)/(P*EXPF(P/(R*R)))
      SUM = -P/R + P*P/(4.0*R**4.0) - P*P*P/(18.0*R**6.0)
      RATIO = -(P*P*P/(18.0*R**6.0))/SUM
      N = R
      M = N/2
      DO 1  I = 1 , N , M
      Y = I
      S = 1.0/(Y*Y)
      W = LOGF(S)
      V = C1*Y*Y*LOGF(Y) + C2*LOGF(Y) + C3*Y*Y + C4
      C = B*EXPF(P*S) - A1  *EXPF(P*S)*(W - P*S + P*P*S*S/4.0 -
     1 P*P*P*S*S*S/18.0) + A2*S*W + A3*W -  A4*S -  A5
      DO 4 L = 1.8
      BL =L
      Z = 15.25 *BL
      CRATIO = C / (C- 103.2 + LOGF (R) *Z)
    4 PRINT 101 , CRATIO , Z
    1 PRINT 100, Y, C, V, S
    3 CONTINUE
    2 CONTINUE
  100 FORMAT (*0*,4(7X,E16.9 ))
  101 FORMAT (*0*, 2(3X, E10.3))
  102 FORMAT (*0 THE RADIUS RATIO FOR THE FOLLOWING IS * )
  103 FORMAT ( *0* , 7X , F7.4)
  104 FORMAT ( *0 THE VALUE OF BETA PRIME IS *)
      END

RUN,3, 4200
```

APPENDIX V

Theoretical Data

Theoretical Data

Table III. Radial concentration ratio data, from Equation (111)

κ	β'	C_i^*/C_o^*
5	0.5	1.5823
5	0.25	1.2618
5	0.125	1.1249
5	0.100	1.099
5	0.05	1.0487
5	0.025	1.0242
10	0.5	1.6151
10	0.25	1.2717
10	0.125	1.1283
10	0.100	1.1016
10	0.05	1.0499
	0.025	1.0248
15	0.5	1.6302
15	0.25	1.2769
15	0.125	1.1302
15	0.100	1.1029
15	0.05	1.0503
15	0.025	1.0250
20	0.5	1.6370
20	0.25	1.2794
20	0.125	1.1312
20	0.100	1.1037
20	0.05	1.0506
20	0.025	1.0250

Table III. (Continued)

κ	β'	C_i^*/C_o^*
25	0.5	1.6406
25	0.25	1.2808
25	0.125	1.1318
25	0.100	1.1041
25	0.05	1.0508
	0.025	1.0251
30	0.5	1.6427
30	0.25	1.2816
30	0.125	1.1321
30	0.100	1.1044
30	0.05	1.0509
30	0.025	1.0251
35	0.5	1.6441
35	0.25	1.2822
35	0.125	1.1323
35	0.100	1.1045
35	0.05	1.0510
35	0.025	1.0252

Table IV. Separation factor data varying L, from Equation (115)

β'	κ	L (cm.)	C_T/C_B
0.025	35	15.25	1.027
0.025	35	30.5	1.056
0.025	35	45.75	1.087
0.025	35	61.0	1.119
0.025	35	76.25	1.153
0.025	35	91.5	1.190
0.025	35	106.75	1.229
0.025	35	122.0	1.270
0.100	35	15.25	1.133
0.100	35	30.5	1.307
0.100	35	45.75	1.545
0.100	35	61.0	1.887
0.100	35	76.25	2.425
0.100	35	91.5	3.391
0.100	35	106.75	5.637
0.100	35	122.0	16.70
0.025	45	15.25	1.013
0.025	45	30.5	1.026
0.025	45	45.75	1.039
0.025	45	61.0	1.053
0.025	45	76.25	1.067
0.025	45	91.5	1.081
0.025	45	106.75	1.096
0.025	45	122.0	1.111

Table V. Separation factor data varying κ, from Equation (115)

β'	L (cm.)	κ	C_T/C_B
0.025	30.5	15	1.847
0.025	30.5	20	1.320
0.025	30.5	25	1.159
0.025	30.5	30	1.091
0.025	30.5	35	1.056
0.025	30.5	40	1.037
0.025	30.5	45	1.026
0.025	30.5	50	1.018
0.025	30.5	55	1.014
0.075	30.5	20	15.16
0.075	30.5	25	1.948
0.075	30.5	30	1.390
0.075	30.5	35	1.211
0.075	30.5	40	1.130
0.075	30.5	45	1.086
0.075	30.5	50	1.060
0.075	30.5	55	1.043

APPENDIX VI

Experimental Resistance and Radioactivity Data

Table VI. Experimental resistance and radioactivity data.

Run 11

Cell I, $C = 0.1$ gm./ℓ., $\alpha' = 15\%$, $M = 96{,}000$,
$V_{avg} = 21$ volts, $P_{avg} = 0.7$ watts

t (hr.)	R_T (ohm)	R_B(ohm)	Separation Factor
0.0	5,450	8,850	1.000
0.5	5,300	8,650	1.041
1.0	5,250	8,500	1.032
1.5	5,175	8,450	1.041
2.5	5,125	8,300	1.034
3.0	5,050	8,400	1.061
3.5	5,100	8,400	1.053
4.5	5,050	8,500	1.073
6.5	5,000	8,250	1.051
10.5	4,900	8,250	1.072
14.5	5,000	8,450	1.077

Run 15

Cell I, $C = 0.01$ gm./ℓ., $\alpha' = 50\%$, $M = 860{,}000$,
$V_{avg} = 50$ volts, $P_{avg} = 1.5$ watts

t (hr.)	R_T (ohm)	R_B (ohm)	Separation Factor
0.00	13,000	11,400	1.000
0.25	12,500	10,900	0.995
0.75	12,400	11,000	1.013
2.75	12,000	11,200	1.064
3.50	11,800	11,200	1.082
4.50	11,550	11,400	1.126
8.75	11,900	11,900	1.141
11.00	11,600	11,600	1.141
12.25	11,500	11,500	1.141

Run 16

Cell I, C = 0.01 gm./ℓ., α' = 50%, M = 860,000,
V_{avg} = 48 volts, P_{avg} = 1.7 watts

t (hr.)	R_T (ohm)	R_B (hm)	Separation Factor
0.00	10,400	11,100	1.000
0.50	9,700	10,500	1.015
1.75	9,500	10,400	1.026
2.25	9,500	10,600	1.045
2.75	9,500	10,600	1.045
3.75	9,400	10,550	1.051
4.75	9.300	10,600	1.067
5.75	9,200	10,600	1.079
6.75	9,100	10,500	1.081
9.75	9,200	10,600	1.079
13.25	9,400	10,800	1.075
14.25	9,400	10,600	1.057

Run 17

Cell I, C = 0.005 gm./ℓ., α' = 50%, M = 860,000,
V_{avg} = 80 volts, P_{avg} = 1.8 watts

t (hr.)	R_T (ohm)	R_B (ohm)	Separation Factor
0.00	26,000	28,700	1.000
0.25	25,400	28,000	1.000
0.75	24,800	27,800	1.016
1.25	24,600	27,800	1.023
1.75	24,200	28,000	1.050
2.25	24,200	27,900	1.045
2.75	23,800	27,700	1.055
4.75	23,300	26,900	1.048

Run 23A

Cell I, $C = 0.07$ gm./ℓ., $\alpha' = 15\%$, $M = 860{,}000$,
$V_{avg} = 75$ volts, $P_{avg} = 1.09$ watts

t (hr.)	R_T (ohm)	R_B (ohm)	Separation Factor
0.00	97,400	109,930	1.000
0.25	95,250	107,950	1.004
0.50	94,730	107,270	1.005
1.00	93.300	106,200	1.010
1.50	92.950	105,600	1.009
2.00	92,700	105,400	1.008
2.50	92,600	105,150	1.007
3.00	92,200	105,100	1.012
5.00	92,150	104,710	1.006
9.00	91,700	105,070	1.005
10.00	91,150	105,150	1.013

Run 23B

Cell I, $C = 0.07$ gm./ℓ., $\alpha' = 15\%$, $M = 860{,}000$,
$V_{avg} = 102$ volts, $P_{avg} = 1.65$ watts

t (hr.)	R_T (ohm)	R_B (ohm)	Separation Factor
0.00	97,400	109,930	1.000
11.00	86,500	105,400	1.081
15.00	85,240	105,900	1.102
16.75	84,400	105,850	1.112
22.50	83,280	105,030	1.121
23.50	82,290	105,020	1.122

Run 25

Cell I, C = 0.225 gm./ℓ., α' = 20%, M = 453,000,
V_{avg} = 35 volts, P_{avg} = 6.2 watts

t (hr.)	R_T (ohm)	R_B (ohm)	Separation Factor
0.00	4,800	5,778	1.000
0.50	4,300	4,910	0.952
1.00	3,920	4,500	0.952
1.50	3,800	4,355	0.951
3.00	3,605	4,010	0.948
4.25	3,590	4,115	0.953
5.00	3,615	4,140	0.951
6.50	3,510	4,055	0.959
9.50	3,535	4,060	0.957
9.75	3,485	4,060	0.968
13.00	3,440	4,035	0.976
21.50	3,365	4,010	0.996

Run 28

Cell I, C = 0.000225 gm./ℓ., α' = 20%, M = 453,000,
V_{avg} = 100 volts, P_{avg} = 2.1 watts

t (hr.)	R_T (ohm)	R_B (ohm)	Separation Factor
0.00	70,850	64,920	1.000
0.05	67,720	59,650	0.961
0.75	67,600	59,400	0.957
4.00	65,150	60,100	1.005
7.25	64,000	60,000	1.021
8.00	63,900	60,300	1.029
20.25	59,850	60,350	1.099
23.25	58,820	59,500	1.035
25.50	58,250	59,550	1.114
43.00	53,650	60,250	1.227
44.50	53,250	60,800	1.244
47.00	52,250	60,375	1.259
50.00	51,300	59,750	1.279
67.50	47,400	59,500	1.372
71.25	46,200	57,900	1.368

Run 30

Cell I, C = 0.000225 gm./ℓ., α' = 20%, M = 453,000,
V_{avg} = 100 volts, P_{avg} = 4.2 watts

t (hr.)	R_T (ohm)	R_B (ohm)	Separation Factor
0.00	34,120	45,450	1.000
0.50	31,100	40,850	1.000
1.00	29,950	39,600	1.016
1.50	29,550	39,050	1.016
2.00	29,100	38,500	1.016
3.75	28,100	37,650	1.030
5.00	28,050	37,700	1.034
12.50	24,650	35,350	1.102
23.00	23,900	33,500	1.077
24.75	23,500	33,300	1.093
26.50	23,200	33,100	1.100

Run 31

Cell I, C = 0.000225 gm./ℓ., α' = 20%, M = 453,000,
V_{avg} = 100 volts, P_{avg} = 1.3 watts

t (hr.)	R_T (ohm)	R_B (ohm)	Separation Factor
0.00	79,050	101,200	1.000
0.25	76,540	95,700	0.978
1.25	74,000	92,300	0.973
2.75	73,250	90,775	0.969
3.50	72,850	91,100	0.974
11.25	71,200	92,050	1.011
14.25	66,500	86,800	1.019
16.75	70,300	90,350	1.005
19.75	69,200	89,600	1.011
29.75	67,450	87,950	1.021

Run 32

Cell I, C = 0.000225 gm./ℓ., α' = 20%, M = 453,000,
V_{avg} = 100 volts, P_{avg} = 2.8 watts

t (hr.)	R_T (ohm)	R_B (ohm)	Separation Factor
0.00	57,660	50,040	1.000
0.50	55,200	46,800	0.978
0.75	54,000	46,150	0.983
1.75	49,100	44,325	1.037
4.75	46,400	41,875	1.041
7.00	46,850	43,850	1.092
8.75	45,350	42,920	1.093
9.75	45,200	43,000	1.098
10.75	45,100	43,100	1.101
11.75	44,000	42,950	1.126
20,75	44,000	43,800	1.149
22.25	44,075	43,800	1.146

Run 34

Cell I, C = 0.000225 gm./ℓ., α' = 20%, M = 453,000,
V_{avg} = 100 volts, P_{avg} = 2.6 watts

t (hr.)	R_T (ohm)	R_B (ohm)	Separation Factor
0.00	70,700	50,900	1.000
0.75	64,850	45,150	0.972
1.50	63,450	43,110	0.949
2.75	60,750	42,150	0.950
4.75	51,500	43,030	1.164
8.00	47,410	44,450	1.303
19.00	45,380	45,480	1.392
21.00	45,100	46,015	1.421
22.50	44,950	45,750	1.417
24.00	44,800	45,750	1.419
26.00	44,500	45,400	1.420

Run 38

Cell I, C = 0.005 gm./ℓ., α' = 20%, M = 1,180,000,
V_{avg} = 121 volts, P_{avg} = 1.75 watts

t (hr.)	R_T (ohm)	R_B (ohm)	Separation Factor
0.00	72,470	67,270	1.000
0.50	69,100	61,100	0.953
1.00	68,650	60,850	0.955
1.75	68,400	61,500	0.969
2.25	68,650	62,100	0.975
2.75	68,550	62,200	0.972
3.25	68,550	62,350	0.979
3.75	68,500	63,950	0.988
4.25	68,400	64,000	0.992
4.75	68,350	63,950	0.992

Run 39

Cell I, C = 0.005 gm./ℓ., α' = 20%, M = 1,180,000,
V_{avg} = 115 volts, P_{avg} = 1.85 watts

t (hr.)	R_T (ohm)	R_B (ohm)	Separation Factor
0.00	63,400	62,800	1.000
0.50	60,600	57,900	0.965
1.00	59,900	56,600	0.955
2.00	59,400	55,200	0.938
2.50	59,400	55,550	0.946
6.00	58,700	55,000	0.945
6.50	58,600	55,500	0.955
7.00	58,600	55,550	0.957
9.50	57,750	54,400	0.957

Run 40

Cell I, C = 0.01 gm./ℓ., α' = 20%, M = 1,180,000,
V_{avg} = 95 volts, P_{avg} = 1.8 watts

t (hr.)	R_T (ohm)	R_B (ohm)	Separation Factor
0.00	43,500	36,460	1.000
0.50	42,675	39,575	0.848
1.25	41,560	38,125	0.839
4.00	40,850	38,625	0.867
9.50	37,700	37,270	0.906
11.00	37,075	36,550	0.902

Run 41

Cell I, C - 0.01 gm./ℓ., α' 20%, M = 1,180,000,
V_{avg} = 104 volts, P_{avg} = 1.5 watts

t (hr.)	R_T (ohm)	R_B (ohm)	Separation Factor
0.00	55,500	66,100	1.000
0.50	54,000	62,550	0.974
1.00	53,000	61,300	0.971
1.50	52,400	60,900	0.976
3.50	51,200	59,700	0.978
4.75	50,800	59,350	0.981
6.50	50,400	59,150	0.987
7.75	50,300	58,900	0.984

Run 43

Cell I, C = 0.01 gm./ℓ., α' = 20%, M = 1,180,000,
V_{avg} = 100 volts, P_{avg} = 1.48 watts

t (hr.)	R_T (ohm)	R_B (ohm)	Separation Factor
0.00	17,020	58,000	1.000
0.50	16,900	54,350	0.944
1.00	16,670	52,835	0.932
2.00	16,550	51,800	0.919
4.50	16,575	51,850	0.919
7.00	16,600	51,550	0.913
8.75	16,450	51,300	0.916
18.50	16,300	51,760	0.932
19.25	16,350	51,900	0.934
20.25	16,300	52,150	0.941
21.25	16,335	51,950	0.936
22.75	16,250	52,600	0.952
25.00	16,260	52,200	0.945
31.75	16,270	52,050	0.943

Run 44

Cell I, C = 0.01 gm./ℓ., α' = 20%, M = 1,180,000,
V_{avg} = 98 volts, P_{avg} = 1.36 watts

t (hr.)	R_T (ohm)	R_B (ohm)	Separation Factor
0.00	18,000	58,000	1.000
1.25	17,490	51,950	0.923
2.00	17,960	51,750	0.922
4.00	17,415	51,600	0.921
5.75	17,445	51,650	0.921
16.75	17,415	52,775	0.940
18.50	17,405	52,700	0.940
19.75	17,325	52,850	0.947
21.75	17,315	52,600	0.944

Run 45

Cell I, C = 0.05 gm./ℓ., α' = 20%, M = 1,180,000,
V_{avg} = 52 volts, P_{avg} = 1.87 watts

t (hr.)	R_T (ohm)	R_B (ohm)	Separation Factor
0.00	13,380	17,000	1.000
0.50	12,750	15,640	0.966
1.00	12,575	15,370	0.963
1.75	12,490	15,260	0.963
2.50	12,435	15,205	0.963
3.50	12,415	15,195	0.964
5.50	12,400	15,185	0.965
6.50	12,370	15,250	0.973
7.75	12,300	15,240	0.978
9.00	12,280	15,250	0.980
21.75	12,185	15,305	0.992
22.25	12,170	15,370	0.996
24.00	12,125	15,295	0.993
25.75	12,100	15,220	0.993
26.00	12,135	15,370	0.997
27.75	12,840	15,240	1.000

Run 47

Cell I, C = 0.05 gm./ℓ., α' = 20%, M = 1,180,000,
V_{avg} = 53 volts, P_{avg} = 2.05 watts

t (hr.)	R_T (ohm)	R_B (ohm)	Separation Factor
0.00	13,140	18,080	1.000
0.50	12,555	16,760	0.971
1.00	12,400	16,395	0.961
2.00	12,000	16,150	0.979
2.75	11,855	16,100	0.987
5.75	11,630	15,915	0.994
6.50	11,710	15,835	0.985
6.75	11,715	15,880	0.986
7.50	11,600	15,790	0.990

Run 48

Cell I, C = 0.05 gm./ℓ., α' = 20%, M = 1,180,000,
V_{avg} = 45 volts, P_{avg} = 1.9 watts

t (hr.)	R_T (ohm)	R_B (ohm)	Separation Factor
0.00	12,660	4,676	1.000
0.50	12,150	4,316	0.959
1.00	11,770	4,260	0.981
1.75	11,950	4,200	0.949
3.75	11,760	4,135	0.947
5.25	11,735	4,115	0.946
7.25	11,700	4,116	0.949
9.75	11,500	4,123	0.970
11.25	11,310	4,138	0.990
18.50	11,350	4,190	0.999

Run 51

Cell I, C = 0.05 gm./ℓ., α' = 20%, M = 1,180,000,
V_{avg} = 50 volts, P_{avg} = 2.15 watts

t (hr.)	R_T (ohm)	R_B (ohm)	Separation Factor
0.00	14,750	4,780	1.000
0.50	13,750	4,412	0.991
1.25	14,100	4,285	0.949
2.00	14,150	4,220	0.935
2.50	14,125	4,245	0.938
13.75	14,150	4,432	0.975
14.50	14,150	4,454	0.986

Run 61

Cell II, C = 0.01 gm./ℓ., α' = 20%, M = 1,180,000,
V_{avg} = 82 volts, P_{avg} = 3.67 watts

t (hr.)	R_T (ohm)	R_B (ohm)	Separation Factor
0.00	47,300	45,400	1.000
0.75	42,300	40,100	0.989
1.75	42,400	38,955	0.958
2.75	42,225	38,015	0.935
3.75	41,485	37,305	0.934
4.75	39,950	36,615	0.956
6.25	39,175	35,725	0.951
9.00	38,250	34,600	0.942
16.75	37,200	33,275	0.934
18,25	36,870	32,970	0.932
19.00	36,800	32,930	0.934
20.25	36,600	32,725	0.932
21.00	36,450	32,700	0.934
22.25	36,425	32,500	0.930

W_T (c.)	W_F (c.)	W_B (c.)	Separation Factor
1,028,780	973,468*	976,353	1.054

Run 63

Cell II, C = 0.01 gm/ℓ., α' = 20%, M = 1,180,000,
V_{avg} = 93 volts, P_{avg} = 5.8 watts

t (hr.)	R_T (ohm)	R_B (ohm)	Separation Factor
0.00	62,400	47,500	1.000
0.50	57,100	42,300	0.972
1.75	56,900	42,450	0.981
2.75	57,500	41,500	0.949
4.75	52,600	42,650	1.067
14.75	47,050	42,665	1.193
16.75	46,700	42,150	1.186
19.00	46,250	42,435	1.190
20.50	46,300	42,515	1.240
21.75	45,800	41,850	1.205

W_T (c)	W_F (c.)	W_B (c)	Separation Factor
844,205	697,594*	809,352	1.043

Run 64

Cell II, C = 0.01 gm./ℓ., α' = 20%, M = 1,180,000,
V_{avg} = 93 volts, P_{avg} = 5.8 watts

t (hr.)	R_T (ohm)	R_B (ohm)	Separation Factor
0.00	67,000	40,000	1.000
0.50	62,700	34,850	0.930
1.25	56,150	36,130	1.075
2.75	46,700	36,260	1.296
6.25	43,950	35,920	1.366
18.00	37,370	35,550	1.590
18.50	37,515	35,630	1.587

W_T (c.)	W_F (c.)	W_B (c.)	Separation Factor
955,674	942,585*	945,412	1.011

Run 65

Cell II, C = 0.01 gm./ℓ., α' = 20%, M = 1,180,000,
V_{avg} = 60 volts, P_{avg} = 4.55 watts

t (hr.)	R_T (ohm)	R_B (ohm)	Separation Factor
0.00	49,200	48,700	1.000
1.00	51,000	52,000	1.062
1.75	51,500	55,250	1.086
2.75	51,200	58,000	1.149
5.50	50,400	58,000	1.169

W_T (c.)	W_F (c)	W_B (c.)	Separation Factor
1,274,690	1,209,489	1,025,020	1.243

Run 66

Cell II, $C = 0.01$ gm./ℓ., $\alpha' = 20\%$, $M = 1{,}180{,}000$,
$V_{avg} = 93$ volts, $P_{avg} = 4.1$ watts

t (hr.)	R_T (ohm)	R_B (ohm)	Separation Factor
0.00	61,300	51,000	1.000
0.75	55,950	47,900	1.030
1.50	57,515	48,835	1.022
2.75	57,710	50,450	1.050
4.00	57,650	50,600	1.055
5.00	57,600	50,420	1.051
5.50	57,500	50,420	1.053
11.00	57,350	50,200	1.055
11.75	57,100	50,120	1.055
22.00	56,500	50,000	1.064
22.50	56,550	50,135	1.065

W_T (c.)	W_F (c.)	W_B(c.)	Separation Factor
967,501	959,873	918,727	1.053

Run 67

Cell II, $C = 0.01$ gm./ℓ., $\alpha' = 20\%$, $M = 1{,}180{,}000$
$V_{avg} = 117$ volts, $P_{avg} = 5.02$ watts

t (hr.)	R_T (ohm)	R_B (ohm)	Separation Factor
0.00	64,400	59,200	1.000
0.50	65,000	61,550	1.029
1.00	64,000	62,410	1.057
2.00	63,700	62,600	1.069
6.25	62,500	61,400	1.067
17.50	61,100	60,425	1.074
22.25	60,875	60,825	1.084

W_T (c.)	W_F (c.)	W_B (c.)	Separation Factor
2,018,588	2,030,858	1,994,262	1.012

Run 68

Cell II, C = 0.01 gm./ℓ., α' = 20%, M = 1,180,000,
V_{avg} = 115 volts, P_{avg} = 4.53 watts

t (hr.)	R_T (ohm)	R_B (ohm)	Separation Factor
0.00	67,700	66,600	1.000
0.25	65,850	66,375	1.025
2.50	63,500	64,750	1.036
4.00	63,150	64,150	1.033
5.75	62,750	63,200	1.025
17.25	63,000	62,300	1.005
18.25	62,650	61,565	0.998
20.25	62,800	61,450	0.995
22.25	62,450	60,900	0.992

W_T (c.)	W_F (c.)	W_B (c.)	Separation Factor
2,018,042	2,121,454	2,111,602	0.956

Run 69

Cell II, C = 0.01 gm./ℓ., α' = 20%, M = 1,180,000,
V_{avg} = 118 volts, P_{avg} = 4.53 watts

t (hr.)	R_T (ohm)	R_B (ohm)	Separation Factor
0.00	72,700	78,600	1.000
1.25	67,600	71,570	0.980
2.25	67,050	70,000	0.967
3.00	66,850	69,700	0.965
4.00	66,550	69,200	0.962
8.25	66,300	69,200	0.966
10.00	65,900	68,815	0.966
20.75	65,250	68,800	0.974
22.50	65,000	68,800	0.979
23.75	64,935	68,800	0.981

W_T (c.)	W_F (c.)	W_B(c.)	Separation Factor
2,102,373	2,136,349	2,074,904	1.013

Run 70

Cell II, C = 0.01 gm./ℓ., α' = 35%, M = 1,180,000,
V_{avg} = 92.5 volts, P_{avg} = 4.48 watts

t (hr.)	R_T (ohm)	R_B (ohm)	Separation Factor
0.00	44,500	48,230	1.000
0.50	42,200	45,640	0.997
1.25	41,800	45,025	0.993
2.25	41,200	44,900	1.003
4.00	40,650	44,960	1.020
4.75	40,650	44,900	1.019
12.50	40,120	44,210	1.017
23.75	39,800	43,800	1.016

W_T (c.)	W_F (c.)	W_B (c.)	Separation Factor
1,610,249	1,623,270	1,547,994	1.040

Run 71

Cell II, C = 0.01 gm./ℓ., α' = 35%, M = 1,180,000,
V_{avg} = 96 volts, P_{avg} = 4.95 watts

t (hr.)	R_T (ohm)	R_B (ohm)	Separation Factor
0.00	44,900	46,400	1.000
1.25	41,450	41,750	0.975
2.50	41,275	41,250	0.967
3.50	41,370	41,060	0.960
5.00	41,050	40,435	0.951
20.50	40,700	39,475	0.938
22.25	40,800	39,600	0.938

W_T (c.)	W_F (c.)	W_B (c.)	Separation Factor
2,157,968	2,186,102	2,188,923	0.986

Run 72

Cell II, C = 0.01 gm./ℓ., α' = 35%, M = 1,180,000,
V_{avg} = 94 volts, P_{avg} = 5.05 watts

t (hr.)	R_T (ohm)	R_B (ohm)	Separation Factor
0.00	42,630	41,200	1.000
1.25	42,000	39,800	0.981
2.25	41,550	39,450	0.983
3.75	40,900	38,800	0.982
5.50	40,500	37,900	0.968
9.75	40,000	36,500	0.945
22.50	39,700	34,880	0.911

W_T (c.)	W_F (c.)	W_B (c.)	Separation Factor
736,547	744,660	742,819	0.991

Run 73

Cell II, C = 0.01 gm./ℓ., α' = 35%, M = 1,180,000,
V_{avg} = 89 volts, P_{avg} = 4.5 watts

t (hr.)	R_T (ohm)	R_B (ohm)	Separation Factor
0.00	44,300	38,200	1.000
3.00	41,500	37,190	0.973
5.75	41,250	36,625	0.964
15.75	40,700	36,190	0.965
17.50	40,650	36,365	0.970
19.25	40,400	36,425	0.972
21.00	40,450	36,460	0.977

W_T (c.)	W_F (c.)	W_B (c.)	Separation Factor
1,466,764	1,483,119	1,477,048	0.993

Run 75

Cell II, C = 0.01 gm./ℓ., α' = 20%, M = 1,180,000,
V_{avg} = 122 volts, P_{avg} = 4.45 watts

t (hr.)	R_T (ohm)	R_B (ohm)	Separation Factor
0.00	64,850	74,500	1.000
1.25	60,650	45,720	0.656
3.00	60,400	43,950	0.634
4.00	60,100	43,600	0.631
6.50	59,700	42,425	0.618
17.75	58,400	41,750	0.624
20.25	57,350	41,300	0.627
23.00	57,250	41,375	0.630
23.50	57,200	41,175	0.628
25.50	56,800	40,300	0.620

W_T (c.)	W_F (c.)	W_B (c.)	Separation Factor
980,763	977,514	970,192	1.010

Run 76

Cell II, C = 0.01 gm./ℓ., α' = 20%, M = 1,180,000,
V_{avg} = 110 volts, P_{avg} = 4.5 watts

t (hr.)	R_T (ohm)	R_B (ohm)	Separation Factor
0.00	57,400	55,000	1.000
1.00	52,650	32,600	0.666
2.00	52,350	31,200	0.613
3.50	52,050	30,250	0.616
12.00	52,550	28,945	0.576
13.25	52,400	28,815	0.575
16.25	52,400	28,645	0.573
18.25	52,400	28,430	0.567
20.25	52,050	28,000	0.562
23.50	52,250	28,050	0.561

W_T (c.)	W_F (c.)	W_B (c.)	Separation Factor
842,937	854,090	875,728	0.961

Run 78

Cell II, C = 0.01 gm./ℓ., α' = 20%, M = 1,180,000,
V_{avg} = 108 volts, P_{avg} = 4.5 watts

t (hr.)	R_T (ohm)	R_B (ohm)	Separation Factor
0.00	58,100	18,325	1.000
1.25	57,600	16,220	0.892
3.00	57,300	16,155	0.894
12.50	57,000	16,120	0.896
14.75	56,200	15,990	0.902
17.50	56,200	15,920	0.900
20.25	56,250	15,860	0.894
23.75	56,050	15,790	0.893

W_T (c.)	W_F (c.)	W_B (c.)	Separation Factor
1,198,185	1,194,367	1,187,437	1.009

Run 82

Cell II, C = 0.0015 gm./ℓ., α' = 20%, M = 1,180,000,
V_{avg} = 140 volts, P_{avg} = 4.45 watts

t (hr.)	R_T (ohm)	R_B (ohm)	Separation Factor
0.00	140,200	98,500	1.000
0.50	125.200	84,700	0.964
1.00	122,700	82,800	0.962
1.75	119,800	81,500	0.972
3.50	116,700	79,700	0.974
5.50	108,200	77,300	1.015
7.00	104,700	77,000	1.050
17.00	99,400	73,300	1.051
19.00	97,600	72,700	1.063
23.00	96,800	71,000	1.052

W_T (c.)	W_F (c.)	W_B (c.)	Separation Factor
321,860	293,449*	298,213	1.097

*Indicates feed sample was in glass sample bottle during run.

APPENDIX VII

Experimental Separation Factor Curves

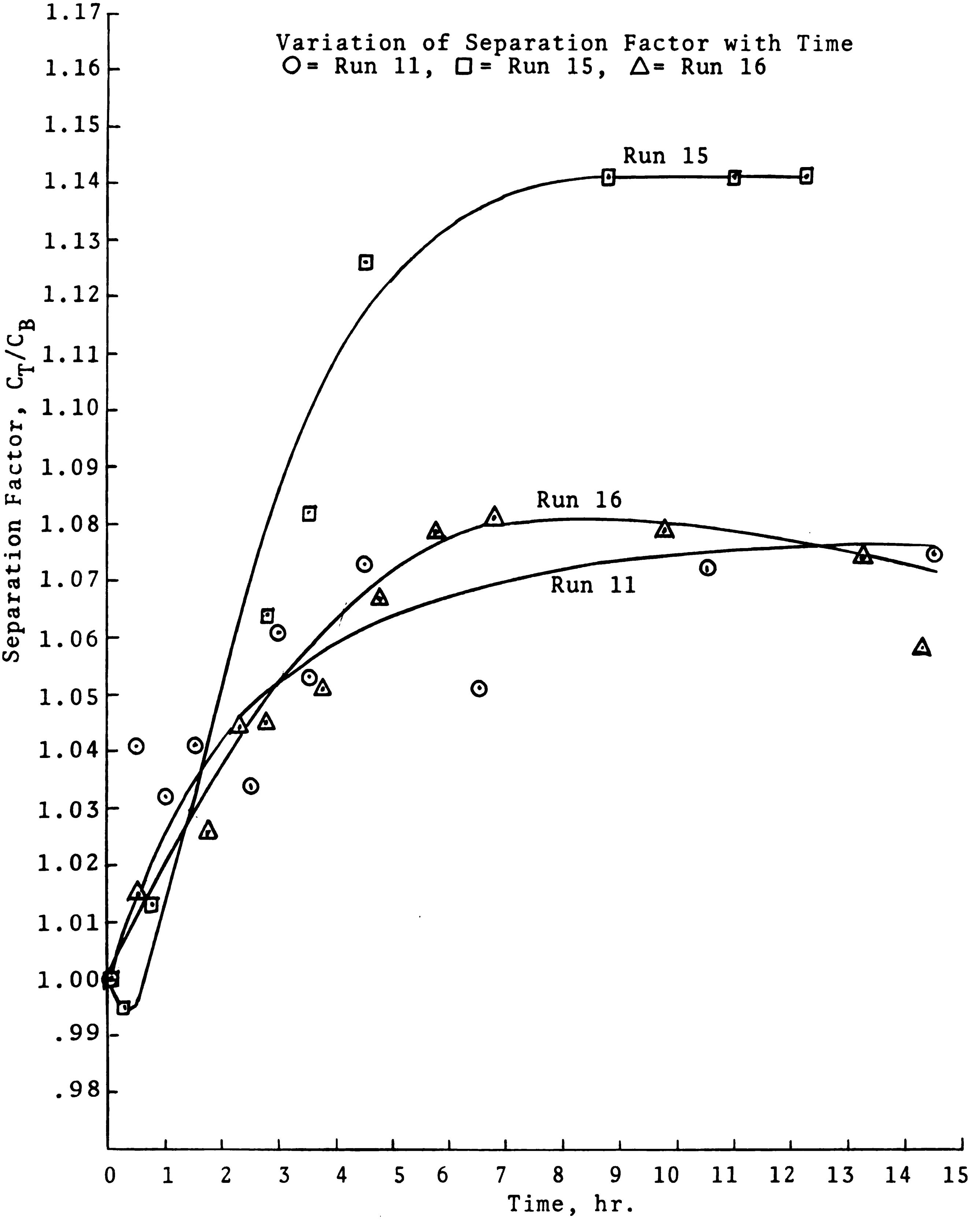
Variation of Separation Factor with Time
○= Run 11, □= Run 15, △= Run 16
Run 15
Run 16
Run 11
Separation Factor, C_T/C_B
1.17
1.16
1.15
1.14
1.13
1.12
1.11
1.10
1.09
1.08
1.07
1.06
1.05
1.04
1.03
1.02
1.01
1.00
.99
.98
0
1
2
3
4
5
6
7
8
9
10
11
12
13
14
15
Time, hr.

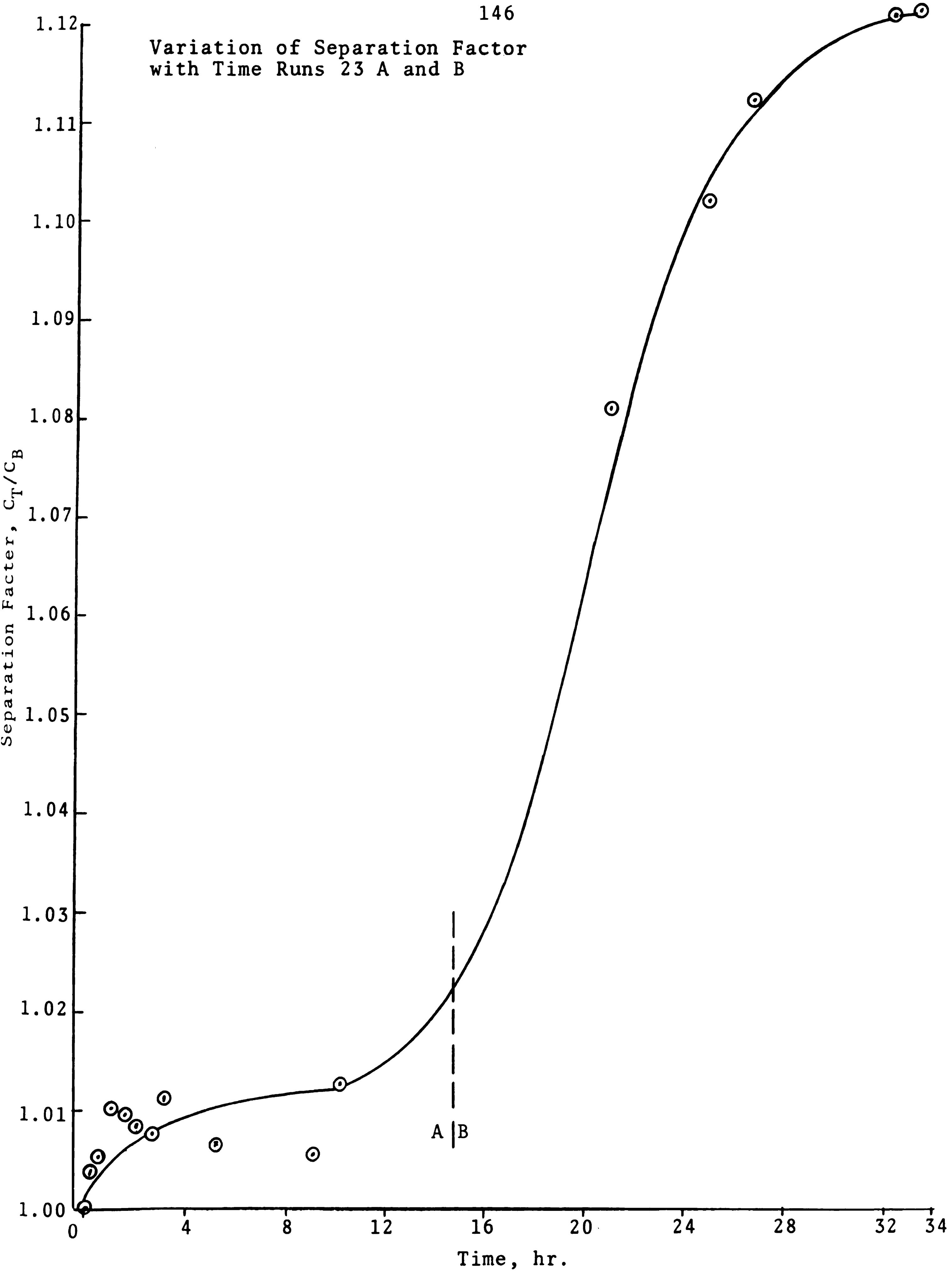

Variation of Separation Factor with Time Runs 23 A and B

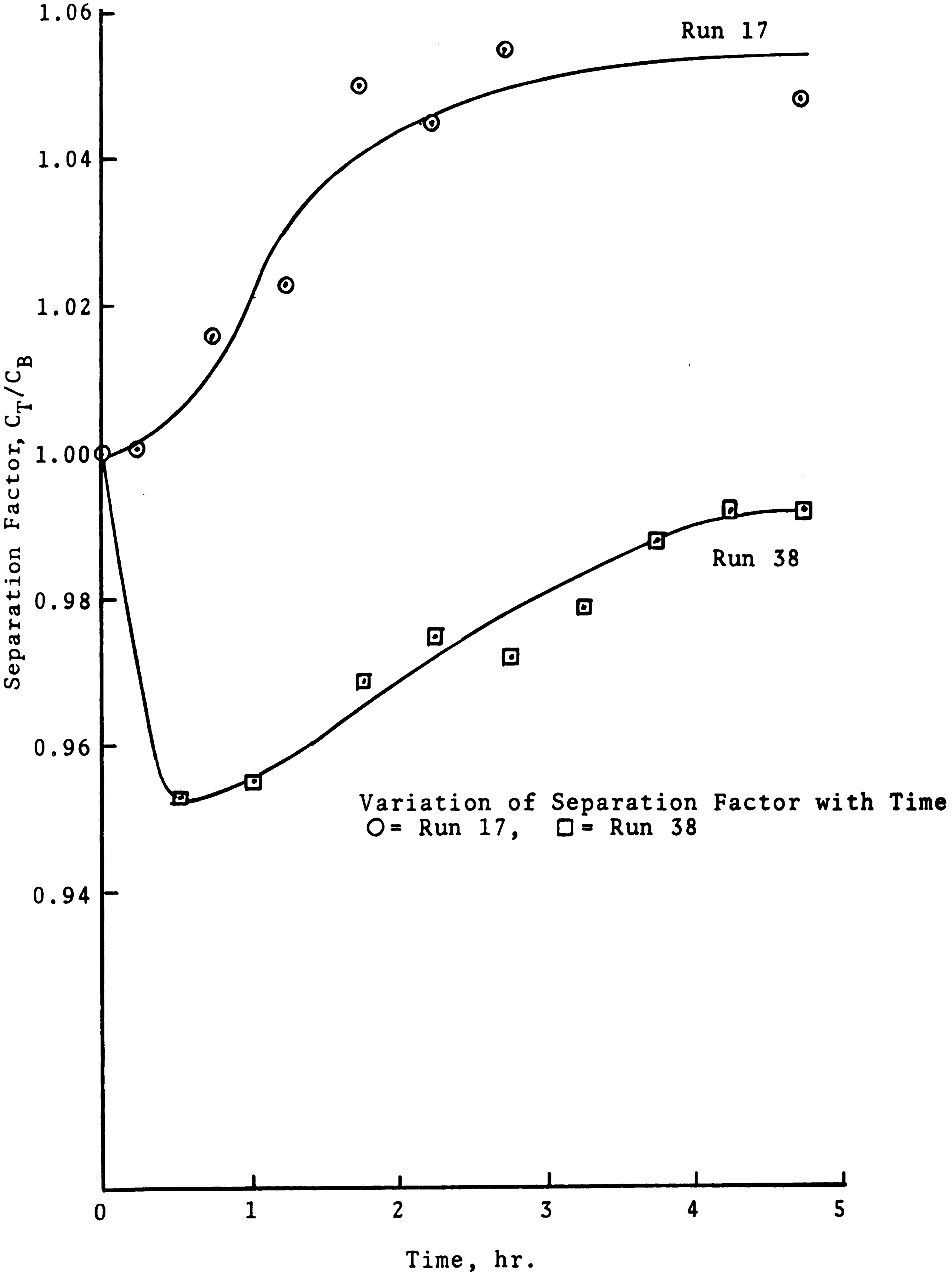

Variation of Separation Factor with Time
○= Run 17, □= Run 38

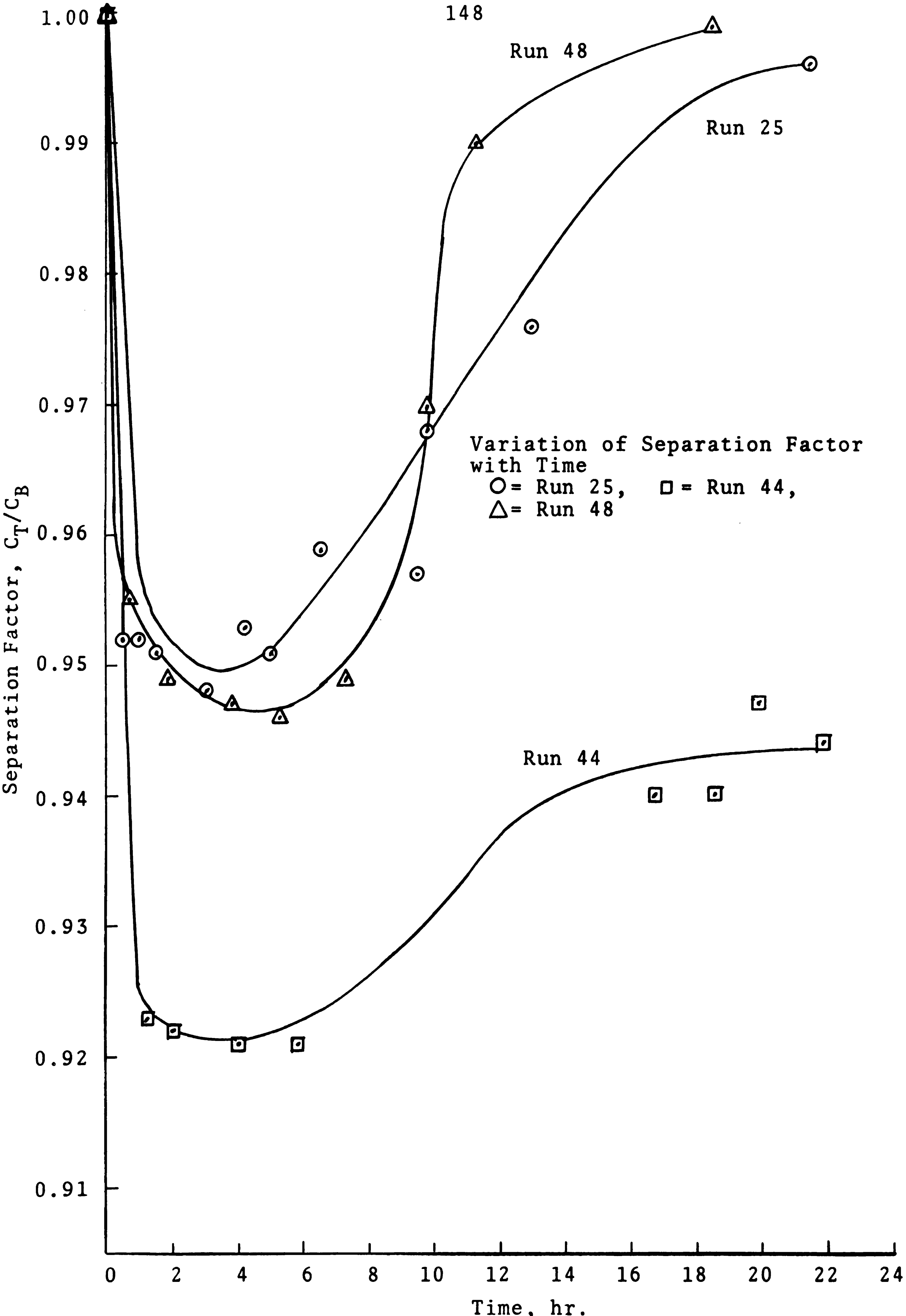

Variation of Separation Factor with Time
○= Run 25, ▫= Run 44,
△= Run 48

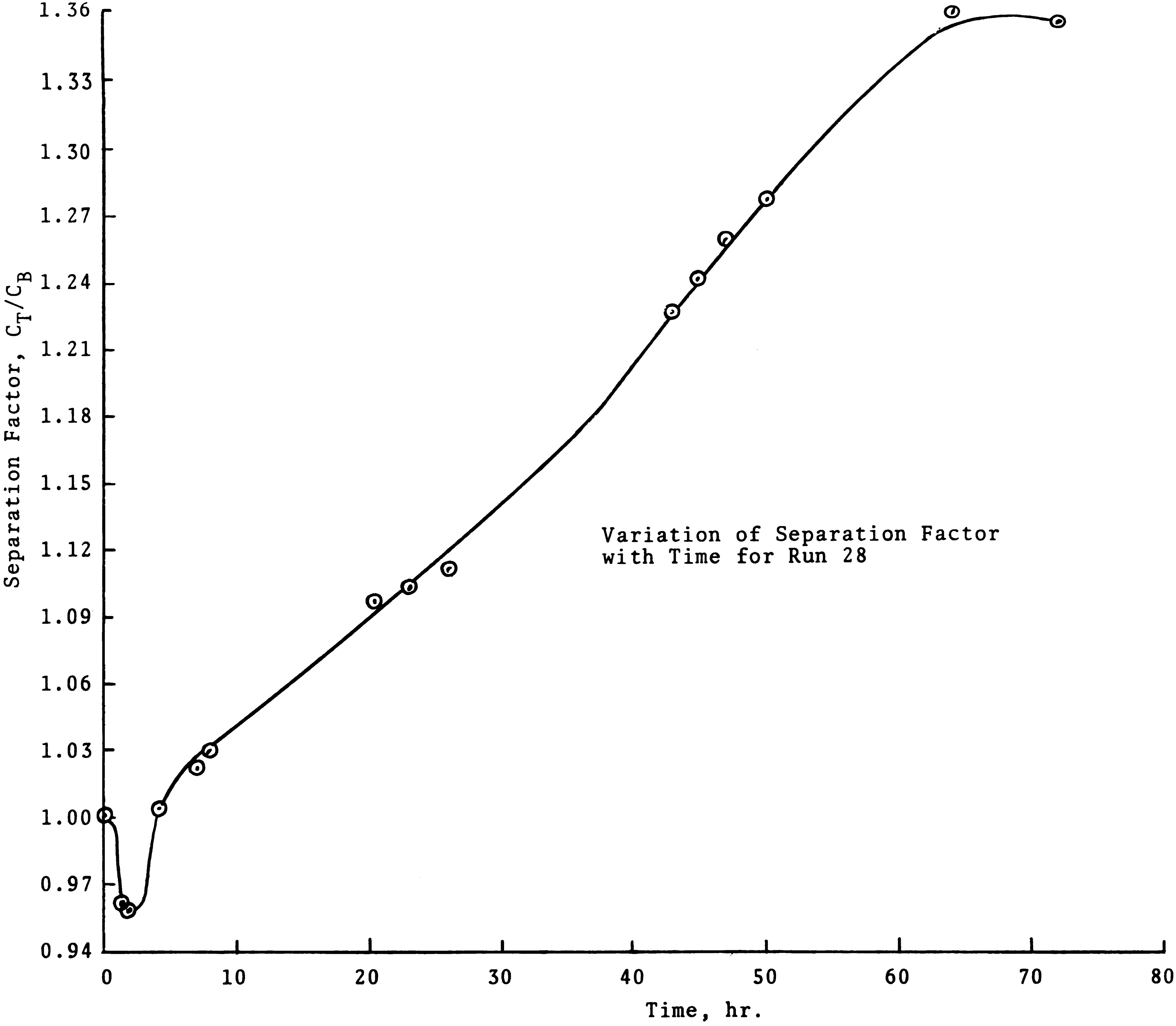

Variation of Separation Factor
with Time for Run 28

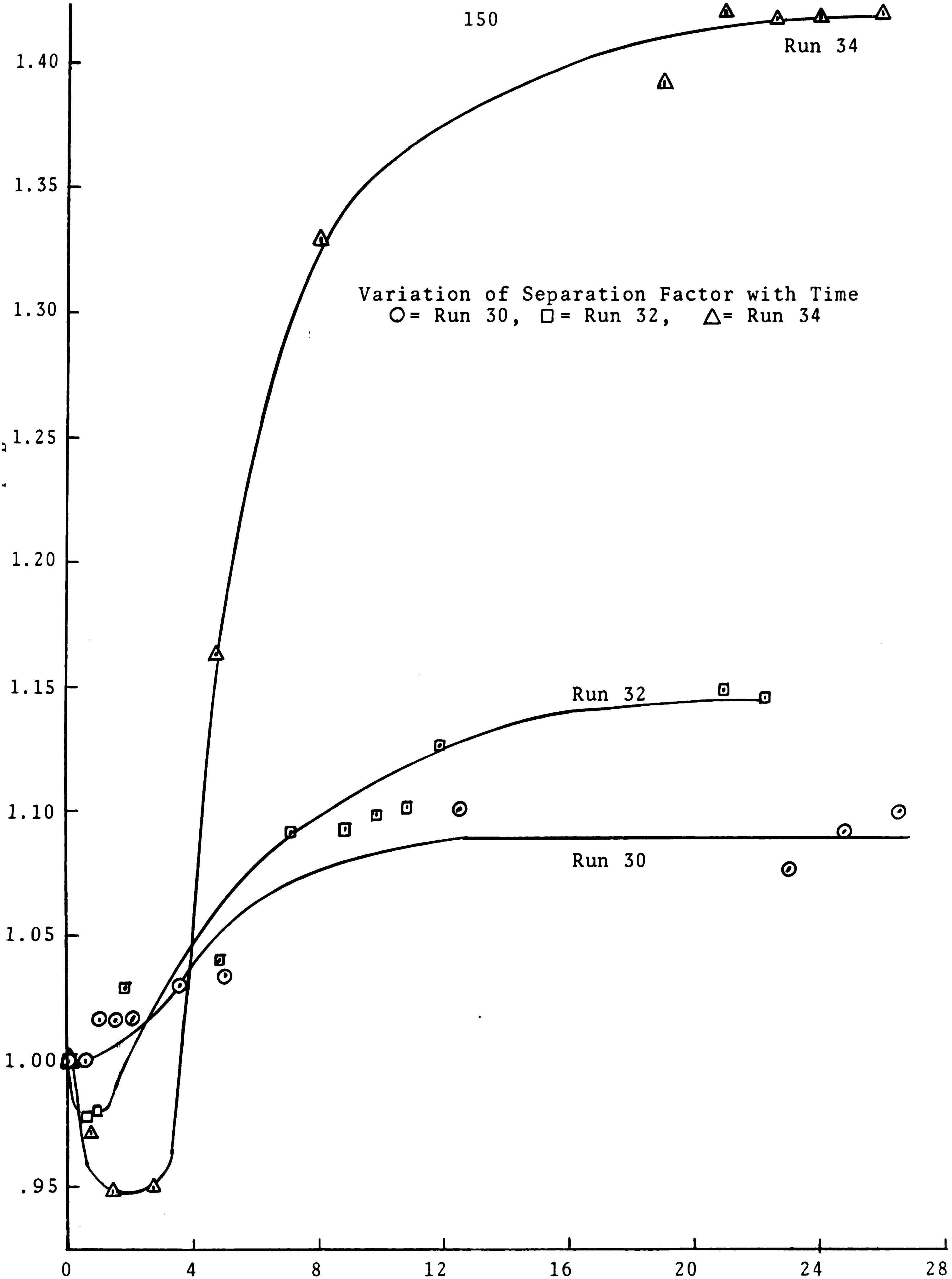
Variation of Separation Factor with Time
○= Run 30, □= Run 32, △= Run 34
Run 34
Run 32
Run 30
1.40
1.35
1.30
1.25
1.20
1.15
1.10
1.05
1.00
.95
0
4
8
12
16
20
24
28

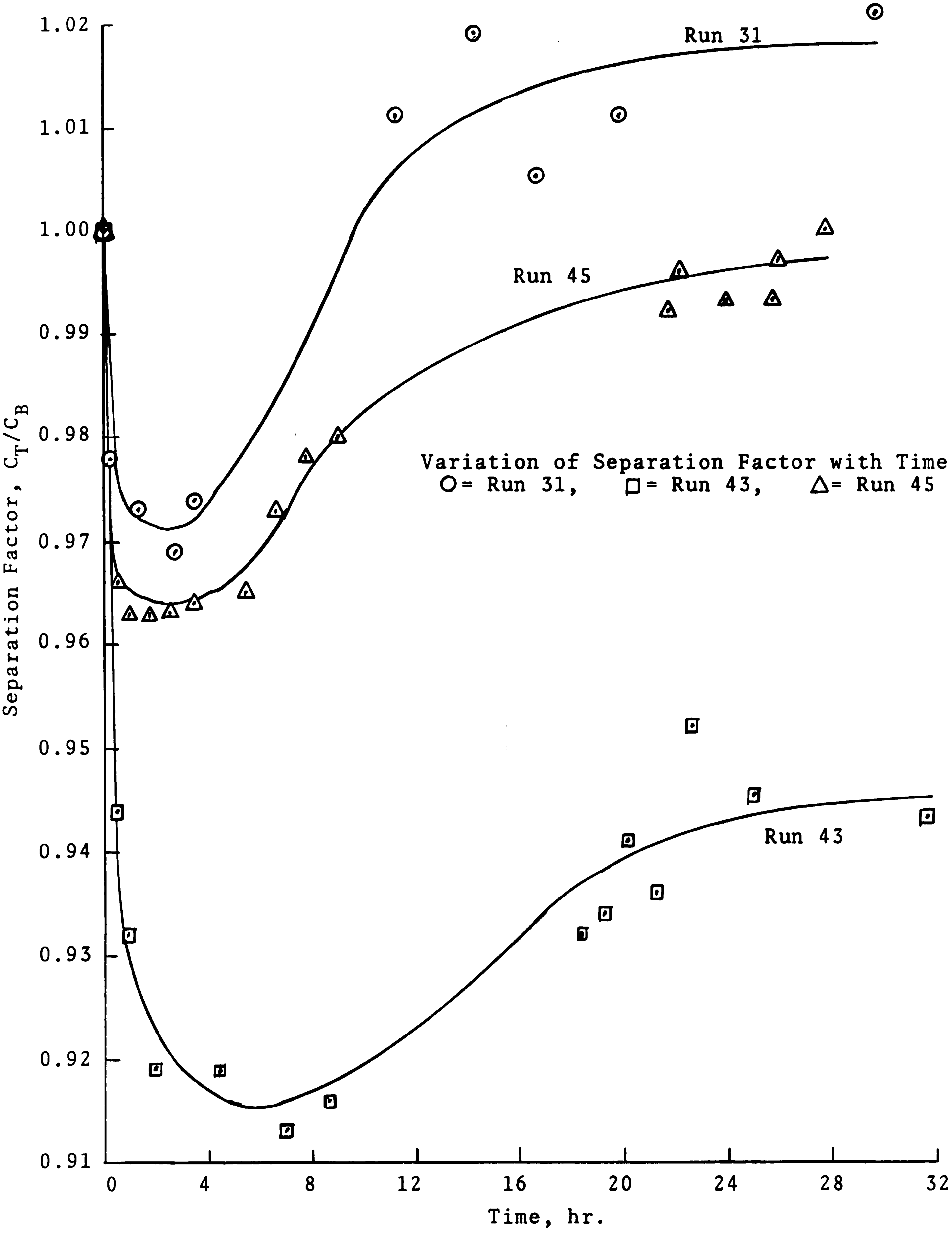
1.02
1.01
1.00
0.99
0.98
0.97
0.96
0.95
0.94
0.93
0.92
0.91
Separation Factor, C_T/C_B
0
4
8
12
16
20
24
28
32
Time, hr.
Run 31
Run 45
Run 43
Variation of Separation Factor with Time
○= Run 31, □= Run 43, △= Run 45

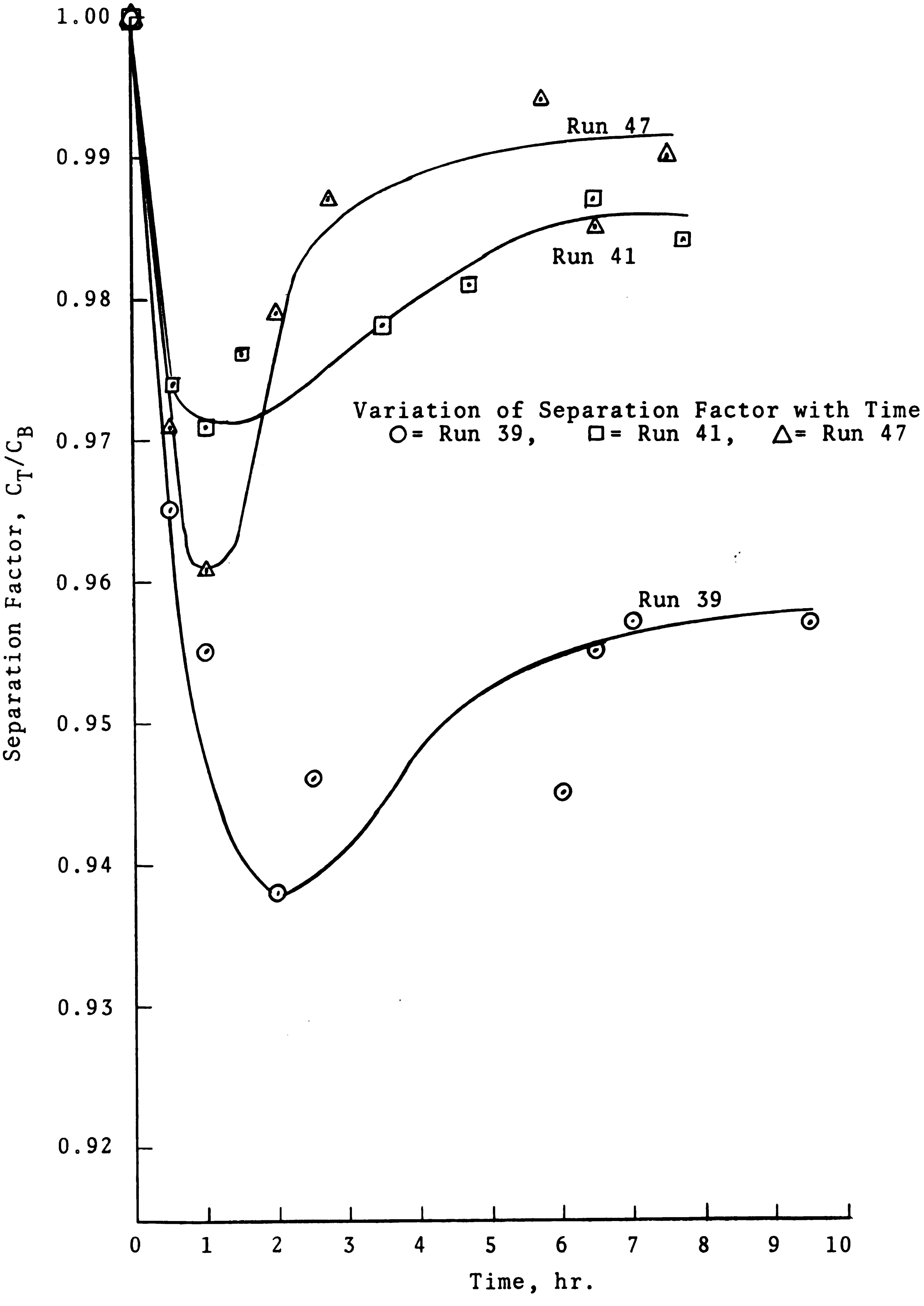

Variation of Separation Factor with Time

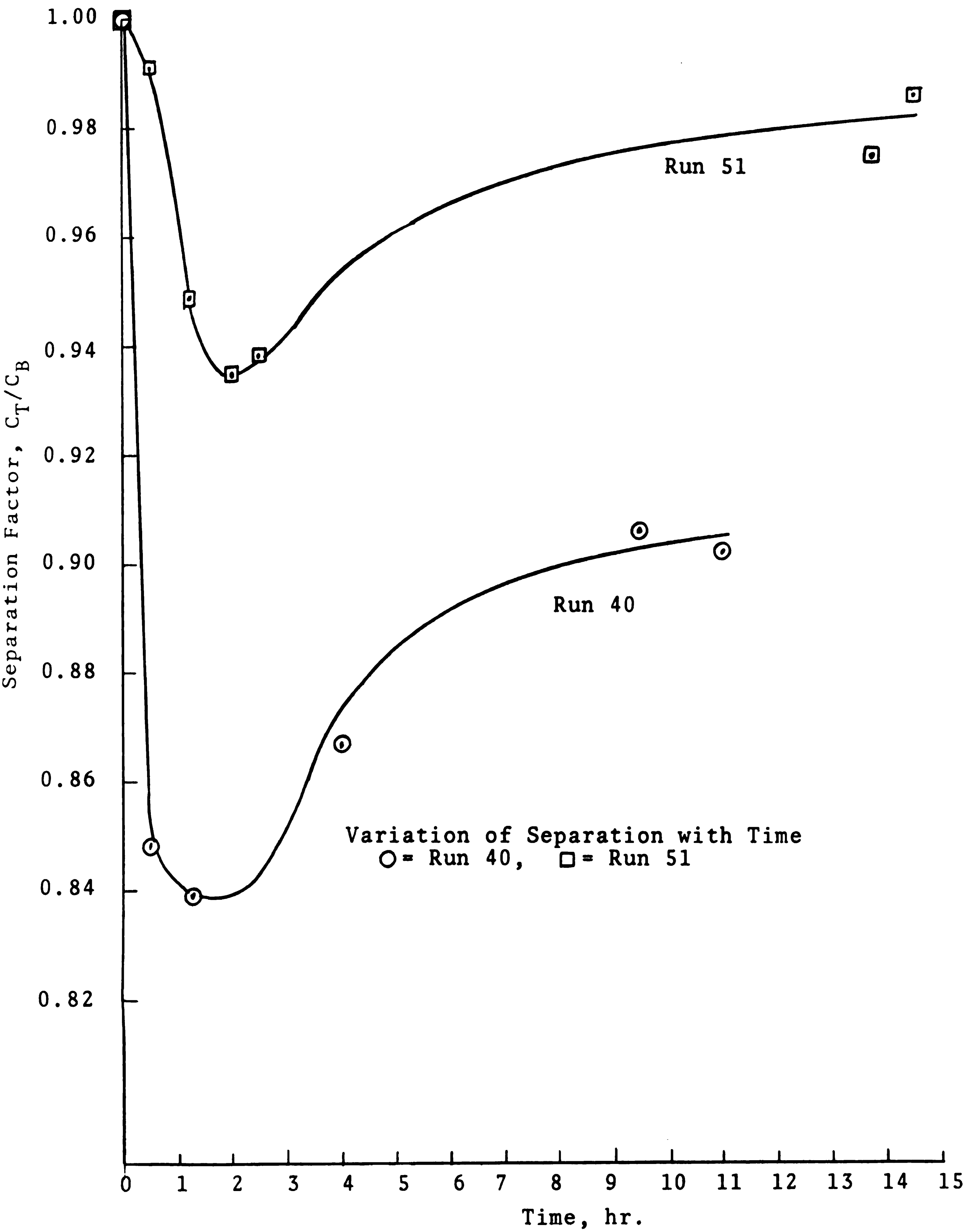

Variation of Separation with Time

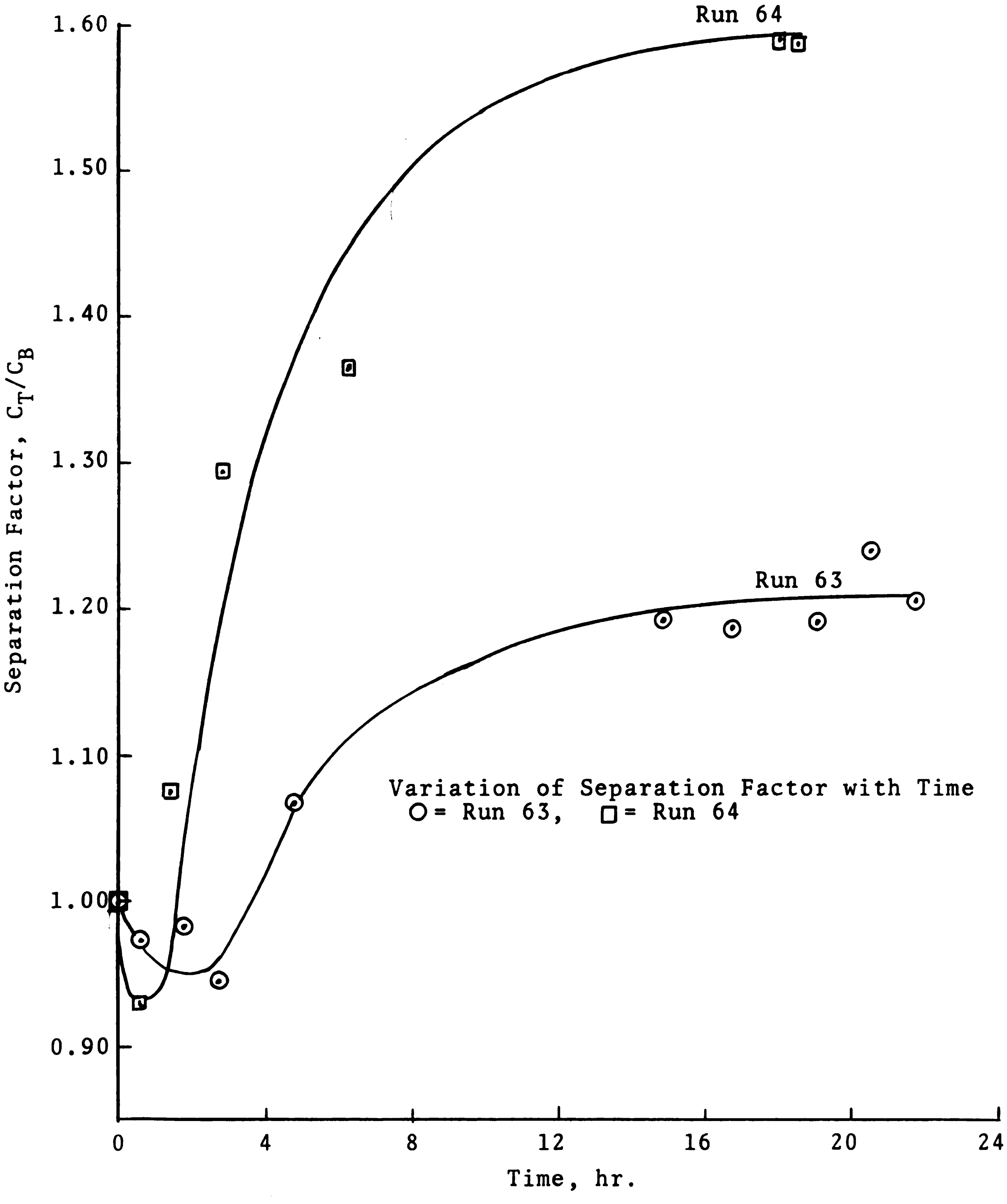

Variation of Separation Factor with Time
○ = Run 63, □ = Run 64

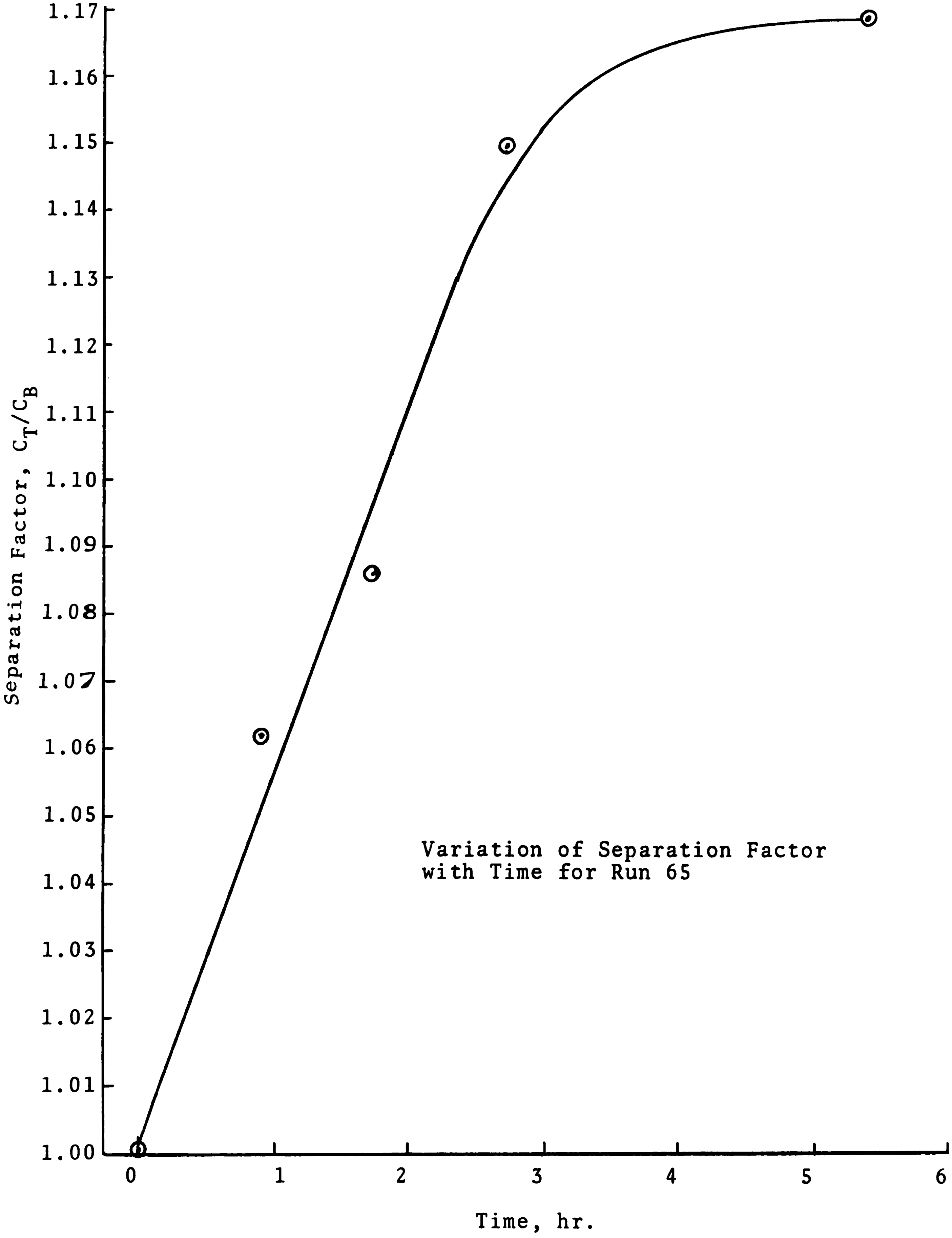

Variation of Separation Factor with Time for Run 65

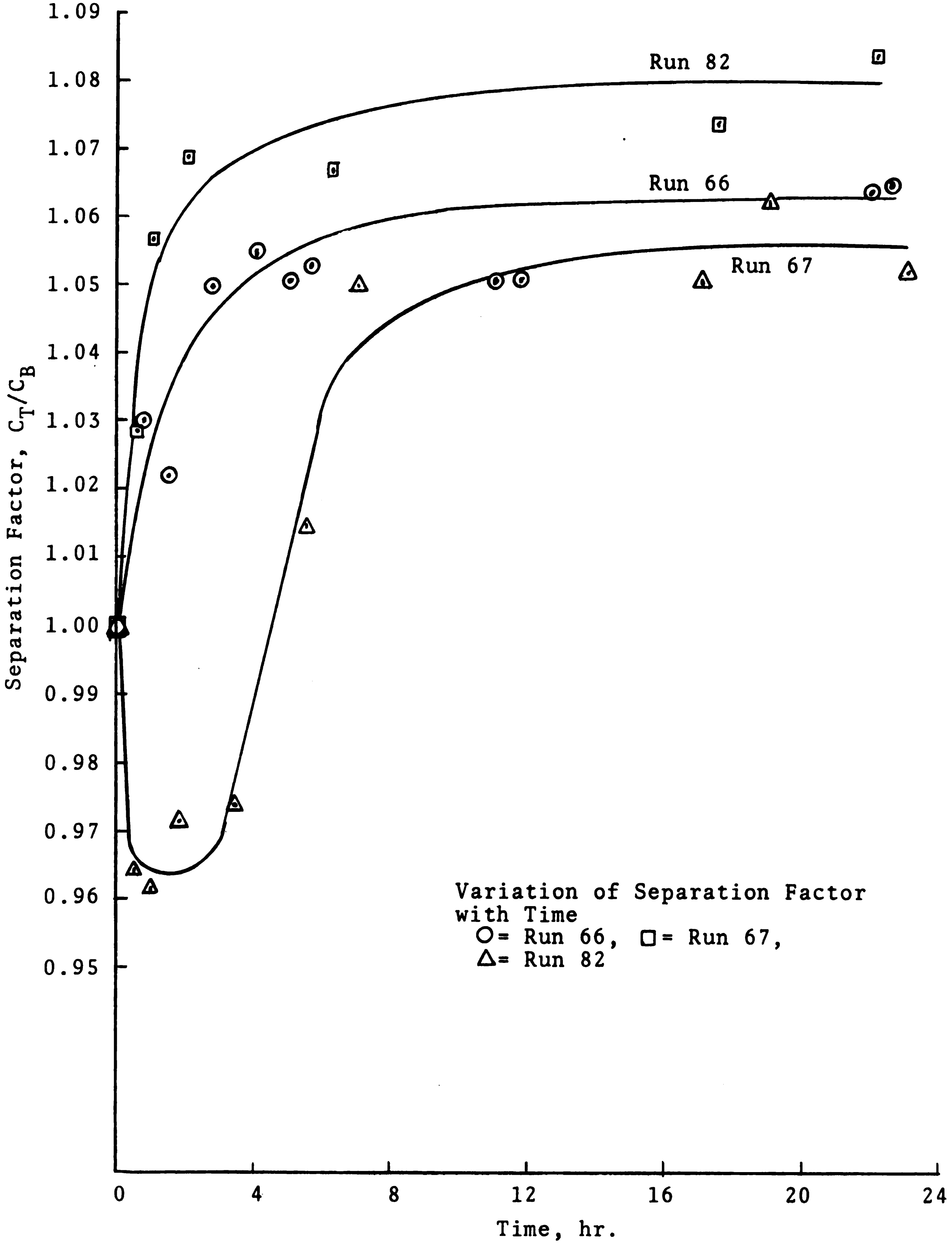

Variation of Separation Factor with Time
○= Run 66, □= Run 67,
△= Run 82

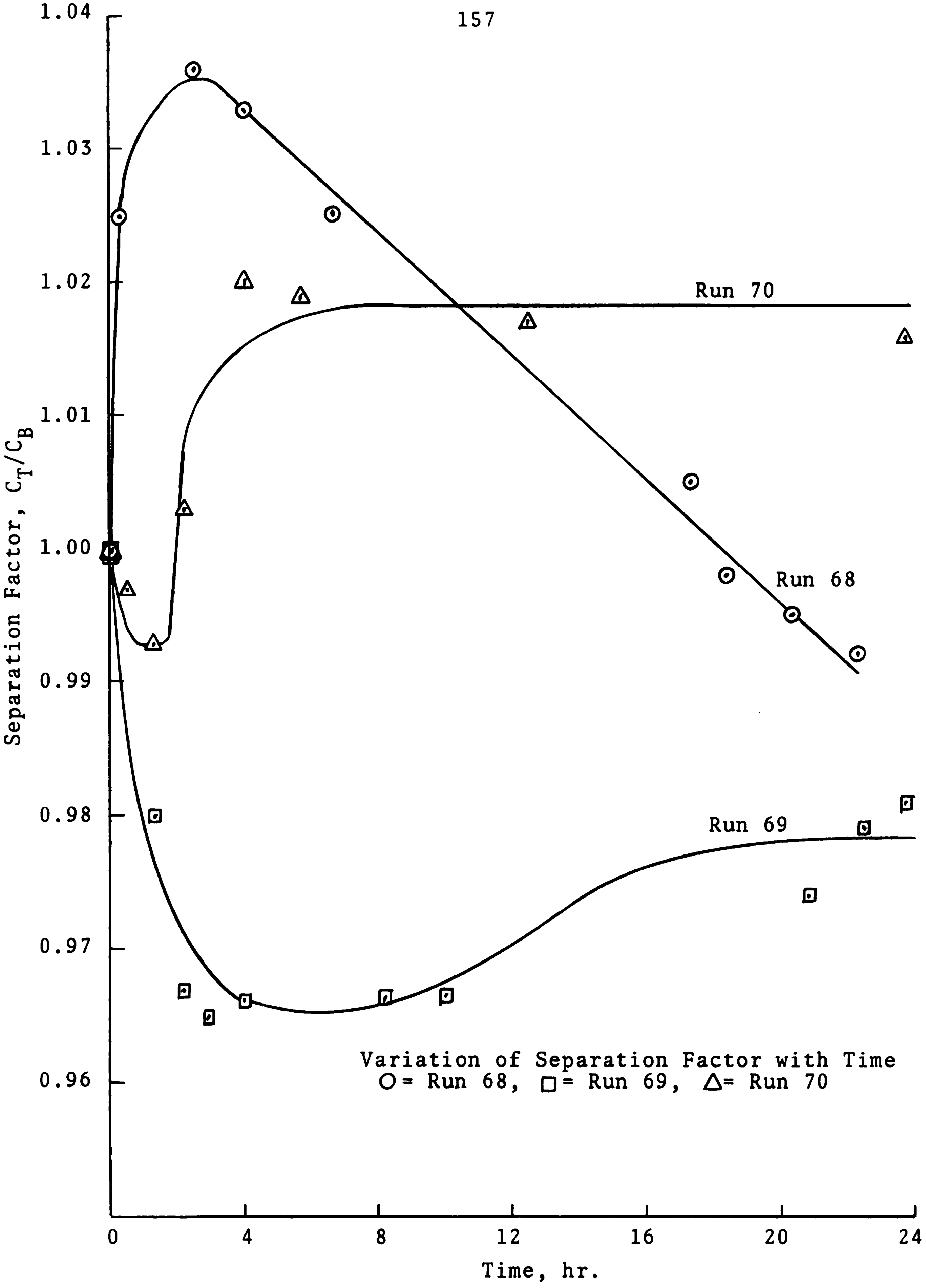

Variation of Separation Factor with Time

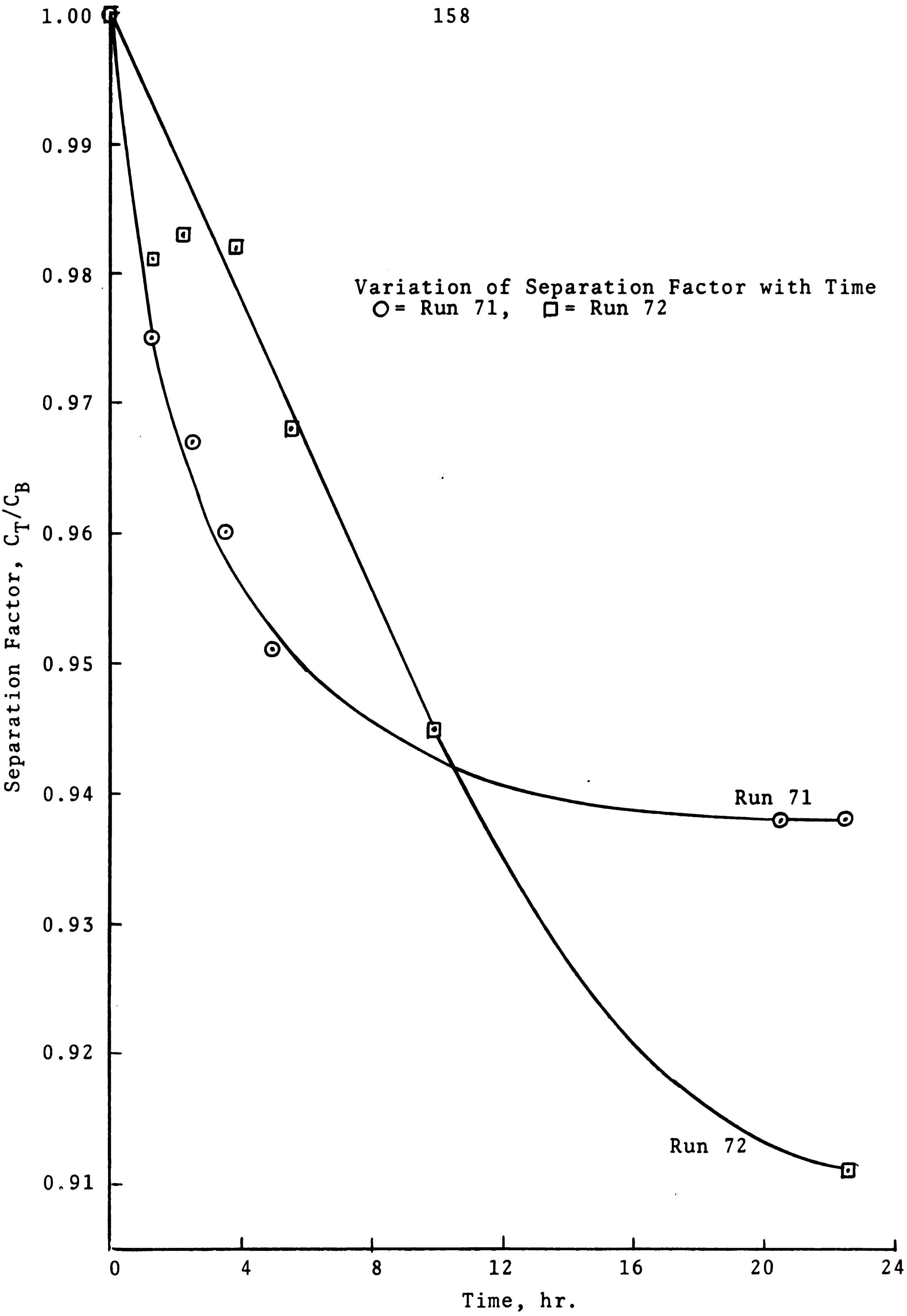

Variation of Separation Factor with Time
○= Run 71, □= Run 72

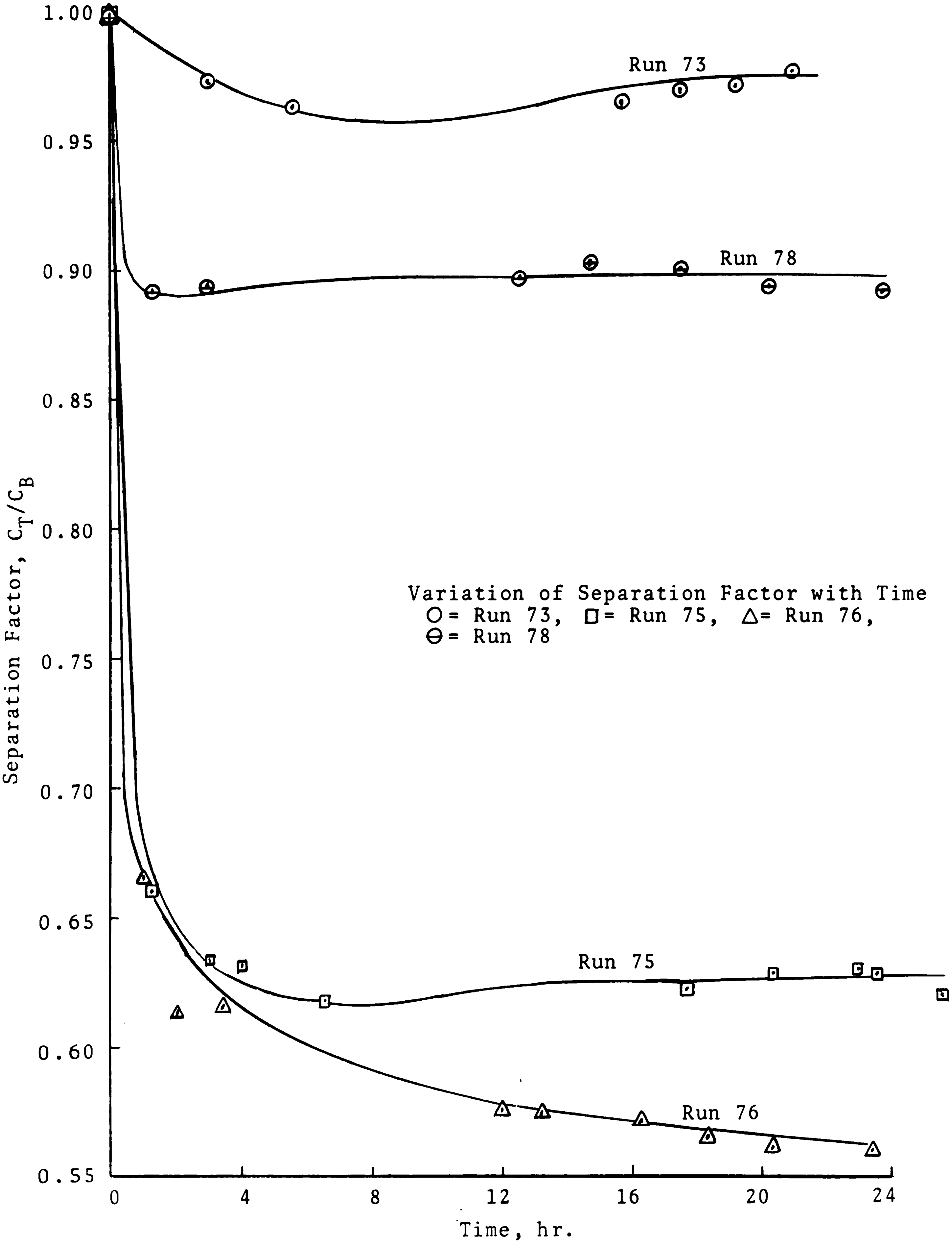
Separation Factor, C_T/C_B
1.00
0.95
0.90
0.85
0.80
0.75
0.70
0.65
0.60
0.55
Time, hr.
0
4
8
12
16
20
24
Run 73
Run 78
Run 75
Run 76
Variation of Separation Factor with Time
○ = Run 73, □ = Run 75, △ = Run 76,
⊖ = Run 78

APPENDIX VIII

Sample Polarizability and Separation Factor Calculations

APPENDIX VIII

Sample Polarizability and Separation Factor Calculations

Theoretical Polarizabilities:

The theoretically predicted polarizability, α_p, is calculated from the approximate expression[10]

$$\alpha_p = \frac{\varepsilon_s \ell^3}{24 \ell n 2p} \qquad \text{(VIII-1)}$$

where

ε_s = the dielectric constant of the solvent

ℓ = end to end length of the molecule

p = ratio of molecular length to diameter.

The end to end length of the molecule is obtained from an expression given by Krause[36] and alternately from molecular bond calculations. Considering the former method, the relationship for the root mean square end to end length for unneutralized polymer is

$$\overline{(\ell^2)}^{\frac{1}{2}} = \ell = GM^d \qquad \text{(VIII-2)}$$

where

G = 0.69 for P.M.A.

d = 0.49 for P.M.A.

M = polymer molecular weight.
For polymer of molecular weight 1.18×10^6, the length calculated from Equation (VIII-2) is 678 A^o.

The expansion ratio for polymethacrylic acid at 20 percent neutralization[49] is 4.935. Multiplying this times the polymer's unneutralized length gives 3.34×10^{-5} cm. as the theoretical length of the 20 percent neutralized P.M.A. molecule. Substituting this in Equation (VIII-1), using $\varepsilon_s \simeq 80$ for water at 20^o C. and and $p \simeq 10^4$, the theoretical polarizability is found to be 1.26×10^{-14} cm.^{3}.

The second method of calculating ℓ is to determine the end to end length of a completely extended P.M.A. molecule from bond length and angle considerations. For P.M.A. the carbon-carbon bond distance along the polymer chain should be 1.54 A^o. Since the angle between neighboring bonds is about 105^o, the length of a repeating unit is 2.46 A^o. Multiplying this by the degree of polymerization ($\simeq$ 1500) gives a fully extended polyion length of 3.72×10^{-4} cm. At 20 percent neutralization, the polyion end to end distance is 29.25 percent of its fully extended length.[49] Multiplying 0.2925 times 3.72×10^{-4} cm. gives the polymer end to end distance equal to 1.09×10^{-4} cm. Using this in Equation (VIII-1) as before, the molecular polarizability is 4.38×10^{-13} cm.^{3}.

Experimental Polarizabilities:

The molecular polarizability may be determined experimentally by calculation from Equation (122) using the equilibrium radial concentration ratios obtained from the forced feed runs for cells I and II. Equation (122) in its appropriate form is

$$\frac{C_i}{C_o} = \exp \frac{\alpha_p (\Delta V)^2}{2\nu kT\, R_i^2\, \ell n^2\, \kappa}, \qquad \text{(VIII-3)}$$

where for the experimental conditions using cell I:

$\Delta V \simeq 100$ volts $\simeq 0.333$ e.s.u.

$k = 1.38 \times 10^{-16}$ ergs/^oC.

$T = 300^oK$

$\kappa = 36$

$\nu \simeq 2,350$ (for 20 percent neutralized polymer, $M = 1.18 \times 10^6$, from reference 32)

$R_i = 0.01$ cm. (taken as the radius of the capillary tube).

Using the above values in Equation (VIII-3) with the separation factor, 1.0265, obtained at optimum power for cell I, the polarizability is 0.59×10^{-13} cm.^{3}. The same calculation performed for cell II where $\kappa = 42$ and the separation factor is 1.0875 yields $\alpha_p = 2.06 \times 10^{-13}$ cm.^{3}.

Theoretical Separation Factors:

The theoretical separation factors for experimental cells I and II operating at optimum power are calculated from

$$\frac{C_T}{C_B} = \frac{C^*}{C^* - 0'(\ln \kappa)\ L} \qquad (115)$$

where

$$0' - \frac{4D_{AB}\ \mu}{R_i^4 \Delta T \bar{\rho} \bar{\beta} g} \qquad (114)$$

and

C* = dimensionless concentration

L = length of separation tube

$\bar{\beta}$ = average volume coefficient of expansion.

Electrical considerations show that at optimum cell power about two watts is dissipated in the separation tube. The ΔT is determined by equating the heat produced from electrical dissipation as a function of r, (Equation 11), to the heat transfer by conduction, (Fourier's Law). Solution of the ensuing differential equation gives

$$(T_i - T_o) = \frac{\Delta VI\ \ln \kappa}{4k_1 \pi L}, \qquad (VIII\text{-}4)$$

which, since

$$I = \frac{\Delta V 2\pi L}{\rho_1\ \ln \kappa}, \qquad (VIII\text{-}5)$$

reduces to

$$\Delta T = \frac{(\Delta V)^2}{2k_1 \rho_1} \qquad (VIII\text{-}6)$$

where

k_1 = thermal conductivity of solution

ρ_1 = electrical resistivity of solution.

Examination of Equation (VIII-6) shows that the theoretical ΔT is dependent only on the solution thermal conductivity and electrical resistivity as well as the applied voltage to the cell. This lack of dependence on cell geometry enables the calculation of a value of 0', which is applicable to both of the experimental cells. The ΔT obtained from Equation (VIII-4) using two watts power, $\kappa = 36$, L 30.5 cm., and $k_1 = 0.35$ Btu/ft. hr. $^{\circ}$C. is 3.08°C. The values of $\bar{\rho}$, $\bar{\beta}$, and μ are calculated at the average solution temperature. An approximate value of the average solution temperature was found to be 35°C. from heat transfer considerations. The calculation included assuming that the heat transfer from the cell wall to the ambient air at 10° C. was due to natural convection. At the approximate average solution temperature,

$\mu = 0.007225$ gm./cm. sec.

$\bar{\beta} = 2.87 \times 10^{-4}$ $^{\circ}C^{-1}$

$\bar{\rho} = 0.994$ gm./cm.^{3}.

Using these values in Equation (114) with

$R_i = 0.00635$ cm.,

$D_{AB} \simeq 5 \times 10^{-6}$ cm.^{2}/sec. (from reference 32), and

$\Delta T = 3.08^{o}C.,$

the value of 0' is 103.2 cm.$^{-1}$.

The calculation of the theoretical separation factor then is accomplished by direct substitution of the cell κ and L as well as the dimensionless concentration from Equation (111) into Equation (115). Using the values for cell I; $\kappa = 36$, $L = 30.5$ cm., and $C^{*} = 2.3624 \times 10^{5}$, the predicted separation factor is 1.049. For cell II with $\kappa = 42$, $L = 61$ cm., and $C^{*} = 1.1574 \times 10^{5}$, the theoretical separation factor is 1.255.

NOMENCLATURE

A	constant defined by Equation (31)
A,B,C,D,E,F	arbitrary constants determined by the method of undetermined coefficients, Equations (93) and (III-14)
A_1',A_2',A_3',A_4',A_5'	constants defined by Equation (108)
A_n	constant determined by the value of n in an infinite series, Equation (III-1)
A_r	cylindrical area at a given value of r
a	activity of dipolar species, Equation (53)
a_1,b_1	constants of integration, Equation (III-11)
B	constant defined by Equation (32)
C	polymer concentration, gm./ℓ.
C^*	dimensionless concentration defined by Equation (110)
C_{iT},C_{iB}	initial reservoir concentrations, gm./ℓ.
C_p	particular solution of Equation (81)
C_I,C_{II}	solutions to Equation (81) obtained by the "Method of Frobenius"
c_1,c_2,c_3,c_4,c_5,c_6	constants of integration
$c_{11},c_{22},c_{33},c_{44}$	constants defined by Equation (79)
c_1',c_2',c_3',c_4'	constants defined by Equation (81)
D	diameter of outer cylinder, cm.
D_{AB}	mutual diffusion coefficient, cm.^{2}/sec.

E	energy difference between polar and non-polar molecules, Equation (5)
F	electric field strength
f	translational force on a dipolar molecule in an electric field
g	acceleration of gravity, 980.665 cm./sec.^{2}
I	electrical current
K	constant defined by Equation (72)
k	Boltzman's constant, 1.380 x 10^{-16}erg/^{o}k.
k_1	thermal conductivity of solution, cal./sec. cm. ^{o}C.
L	length of separation tube
$L_{(x)}$	Langevin function
ℓ	average end to end length of polymer molecule, Equation (VIII-1)
ℓ	dummy variable, Equation (III-1)
M	average polymer molecular weight
M	total dipole moment, Equation (1)
m	molality of solute
m_i	magnitude of an induced dipole moment
N	Avogadro's number, 6.023 x 10^{23} molecules/mole
N	number of molecules of a particular type, Equation (5)
N_{Ar}	molar flux of component A in the r direction
$N_{A\theta}$	molar flux of component A in the θ direction
N_{Az}	molar flux of component A in the z direction

n	degree of polymerization
n	summation index for infinite series, Equation (103)
O'	constant defined by Equation (114)
P	power produced by Joule heating, watts
p	ratio of molecular length to diameter, Equation (VIII-1)
Q	variable defined by Equation (18)
R	solution resistance, Equation (10)
R	universal gas constant, 8.31×10^7 ergs / mole °K, Equation (53)
R_A	rate of production of species A per unit volume by chemical reaction
R_{iB}	initial solution resistance in bottom cell reservoir, ohm
R_{iT}	initial solution resistance in top cell reservoir, ohm
r	radial variable
r_m	equivalent radius of a dipolar molecule
S_t	frictional force on a moving particle defined by Stoke's Law
S_e	power per unit volume produced from Joule heating
s	variable defined by Equation (75)
T	temperature
$\bar{T}$	average solution temperature, Equation (47)
T'	constant defined by Equation (79)
t	time

$U_{(s)}$	variation of parameters variable, Equation (III-9)
V	electrical voltage
V_z	fluid velocity in the z direction
V'	dimensionless velocity defined by Equation (43)
V^*	dimensionless velocity defined by Equation (49)
v	molecular velocity in the direction of molecular movement
W	number of radioactive counts in a given time
x	mole fraction of polymer in solution
y	dimensionless radial variable, Equation (13)
Z	variable defined by Equation (35)
z	length variable

Gr	Grashof number
Re	Reynolds number
Sc	Schmidt number

α	molecular polarizability
α'	degree of neutralization, percent
β	volume coefficient of expansion, $^{o}C^{-1}$
β	variable defined by Equation (67)
$\bar{\beta}$	volume coefficient of expansion evaluated at $\bar{T}$
β'	variable defined by Equation (80)

$\Gamma_1, \Gamma_2, \Gamma_3, \Gamma_4, \Gamma_5$	variables defined by Equation (103)
Δ	indicates difference
ε_s	dielectric constant of solvent
Θ	dimensionless temperature defined by Equation (16)
θ	angular variable
κ	ratio of outer to inner cylinder radii
μ	permanent dipole moment, Equation (3)
μ	solution viscosity, Equation (23)
μ_c	total molecular chemical potential in an electric field
μ_0	constant, Equation (53)
ν	number of ionized groups per polyion
π	mathematical constant, 3.14159
ρ	density of solution, gm./ℓ.
$\bar{\rho}$	density of solution at temperature $\bar{T}$
ρ_1	resistivity of solution
ϕ	variable defined by Equation (85)
ϕ_c	complimentary solution of Equation (87)
ϕ_p	particular solution of Equation (87)

Subscripts

p	refers to polar molecule
n	refers to non-polar molecule
i	refers to inner cylinder radius

o	refers to outer cylinder radius
r	refers to radial direction
z	refers to vertical direction
T	refers to top reservoir
B	refers to bottom reservoir
F	refers to feed solution
avg	refers to the average value of a parameter
min	refers to minimum value of a parameter
max	refers to maximum value of a parameter

BIBLIOGRAPHY

1. Alfrey Jr., T., Berg, P. W., and Morawetz, H., J. Polymer Sci., 7, 543 (1951).

2. Bailey Jr., F. E., Patterson Jr., A., and Fuoss, R. M., J. Am. Chem. Soc., 74, 1845 (1952).

3. Bird, R. B., Stewart, W. E., and Lightfoot, E. N., Transport Phenomena, Wiley, N.Y., 1960, p. 85 Eq. F.

4. Bird, R. B., Stewart, W. E., and Lightfoot, E. N., Transport Phenomena, Wiley, N. Y., 1960, p. 319 Eq. B.

5. Bird, R. B., Stewart, W. E., and Lightfoot, E. N., Transport Phenomena, Wiley, N. Y., 1960, p. 559 Eq. B.

6. Bockris, J. O'M., Modern Aspects of Electrochemistry, Academic Press, N.Y., 1954, pp. 3-11.

7. Debye, P., Polar Molecules, Dover, N. Y., 1929, pp. 27-30.

8. Debye, P., and Bueche, F., J. Chem. Phys., 19, 589 (1951).

9. Debye, P., Debye, P. P., Eckstein, B. H., Barber, W. A., and Arquette, G. J., J. Chem. Phys., 22, 152 (1954).

10. Eigen, M., and Schwarz, G., J. Colloid Sci., 12, 181 (1957).

11. Eisenberg, H., J. Polymer Sci., 30, 47 (1958).

12. Flory, P. J., J. Am. Chem. Soc., 65, 375 (1943).

13. Flory, P. J., J. Chem. Phsy., 21, 162 (1953).

14. Frame, J. S., Private communication.

15. Frank, H. S., J. Chem. Phys., 23, 2023 (1955).

16. Fuoss, R. M., J. Polymer Sci., 12 185 (1954).

17. Fuoss, R. M., and Cathers, G. I., J. Polymer Sci., 2, 12 (1947).

18. Fuoss, R. M., and Strauss, U. P., J. Polymer Sci., 3, 246, 602 (1948).

19. Harris, F. E., and Rice, S. A., J. Phys. Chem., 58, 725, 733 (1954).

20. Harris, F. E., and Rice, S. A., J. Polymer Sci., 15, 151 (1955).

21. Hermans, J. J., and Overbeek, J. T. G., Rec. Trav. Chim., 67, 761 (1948).

22. Howard, G., and Jordan, O. O., J. Polymer Sci., 12, 209 (1954).

23. Inagaki, H., and Oda, T., Macromol. Chem., 21, 1 (1956).

24. Jacobson, B., Rev. Sci. Instr., 24, 949 (1953).

25. Kagawa, I., J. Chem. Soc. Japan, 47, 574 (1944).

26. Kagawa, I., Oosawa, F., and Imai, N., J. Polymer Sci., 13, 93 (1954).

27. Karagounis, G., Nature, 161, 855 (1948).

28. Karagounis, G., Helv. Chim. Acta, 31, 1929 (1948).

29. Katchalsky, A., and Eisenberg, H., J. Polymer Sci., 6, 145 (1951).

30. Katchalsky, A., and Lifson, S., J. Polymer Sci., 11, 409 (1953).

31. Katchalsky, A., and Lifson, S., J. Polymer Sci., 13, 43 (1954).

32. Kern, E. E., Ph.D. Thesis, Michigan State University (1966).

33. Kern, W., Z. Physik. Chem., A181, 240, 283 (1938).

34. Kimball, G. E., Cutler, M., and Samelson, H., J. Phys. Chem., 56, 47 (1952).

35. Kotliar, A. M., and Morawetz, H., J. Am. Chem. Soc., 77, 3692 (1955).

36. Krause, S., Private communication.

37. Kraut, J., J. Polymer Sci., 14, 222 (1954).

38. Loesche, A., and Hultschig, H., Kolliod. Zhur., 141, 177 (1955).

39. Kuhn, W., Kunzle, O., and Katchalsky, A., Helv. Chim. Acta, 31, 1994 (1948).

40. Kuhn, W., Kunzle, O., and Katchalsky, A., J. Polymer Sci., 5, 283 (1950).

41. Mandel, M., and Jenard, A., Trans. Faraday Soc., (To be published).

42. Mandel, M., and Leyete, J. C., J. Polymer Sci., (To be published).

43. Mandel, M., and Leyete, J. C., J. Polymer Sci., (To be published).

44. Miller, M. L., The Structure of Polymers, Reinhold, N.Y., 1966, Chap. 13.

45. Morawetz, H., Macromolecules in Solution, Interscience, N.Y., 1965, pp. 320-330.

46. Mueller, F. H., Wiss. Verofentl. a. d. Siemens-Werken, 17, 20 (1938).

47. O'Konski, C. T., J. Phys. Chem., 64, 605 (1960).

48. Orofino, T. A., and Flory, P. J., J. Phys. Chem., 63, 283 (1959).

49. Oth, A., and Doty, P., J. Phys. Chem., 56, 43 (1952).

50. Pohl, H. A., J. Appl. Phys., 22, 869 (1951).

51. Pohl, H. A., J. Appl. Phys., 29, 1182 (1958).

52. Rice, S. A., and Nagasawa, M., Polyelectrolyte Solutions, Academic Press, N.Y., 1961, pp. 283-390.

53. Schindewolf, U., Z. Physik. Chem., 1, 129 (1954).

54. Schindewolf, U., Z. Physik. Chem., 1, 134 (1954).

55. Steiner, R. F., and Doty, P., J. Chem. Phys., 20, 85 (1952).

56. Strauss, U. P., Gershfeld, N. L., and Spiera, H., J. Am. Chem. Soc., 76, 5909 (1954).

57. Swinkels, D. A., and Sullivan, E. B. A., Aust. J. Chem., 14, No. 4, 487 (1961).

58. Tanford, C., Physical Chemistry of Macromolecules, Wiley, N.Y., 1961, pp. 458-504.

59. Vinks, H., Makro. Chem., 67, 105 (1963).

60. Vithani, K. K., M. S. Thesis, Michigan State University (1960).

61. Wall, F. T., J. Phys. Chem., 61, 1344 (1957).

62. Wall, F. T., Huizenga, J. R., and Greiger, P. F., J. Am. Chem. Soc., 72, 2636 (1950).

63. Wall, F. T., Huizenga, J. R., and Greiger, P. F., J. Am. Chem. Soc., 72, 4228 (1950).

64. Wall, F. T., Teryama, H., and Techakumpuch, S., J. Polymer Sci., 20, 477 (1956).

65. Wojtczak, Z., J. Polymer Sci., 3A, 3613 (1965).